1-1-2002

The chloroplast terminal oxidase is involved in multiple physiological responses

Jason Edward Barr
Iowa State University

The chloroplast terminal oxidase is involved in multiple physiological responses

by

Jason Edward Barr

A thesis submitted to the graduate faculty

in partial fulfillment of the requirements for the degree of

MASTER OF SCIENCE

Major: Genetics

Program of Study Committee:
Steven R. Rodermel, Major Professor
David Oliver
Thomas Baum

Iowa State University

Ames, Iowa

2002

Graduate College
Iowa State University

This is to certify that the master's thesis of

Jason Edward Barr

has met the thesis requirements of Iowa State University

Signatures have been redacted for privacy

TABLE OF CONTENTS

CHAPTER 1

GENERAL INTRODUCTION

OVERVIEW AND BACKGROUND

The biology of plant photosynthesis and greening has been studied for many decades. The effects of these studies have broadened the general knowledge of the physiology of the plant, and the knowledge accumulated has allowed the continuous improvement of commercially and agronomically important plants. Many recent studies have utilized modern genetic experiments to elucidate mechanisms of phenotypic expression in plants by either artificially creating genetic aberrations or by analyzing natural variants. Recently, these studies have been particularly poignant in defining the mechanisms of chloroplast biogenesis and function.

Chloroplasts: nuclear-organelle interactions

It has been hypothesized that chloroplasts arose from progenitor photosynthetic green algae millions of years ago through the process of endosymbiosis. According to this hypothesis, proto-eukaryotic cells endosymbiosed, or took internally, prokaryotic green algae cells to benefit symbiotically from the photosynthesis in the algae cells. Both the host cell and the endosymbiosed algal cell both have deoxyribonucleic acid (DNA) as the chemical that determines cellular proteins, products and processes and through which heredity functions. During the evolutionary process to modern times, the algal DNA has been transferred to the eukaryotic nucleus, and the genes that are carried on this transferred DNA undergo transcription and translation outside the envelope. Protein products from the genes transferred to the eukaryotic nucleus are translated on 80S ribosomes and then are imported post-transcriptionally into the chloroplast. An example is the small subunit of ribulose bis-phosphate carboxylase-oxygenase (RUBISCO), which is encoded by the *rbcS* gene family located in the nucleus. Although many genes have been transferred into the nuclear compartment of eukaryotic cells, many genes, such as the gene *rbcL*, which encodes for the large subunit of RUBISCO, remain inside the chloroplast and are transcribed and translated therein. This post-translational import of proteins into the chloroplast begs the question of regulation, wherein there exist at least two separate and active chromosomal DNA compartments inside the eukaryotic cell: the

nucleus and the chloroplast. Recent experiments have shown the eukaryotic cell has anterograde and retrograde signaling between the nucleus and the chloroplast to control transcription of nuclear encoded genes (Rodermel, 2001).

Variegation mutants as model systems: *immutans*

Variegated mutants were used to demonstrate the genetics of maternal inheritance, or extra-nuclear inheritance, thereby defining the question of nuclear-chloroplast interactions. These mutants are composed of leaves that contain two distinct phenotypic regions: white chlorotic sections and green morphologically normal sections. Many of these mutants arise from lesions in the chloroplast or mitochondrial DNA, and during normal cellular division, the mutant organelles segregate to form the phenotypically distinct leaf regions (Rodermel, 2002). This thesis discusses experiments with the *Arabidopsis thaliana* (Col.) variegated mutant *immutans* (*im*). *im* was first described and characterized by G. P. Redei over 50 years ago, and the mutant was given the Latin name *immutans* ("*im*" a prefix meaning "not" and "*mutans*" the nominative present active participle of the Latin verb "*mutare*" meaning "to change", thus "*immutans*" means literally "it is not changing") to designate the non-segregation of the variegated phenotype. Experiments have shown that the degree of variegation, or ratio of white leaf surface area to green leaf surface area, depends upon the intensity and quality of light for the growth conditions of the plant (Wetzel et al, 1994; Wu et al, 1999). Under higher light intensities, *im* is nearly entirely composed of white tissue or completely albino, while under low light intensities little variegation is apparent. Seed collected from even extremely chlorotic siliques gives rise to green, variegated and white plants (depending on ambient light intensities) for many generations and completely green siliques produce the same phenotypic distribution. Reciprocal crosses of known *im* alleles to wild type plants have shown these *im* alleles are caused by a completely recessive single nuclear gene (Chapter 2). The green sections produced by *im* show normal photosynthetic gene transcription and many *im* mutants accumulate normal pigment levels (Chapter 2). In the *im* mutant *spotty*, the green sectors are thicker (due to an elongation of the cells in the palisade layer) than wild type tissues and contain a higher chlorophyll a/b ratio (Aluru et al, 2001). The green *spotty* sections also have higher photosynthetic rates and have a higher number of

chloroplasts per cell. By contrast, the white leaf tissues are thinner than wild type leaf tissues due to a reduction of the cell length and organization in the palisade layer and exhibit no detectable photosynthetic capacity (Aluru et al, 2001). Experiments conducted with the bleaching herbicide norflurazon have shown it to cause white sectoring similar to *im* in which white sections have photooxidized plastids, altered transcription of nuclear genes and accumulate the colorless carotene precursor phytoene (Wetzel et al, 1994). Past experiments on *im* have shown that the white chlorotic sections of the mutant also accumulate phytoene and contain plastids that are photooxidized or lacking pigments and organized lamellar structures with large vacuolar structures (Wetzel et al, 1994). Additionally, the nuclear transcription of photosynthetic genes, such as *Lhcb*, which encodes a chlorophyll a/b binding protein, have been abated in these white sections. However, the accumulation of phytoene in white tissues is not due to lower amounts of the enzyme phytoene desaturase (PDS), which converts phytoene to ζ-carotene in the carotenoid pathway, as Western analysis has shown PDS levels to be equivalent in both green and white *im* tissues (Wetzel and Rodermel, 1998). There are studies that agree with this result, such as analysis of *Capsicum annuum* treated with norflurazon (Simkin et al., 2000), yet recent studies of the *ghost* (*gh*) mutant (the tomato homolog of *im*) disagree and conclude that higher PDS levels exist (Scolnik et al., 1987; Josse et al., 2000). Regulation of carotenogenesis and PDS levels, along with other enzymes of the carotenoid biosynthetic pathway, are discussed further in Chapter 3. Thus, variegated mutants provide an excellent model in which nuclear-chloroplast interactions may be studied.

Carotenoid Biosynthesis

Carotenoid biosynthesis is a process in which pigmented compounds are synthesized for photoprotection and light harvesting activities. Carotenoids are C_{40} terpenoid compounds that are yellow, orange, and red pigments that exist in high levels in chloroplasts and chromoplasts (McGarvey and Croteau, 1995; Cunningham and Gantt, 1998). In chloroplasts, carotenoids have essential functions in the photosynthetic light harvesting and photoprotection. In some flowers and fruits, which have chromoplasts, carotenoids serve as attractants for pollinators as agents for seed dispersal (Bartley et al., 1995). Nuclear genes encode all the enzymes that control plant carotenoid

biosynthesis, and the protein products are imported into plastids (Cunningham and Gantt, 1998). Carotenoid synthesis begins in the plant when two molecules of geranylgeranyl diphosphate are condensed into phytoene, the first colorless carotenoid, by phytoene synthase (PSY) (Fraser et al., 1999). Phytoene is synthesized into the red pigment, *trans*-lycopene, by four consecutive desaturation reactions and an isomeration reaction forming carbon-carbon double bonds. Two enzymes in plants catalyze the desaturation reactions: two membrane-associated enzymes, phytoene desaturase (PDS) and ζ-carotene desaturase (ZDS) (Beyer et al., 1989). Phytofluene and ζ - carotene are the first two products from the desaturation reaction by PDS. ZDS catalyzes the last two steps of desaturation to produce neurosporene and *cis*-lycopene. The isomeration reaction transforming *cis*-lycopene into *trans*-lycopene is catalyzed by the recently identified lycopene isomerase (CRTISO) (Park et al., 2002, Isaacson et al., 2002). *Trans*-lycopene is cyclized to synthesize either α- or β-carotene by lycopene ε-cyclase (LCYE), lycopene β-cyclase (LCYB) and BETA (Ronen et al., 2000). The addition of molecular oxygen to the rings forms zeaxanthin, which is catalyzed by β-carotene hydroxylase (CHYB); hydroxylase reactions can also utilize α-carotene to produce lutein and other xanthophylls. Transcriptional regulation is the major regulatory mechanism of carotenoid biosynthesis in flowers and fruits (Giuliano et al., 1993; Pecker et al., 1996; Ronen et al., 1999; Mann et al., 2000). The tomato and tobacco plant genomes contain two *PSY* genes (Fraser et al., 1999; Busch et al., 2002). In tomato, *PSY1* is up-regulated during fruit ripening, reaching a peak at the breaker (BR) stage, while *PSY2* transcripts are more abundant in mature leaves, and PSY2 is not active in tomato fruit carotenoid biosynthesis (Bartley and Scolnik, 1993; Giuliano et al., 1993; Fraser et al., 1999). Prior research has suggested that IM is involved in carotenoid biosynthesis because white *im* tissues accumulate phytoene, but *im* is not required for PDS translation, as PDS was detected at wild type levels in green tissue of *im* (Wetzel and Rodermel, 1998).

The *Arabidopsis* alternative oxidase (AOX)

In 1999, the *im* locus was cloned in *Arabidopsis*, and *im* was found to be a single copy nuclear-localized gene that encodes a homolog of the *Arabidopsis* alternative oxidase (AOX) (Wu et

al, 1999; Carol et al, 1999). AOX is a mitochondrial protein encoded, in many plant species, by a gene family of four members (Wu et al., 1999). AOX acts in the mitochondrial electron transport chain (mitETC) by oxidizing ubiquinol (UQH_2) to ubiquinone (UQ) and using molecular oxygen as an electron acceptor to form water. AOX is believed to function as a homodimer in the mitochondrial inner membrane. UQ exists in mitochondria as a high-energy electron carrier between nicotinamide adenine dinucleotide (NADH) dehydrogenase and the cytochrome complex. AOX activity is not sensitive to cyanide inhibition but rather is inhibited by propyl gallate. Thus, AOX activity seems to remove electrons from an early stage in the mitETC, and has been termed an alternative pathway of mitochondrial respiration (Maxwell et al, 1999).

IM has been shown to have biochemical activity in the chloroplast analogous to AOX. IM oxidizes plastoquinol (PQH_2) to plastoquinone (PQ) and transfers the electrons to molecular oxygen forming water (Bennoun et al, 2000; Joet et al., 2002). PQ exists in the chloroplast as a high-energy electron carrier, which transfers electrons from photosystem I to the cytochrome complex. Recently, *im* homologs have been identified in pepper (*Capsicum annum*) and tomato (*Lycospersicon esculentum*), and in *Arabidopsis*, as well as other species, *im* is a single locus, which is a contrast to the gene family of AOX (Wu et al., 1999; Josse et al, 2000; Rodermel, 2002). The tomato homolog of *im*, called *ghost* (*gh*), was identified by spontaneous mutation in a commercial population (Rick et al, 1959). The carotenoid composition of *gh* green tissues is similar to that in the wild type, and green *gh* tissues also have normal chloroplasts. In contrast, the white tissues of *gh* leaves or fruits have plastids that lack organized membrane structures (Scolnik et al., 1987). Under normal illumination conditions, *gh* plants have pale cotyledons and the first true leaves that emerge are completely chlorotic. When germinated under lower than normal illumination and shifted to normal illumination conditions 4-6 weeks later, gh leaves are white and/or variegated with pale yellow to white petals emerging during flowering and fruits are white in their immature stage, proceed through a yellow intermediate turning stage, and turn orange as development proceeds to ripening (Rick et al., 1959; Scolnik et al., 1987; Chapter 3). However, when *gh* plants are grown under lower than normal illumination and never transferred to normal conditions, leaves are all green or very slightly variegated

with pale yellow to yellow petals emerging during flowering, and *gh* fruits are almost entirely green or variegated with darker green streaks or patches and proceed through the intermediate yellow stage and later turn orange (Rick et al., 1959).

RATIONALE FOR THESIS

Although the biochemical nature of *im* is known, there is no clear evidence about how IM function is involved in physiological processes. No data suggest that *im* has an impact on the flow of electrons from PQ to the cytochrome b_6/f complex, and the involvement of *im* in many other processes is yet undetermined. Through my studies of both *im* and *gh*, I wanted to identify and characterize new mutations of *im* for further analysis and suppressor identification. *im* mutants currently under study have varying phenotypes of variegation severity, yet reportedly only carry null mutation in *im* (as mentioned above). The *im* homolog *gh* has been identified in tomato (*Lycospersicon esculentum* Mill). *gh* has light sensitive variegated leaves and branches that emerge similarly to *im*, and *gh* produces unusually orange colored ripe fruit from either white or green mature fruit that originates from branches grown under high light or low light, respectively. These unusually colored fruits prompted my study of *gh* and its role in chromoplast development (Chapter 3). As engineering carotenogenesis becomes increasingly popular to supplement plants used for human foods, such as tomatoes, maize and rice, the understanding of the function *gh* plays in the transcriptional regulation of carotenoid synthesis is pertinent to the development of these plants and to the understanding of the chloroplast to chromoplast transition. As *im* has been identified as a PQH_2 oxidase and operates in between the photosystems, I suspected that *im* might respond to the effects of light stress (Chapter 5). This response would show the importance of *im* in *Arabidopsis* compensation response for extreme variations in light intensity, as may be found in nature.

This thesis is organized into four additional chapters that are comprised of: new mutant identification, analysis, and suppressor genes; general introduction to carotenoid biosynthesis and tomato fruit development; involvement of the plastid terminal oxidase in chromoplast development and regulation of carotenogenesis during fruit ripening; and studies that implicate IM in plant response to light stress. In Chapter 6, there is written a conclusion to this thesis, which discusses the

more broad ideas not stated in the previous chapters. Included in the Appendix is a manuscript addendum to Chapter 5, which contains some of my work discussed more completely within Chapter 5.

LITERATURE CITED

Aluru, M., Hanhong, B., Dongying, W., and Rodermel, S. (2001). The *Arabidopsis immutans* mutation affects plastid differentiation and the morphogenesis of white and green sectors in variegated plants. Plant Physiol. Sept; 127: 67-77.

Bartley G. and Scolnik, P. (1993). cDNA cloning, expression during development, and genome mapping of PSY2, a second tomato gene encoding phytoene synthase. J. Biol. Chem. Dec 5;268(34): 25718-21.

Bartley, G. and Scolnik, P. (1995). Plant carotenoids: pigments for photoprotection, visual attraction, and human health. Plant Cell 7: 1027-1038.

Beyer P, Mayer M, and Kleinig H. (1989). Molecular oxygen and the state of geometric isomerism of intermediates are essential in the carotene desaturation and cyclization reactions in daffodil chromoplasts. Eur. J. Biochem. Sep 1;184(1):141-50.

Busch, M., Seuter, R., Rüdiger, H. (2002). Functional analysis of the early steps of carotenoid biosynthesis in tobacco. Plant Physiol. 128:439-453.

Carol, P., Stevenson, D., Bisanz, C., Breitenbach, J., Sandmann, G., Mache, R., Coupland, G., and Kuntz, M. (1999). Mutations in the *Arabidopsis* gene *IMMUTANS* cause a variegated phenotype by inactivating a chloroplast terminal oxidase associated with phytoene desaturation. Plant Cell 11: 57-68.

Cunningham, Jr., F. and Gantt, E. (1998). Genes and enzymes of carotenoid biosynthesis in plants. Annu. Rev. Plant Physiol. Plant. Mol. Biol. 49: 557-583.

Fraser, P., Kiano, J., Truesdale, M., Wolfgang, S., and Bramley, P. (1999). Phytoene synthase 2 enzyme activity in tomato does not contribute to carotenoid synthesis in ripening fruit. Plant Mol. Biol. 40: 687-698.

Giuliano, G., Bartley, G., and Scolnik, P. (1993). Regulation of carotenoid biosynthesis during tomato fruit development. Plant Cell 5(4): 379-387.

Isaacson, T., Ronen, G., Zamir, D., and Hirshberg, J. (2002). Clonong of *tangerine* from Tomato Reveals a Carotenoid Isomerase Essential for Production of β-Carotene and Xanthophylls in Plants. Plant Cell 14: 333-342.

Joet, T., Genty, B., Josse E-M., Kuntz, M., Cournac, L., Peltier, G. (2002). Involvement of a plastid terminal oxidase in plastoquinone oxidation as evidenced by expression of the arabidopsis thaliana enzyme in tobacco. J. Biol. Chem. [in press].

Josse, E-M., Simkin, A., Joël, G., Labouré, A-M., Kuntz, M., and Carol, P. (2000). A plastid terminal oxidase associated with carotenoid desaturation during chromoplast differentiation. Plant Physiol. Aug; 123: 1427-1436.

Mann, V., Harker, M., Pecker, I., and Hirschberg, J. (2000). Metabolic engineering of astaxanthin production in tobacco flowers. Nat. Biotechnol. Aug;18(8): 888-92.

Maxwell, D.P., Wang, Y., and McIntosh, L. (1999). The alternative oxidase lowers mitochondrial reactive oxygen production in plant cells. PNAS Jul 6; 96(14):8271-6.

McGarvey, D. and Croteau, R. (1995). Terpenoid metabolism. Plant Cell 7(7): 1015-1026.

Park, H., Kreunen, S., Cuttriss, A., DellaPenna, D., and Pogson, B. (2002). Identification of the Carotenoid Isomerase Provides Insight into Carotenoid Biosynthesis, Prolamellar Body Formation, and Photomorphogenesis. Plant Cell 14: 321-332.

Pecker, I., Gabbay, R., Cunningham, Jr, F., and Hirschberg, J. (1996). Cloning and characterization of the cDNA for lycopene beta-cyclase from tomato reveals decrease in its expression during fruit ripening. Plant Mol. Biol. Feb; 30(4): 807-19.

Rick, C., Thompson, A., and Brauer, O. (1959). Genetics and development of an unstable chlorophyll deficiency in *Lycospersicon esculetum*. Am. J. Bot. 46(1): 1-11.

Rodermel, S. (2001). Pathways of plastid-to-nucleus signaling. Trends in Plant Science. Oct;6(10):471-478.

Rodermel, S. (2002) Arabidopsis Variegation Mutants, The Arabidopsis Book, eds. C.R. Somerville and E.M. Meyerowitz, American Society of Plant Biologists, Rockville, MD, doi/10.1199/tab.0079, http://www.aspb.org/publications/arabidopsis/

Ronen, G., Cohen, M., Zamir, D., and Hirschberg, J. (1999). Regulation of carotenoid biosynthesis during tomato fruit development: expression of the gene for lycopene epsilon-cyclase is down regulated during ripening and is elevated in the mutant *Delta*. Plant J. 17(4): 341-351.

Ronen, G., Carmel-Goren, L., Zamir, D., and Hirschberg, J. (2000). An alternative pathway to β-carotene formation in plant chromoplasts discovered by map based cloning of *Beta* and *old-gold* color mutations in tomato. Proc. Natl. Acad. Sci. U. S. A. 97(20): 11102-11107.

Scolnik, P., Hinton, P., Greenblatt, I., Giuliano, G., Delanoy, M., Spector, D., and Pollock, D. (1987). Somatic instability of carotenoid biosynthesis in the tomato *ghost* mutant and its effect on plastid development. Planta 171: 11-18.

Wetzel, C., Jiang, C-Z., Meehan, L., Voytas, D., and Rodermel, S. (1994). Nuclear-organelle interactions: the *immutans* variegation mutant of *Arabidopsis* is plastid autonomous and impaired in carotenoid biosynthesis. Plant J. 6(2): 161-175.

Wetzel, C. and Rodermel, S. (1998). Regulation of phytoene desaturase expression is independent of leaf pigment content in *Arabidopsis thaliana.* Plant Mol. Biol. 37(6):1045-53.

Wu D., Wright D., Wetzel C., Voytas D., and Rodermel S. (1999). The *IMMUTANS* variegation locus of *Arabidopsis* defines a mitochondrial alternative oxidase homolog that functions during early chloroplast biogenesis. Plant Cell 11: 43-56.

CHAPTER 2

CHARACTERIZATION OF *IMMUTANS* ALLELES

ABSTRACT

A recent mutant screen has identified many new *immutans* (*im*) alleles that have distinct physiological differences in variegation severity. Many of the new mutants exhibit a less severe variegated phenotype than the extensively studied *im* allele *spotty*. These mutants have been characterized by crosses to wild type and *spotty*, Northern analysis, Western analysis, chlorophyll and carotenoid content and DNA sequencing. The alleles V189, cs3157, cs3639, cs3630 and cs3627 contain intronic mutations that cause aberrant *im* mRNA products to be formed. These aberrations in splicing can be described as intron inclusion, exon skipping and activation of cryptic splice sites. It is yet undetermined why these mutants show a variable severity of phenotype, as they are all null for the IM protein, but some early crosses suggest that the yellow seed phenotype of cs3630 may suppress the variegation caused by its *im* lesion. Alleles cs3628, cs3643 and cs3660 also show this yellow seed phenotype and have a less severe variegated phenotype.

INTRODUCTION

Suppressor screens using a mutant background is a common method to detect genetic aberrations that may suppress, or reduce the severity, of the background mutant phenotype used. This is an excellent method to discover new interacting genes and mechanisms of the mutant phenotype, and I employed this method to search for suppressors of the *im* variegated phenotype. There exist three *Arabidopsis thaliana immutans* (*im*) variegated mutants previously identified, and their genomic DNA has been sequenced: *im-1*, *spotty* and *cs3157* (Wu et al., 1999). Each mutant possesses a defective genomic *im* sequence and has a unique phenotype of variegation and pigmentation. This variegation is light-sensitive, meaning the percentage of white chlorotic tissue is approximately proportional to the ambient light intensity. Secondary site mutations that suppress the variegated phenotype of *im* might explain how the mechanism of variegation occurs and identify other genes that may be involved in the process of variegation or influence the mechanism by which leaf tissue becomes variegated. In a screen to find suppressor mutations, multiple lines generated by

ethylmethanosulfate (EMS) and stored at the Arabidopsis Biological Resource Center (ABRC) at Ohio State University were grown that showed a light-sensitive variegated phenotype less severe but similar to the *spotty* allele of *im*. Additionally, many of the lines were double mutants in which they have two unique phenotypes caused by seemingly different loci: light-sensitive variegation and yellow seed production. Many of these mutants have been characterized by crosses to wild type *Arabidopsis* (WT) and *spotty*, DNA sequencing, and both Northern and Western analysis. It is possible that the varying phenotypes of some mutants can be explained if the yellow seed phenotype can act as a suppressor of variegation in *im* mutants.

The yellow seed phenotype is similar to the transparent testa phenotype described by recent studies as a set of mutant loci that, when defective, produce yellow seed instead of the normally dark brown seed produced by wild type *Arabidopsis* (Sagasser et al., 2002). The mutants obtained from the stock center were selfed for at least 2 generations and showed a stable transmission of the *im* phenotype and , where applicable, the yellow seed phenotype. The mutant cross to WT shows the nature of the lesion in the manner of dominance and loci number, and the mutant cross to *spotty* detects allelism to *im*. Additionally, molecular characterization of *im* mRNA levels and IM protein levels in the mutant lines detected effects of mutations on the transcription and translation of *im*.

MATERIALS AND METHODS

Plant Materials

Arabidopsis thaliana Col. seeds stock lines cs3612, cs3620, cs3627, cs3628, cs3630, cs3633, cs3639, cs3641, cs3643 and cs3660 were obtained from Arabidopsis Resource Center at Ohio State University and germinated on soil at 22°C 60 μmol m^{-2} sec^{-1} continuous light and grown under this light intensity in a growth chamber for 1 week after cotyledon emergence. Seedlings were then transferred to 100 μmol m^{-2} sec^{-1} continuous light for the duration of the growth period. Seed stock lines used for crossing were self-fertilized and offspring seed from each plant collected separately for at least 2 generations prior to crosses to determine stability of the phenotypes. Flowers used for the pollen receptor (female) had the anthers and filaments dissected out pre-dehiscence using fine tipped forceps dipped in 50% ethanol in water and allowed to air dry, and test

flowers that did not receive pollen treatment did not generate seed. Pollen donors (male) were utilized by removing an anther 2 to 7 days post-dehiscence and distributing the pollen from the anther to the female stamen, and the flower was marked with a loop of colored cotton thread for recording position and development of the resultant silique. For all crosses, the seed stock mutant flowers were pollen receptors (female) and the wild type (WT) or *spotty* flowers were used as pollen donors (male). Siliques from each cross were kept separate for seed collection, and the F_1 generation was grown as described above. The F_1 and F_2 were allowed to self pollinate, were scored for phenotype, and seed was collected from each plant individually.

Chlorophyll Assay

For determining the concentration of chlorophyll in mutant leaf tissues, mutant alleles were grown as described above and 0.351 cm^2 leaf punches were taken from green sections of leaves with a #3 cork borer, weighed on an analytical balance, and imbibed in 1 mL of N,N-dimethylformamide in a 2 mL centrifuge tube. For each genotype, nine leaf punches were taken from the green leaf sections of nine different plants grown under the same growth chamber conditions at the same time. The centrifuge tubes were place inside a completely dark environment and shaken at 4°C on a orbital shaker at 200 rpm for 24 hours. Chlorophyll and carotenoid concentrations were determined using spectrophotometry according to Moran, 1982. Statistical calculations and graphic representations of data were generated using Microsoft® Excel 2000.

Nucleotide Analysis and RT-PCR

Leaf tissue from plants grown under the same conditions and the same age (see above for conditions) were collected for RNA analysis was weighed and immediately frozen in liquid nitrogen and stored at -80°C until RNA extraction. Leaves collected from *im* alleles were usually variegated, and often the ability to detect *im* mRNA in *spotty* was dependant on the percent variegation of the leaf, as it was previously reported that *im* mRNA was undetectable by Northern blot (Wu et al., 1999). Total RNA was extracted by grinding the leaf tissue to a powder under liquid nitrogen and immediately using Concert RNA plant reagent (Invitrogen) according to the manufacturer's suggestions to extract total RNA from the powdered leaf tissue. RNAs were electrophoresed on 3%

formaldehyde-1% agarose gels and blotted onto a GeneScreen Plus® Hybridization Transfer Membrane (NEN™ Life Science Products, Boston, MA). *im* cDNA was ^{32}P-labeled by random priming and used as a probe (Ausubel et al., 1998). Hybridization and washing of the membranes were performed as described (Wetzel et al., 1994). All RNA blot analyses were repeated at least twice from different RNA isolations from different plants to confirm the reproducibility of the results.

Total RNA was isolated (see above) and used to perform RT-PCR. The quantity and quality of RNA was verified by spectrophotometer absorbance at 260nm and 280nm and by electrophoresing the RNAs on a 3% formaldehyde-1% agarose gel. To remove any genomic DNA contamination, 1µg total RNA was treated with RNase-free DNase according to manufacturer's recommendation (Life Technologies, Rockville, MD). RNA quality was re-checked by electrophoresing the DNase-treated RNA on a 3% formaldehyde-1% agarose gel. Superscript™ first-strand cDNA synthesis for RT-PCR kit (Life Technologies, Rockville, MD) was used according to manufacturer's recommendation to generate first-strand cDNA prior to PCR except primer DV0514 was used as a reverse primer to generate cDNA instead of the oligo T or random primers, which were provided by the manufacturer. PCR included an initial denaturation of 3 min at 94°C, followed by 30 cycles of 1 min at 94°C, 1 min at 52°C, 1 min at 72°C, and a final 10-min extension at 72°C. The PCR products were electrophoresed in a 0.8, 1.5, or 3.0% agarose gels and purified by using QIAEX II Gel Extraction System (Qiagen Inc., Valencia, CA) for sequencing. Primers used for PCR and sequencing were: forward IM100A 5'-GCTCAAATCTTTGGTTCCTGACGGAG -3'; and reverse DV0514 5'-GCAGACTGCCTAGAGTCTGACAAG -3', DV0549 5'- TCAGAAGACAGTAAGATTGTGAAC -3', DV0550 5'- GCCTTTTGTTGTTAAGAGTTGAAC -3', reverse DV0574 5'-ATGAGCAAGTGATGCATTTCATTC -3', IM7R 5'- GCGATARCCGGTGCAGGC -3', DV0536 5'-TACAACAGAATGGTGGAGAAAGAAG -3'. forward IM5F 5'- GGCTCAGCACATAGCAACC -3', DV0551 5'- TACTCGAAGACCAGTAATAG -3', DV0534 5'- TGTGGTTCGACGGAATCAGAGATG -3'. DNA sequence alignments were performed using the Pairwise BLAST option on the NCBI web server, and all mutations were validated by sequencing both forward and reverse DNA strands. For electrophoresis, PCR fragments were electrophoresed on either 0.8, 1.5, or 3.0% agarose, and

difference in PCR fragment sizes of less than 20 nucleotide base pairs was detected by electrophoresis of PCR products on 12% acrylamide gels. For acrylamide gel electrophoresis, TAE buffer was used, and the acrylamide gel was soaked in TAE buffer with ethidium bromide (50mg/100mL) for 1 hour for DNA visualization. Mutant plant photographs were captured digitally with a Kodak DC3400 digital camera or scanned into digital format from 35mm color prints and formatted for presentation using Adobe Photoshop 5.0, and plants were grown as described above and photographed at the same stage in development at the same magnification.

Chloroplast isolation and Western analysis

From plants grown in conditions described in the plant materials section, 5 to 10 g of leaf tissue (multiple whole rosettes) was collected and any soil was rinsed from the tissue with ddH_20. The tissue was immediately moved to a 4°C environment where the remaining procedure was executed. Tissue was placed into a commercial blender with 200 to 500 mL of CP grinding buffer (per 1 L: 3.722 g EDTA-Na, 12 g HEPES adjust to pH 8.0 with KOH, 60.1 g sorbitol, 0.5 g BSA, and 0.88 g sodium ascorbate is added just before use) and pulsed on the highest setting for 2 times, then homogenized on highest setting for 2 to 3 seconds. The homogenate was filtered through 2 layers of Calbiochem® Miracloth (CNbiosciences, Inc., LaJolla, CA 92039-2087), placed into a 200 mL centrifuge bottle in ice, and wrapped in aluminum foil to keep the homogenate in dark conditions . The homogenate was centrifuged at 8,000 times G at 4°C for 3 minutes in a Sorvall centrifuge using a GSA rotor. The supernatant was decanted and discarded, and the pellet was re-suspended in 25 mL of 10 mM HEPES-KOH pH 8.0. The slurry was homogenized in a pyrex tissue homogenizer for 30 seconds and placed in a 50 mL centrifuge tube in ice, and wrapped in aluminum foil to keep the homogenate in dark conditions . The homogenate was centrifuged at 10,000 times G at 4°C for 10 minutes in a Sorvall centrifuge using a SS-34 rotor. The supernatant was decanted and discarded, and the pellet was re-suspended in 0.25 mL to 2 mL of SH Buffer (per 50 mL: 3 g HEPES adjust to pH 8.0 with KOH, 15.175 g sorbitol). The slurry was homogenized in a pyrex tissue homogenizer for 30 seconds and transferred into a 1.5 mL microcentrifuge tube and placed on ice. Chlorophyll concentrations of the samples were determined by using 95% ethanol according to Lichtenthaler,

1987 (additionally to the published assay: aliquots of the samples were centrifuged prior to chlorophyll determination and the supernatant was used in this assay). Samples were stored in the dark at -80°C until use.

For Western analysis, volumes of chloroplast preparations containing equal concentrations of chlorophyll (see Figure 6 for concentrations) were prepared for gel loading by adding enough 2X loading buffer (per 10 mL buffer: 1 mL 1M Tris-HCl pH 6.8, 0.31 g dithiothreitol, 2 mL 20% w/v sodium dodecyl sulfate, 5 mL 40% glycerol, 0.02 g bromophenol blue) to bring the samples to the same volume and incubating the samples in boiling water for 5 minutes. The samples were then loaded onto a 12% polyacrylamide gel with a 5% polyacrylamide stacking gel and electrophoresed at 125V for 1.5 to 2 hours. The gel was transferred to a Immobilon™-NC nitrocellulose membrane (Millipore, 80 Ashby Road, Bedford, MA 01730-2271) and using a BioRad transfer apparatus in 4°C at 300mA current for 1.5 hours. The membrane was blocked by agitation on an orbital shaker (150 rpm, 22°C) for more than 30 minutes in 38 mL of TBST Buffer (per 1 L: 2.42 g Tris adjust to pH 7.6 with HCl, 8 g NaCl, 1 mL Tween-20) with 5% w/v powered fat-free milk (Nestlé® Carnation® Instant Nonfat Dry Milk, Nestlé USA, Inc., Solon, Ohio 44139). IM primary antibody (antibody raised to C-terminus of IM) was diluted to 1:1000 in 12 mL of TBST Buffer with 5% w/v powered fat-free milk. Blocking solution was decanted and discarded and membrane was incubated in solution containing primary antibody by agitation on a orbital shaker (150 rpm, 4°C) for 12 hours. Membrane was rinsed with 50 to 100 mL TBST Buffer 3 times (for 5 minutes each time) by agitation on an orbital shaker (150 rpm, 22°C). Secondary antibody was diluted 1:3000 in TBST Buffer with 5% w/v powered fat-free milk, and the membrane was incubated in the secondary antibody solution for more than 1 hour on a orbital shaker (150 rpm, 22°C). Membrane was rinsed with 50 to 100 mL TBST Buffer 3 times (for 5 minutes each time) by agitation on an orbital shaker (150 rpm, 22°C) and one time (for 5 minutes) with TBS Buffer (per 1 L: 2.42 g Tris adjust to pH 7.6 with HCl, 8 g NaCl). Secondary antibody was detected by horseradish peroxidase activity using a chemiluminescent reagent and exposing to audoradiograph film. Images were digitized using a UMAX GS-800 Calibrated Densitometer and formatted for presentation using Adobe Photoshop 5.0.

RESULTS

Previously described *immutans* mutants.

The *Arabidopsis* variegated mutant *immutans* was first described by G.P. Rédei in 1963. Subsequent studies of *im* have concluded that *IM* is a nuclear locus that encodes a plastid terminal oxidase (Wu et al., 1999; Aluru et al., 2001; Bennoun et al, 2001; Joet et al, 2002). Null mutations in *IM* cause a variegated phenotype in which green and white sectors are produced. Green sections appear to contain morphologically normal chloroplasts, while white sections contain vacuolated plastids that lack internal lamellar structures (Wu et al., 1999; Aluru et al., 2001). White sections are devoid of pigmentation, and accumulate the carotenoid precursor phytoene (Wetzel et al., 1994). These chlorotic sections can rarely contain heteroplastidic cells that possess very few (if any) normal chloroplasts, and production of the white sections can be promoted by increasing growth light intensity (Wetzel et al., 1994; Wu et al., 1999). Three mutants of *im* were previously characterized by Wu. et al., 1999. *im-1* contains an inversion breakpoint that disrupts the coding region of *im*, and cs3157 contains a G to A transition at the exon 6 / intron 6 splice site that causes the splicing to shift 14 nucleotides downstream to an alternative site. Both of these mutants were generated by x-ray treatment. *spotty* was generated by EMS treatment and contains a G to A transition in exon 4 that converts a tryptophan codon to a stop codon (TAA). *spotty* is the only *im* allele identified that is due to an early stop codon, and it has lower total chlorophyll amounts in green sections but a higher chlorophyll a/b ratio (Figure 3; Aluru et al., 2001). However, the majority of other *im* alleles do not show this phenotype, suggesting either wild type IM is produced and functioning at lower levels than detectable by Western or there exists an enhancing secondary mutation in *spotty* that causes this phenotype. In order to identify a non-null or modifier mutant in *im*, mutants with similar phenotypes to *im* were ordered from the *Arabidposis* Biological Resource Center for characterization. Mutant identification was conducted by growth with wild type and *spotty* as controls (Figure 1). These plants were selfed for at least 2 generations to observe the stable transmission of the variegated phenotype and then crossed to both *spotty* to observe allelism to *im* and to wild type for identifying dominance characteristics of the genes (Figure 2; Table 2). Five of the mutant alleles were sequenced and were

all found to be aberrations in the splicing of *im*. Four alleles obtained show the yellow seed phenotype, but only two have been determined to carry *im* alleles by crosses to *spotty* (see below).

Sequencing PCR fragments from genomic DNA and cDNA reveals mutants cs3157, V189, cs3639, cs3630 and cs3627 are perturbed in *im* mRNA splicing

All other alleles identified and sequenced in this study had mutations in intron *immutans* genomic DNA sequences that effect the splicing of the *im* pre-mRNA and consequently the translation of IM as well. Preliminary data suggested *IM* might be alternatively spliced around exon 6, but this was not confirmed (Figure 4). All mutants characterized herein had no detectable IM protein via Western analysis and had varying degrees of *im* mRNA as detected by Northern analysis with mutants cs3639 and cs3641 having wild type *im* mRNA levels (Figure 5 and Figure 6). Mutants cs3612 and cs3643 have not been analyzed by Western blot. The sequencing of genomic DNA isolated from mutants allelic to *spotty* identified 5 new *im* mutants that were all splicing mutations, and the resulting cDNA mutations showed the effects of the splicing aberrations (Figures 4 and 7). The G to A point mutation at the first nucleotide of intron 5 caused an additional 14 nucleotides of intron 5 to be attached to exon 4 and not spliced out (Figure 7). This larger mRNA product was detected by RT-PCR and electrophoresis on 12% polyacrylamide gels and verified by sequencing. This larger RT-PCR product was the more dominant species with very faint or no detectable wild type-sized transcripts (Figure 4). *im* allele V189 (*A. thaliana* En) was previously described (A. Manuel, Thesis) and was chosen for sequencing as a possible splicing mutant. V189 contains a single G to A point mutation in the last nucleotide of intron 1, and this mutation causes the formation of 2 mRNA species: a larger mRNA that includes intron 1 and a smaller mRNA that is missing the first 14 nucleotides of Exon 2 in addition to the lack of intron 1 (Figures 4 and 7). The RT-PCR product size differences were detected by electrophoresis on 12% polyacrylamide gels and verified by sequencing (Figure 4A). Mutant cs3639 has wild type levels of *im* mRNA, and it was surprising to find this mutant allelic to *im* in its crosses to *spotty*. Genomic sequencing revealed a single G to A point mutation in the last nucleotide of intron 7. This mutation causes exon 8 (48 bp) to be removed from the mRNA and does not affect the reading frame of the mRNA for translation (Figure 7). The resulting IM protein is

presumably missing 16 amino acids and unstable, as it was undetectable by Western analysis (Figure 6). Mutant cs3630 contains a single G to A point mutation in the 15th nucleotide from the end of intron 6 (Figure 7). This mutation causes the last 14 nucleotides of Intron 6 to be included in the mRNA as detected by cDNA sequencing. No IM protein was detected by western analysis (Figure 6). The *im* mutant cs3627 was identified as allelic to *spotty* through crosses and confirmed deficient in IM protein and *im* mRNA by Western and Northern blot analysis, respectively (Figures 5 and 6). The mutant has a single point mutation in the last nucleotide of intron 5, and this point mutation causes many mRNA products to be formed, as detected by RT-PCR (Figure 4). By selective PCR reactions, the mutation causes many different intron and exon combinations between exon 5 and exon 9, as PCR amplification of the cDNA region between exon 1 to 5 resulted in one single wild type sized fragment (Figure 4). Sequencing of the many PCR products from cDNAs revealed a larger PCR product that included intron 5 and a smaller PCR product that was missing exon 6 in addition to a wild type PCR product (Figures 4 and 7). Sequencing of other PCR products was attempted but has been unsuccessful.

The variegation and yellow seed phenotypes of characterized mutants

Mutants cs3628, cs3630, cs3643, cs3660 analyzed had a yellow seed phenotype similar to the transparent testa mutations previously identified in addition to the light sensitive variegation (Figure 1 and 8; Sagasser et al., 2002). The results of crosses showed mutants (see Table 1) that were crossed carry a single recessive nuclear gene allelic to *im*, and the yellow seed allele was not linked to *im* (Figure 9 and Table 2). The yellow seed phenotype was determined to be recessive and have a maternal expression in phenotype in which the nuclear genotype of the parental plant was the sole factor in determining the expression of the yellow seed phenotype (shown as purple arrows in Figure 9). This has been shown for other mutants having a yellow seed phenotype, such as the transparent testa mutants (Sagasser et al., 2002). Mutants that carry this yellow seed allele have a less severe variegation phenotype than F_3 plants that had the yellow seed allele removed by segregation (Figure 8). It was not determined if all mutants examined here that show the yellow seed phenotype carry the same mutant allele that causes yellow seed, and it is quite possible that these

mutants may have different mutations that cause the same yellow seed phenotype, which would agree with their generation by EMS treatment. One yellow seed allele was isolated (i.e. crossed away from *im*) from the cs3630 mutant by a cross to wild type using wild type as the pollen donor (Figure 9). The F_1 generation was grown and was all green and produced all yellow seed indicating that the variegated locus was recessive and the yellow seed locus was dominant, and this suggested the two phenotypes were caused by different loci. The F_2 generation appeared to have an approximate 3 green : 1 variegated ratio of plants suggesting a single nuclear gene was responsible for the variegation phenotype, and this agreed with the cs3630 cross to *spotty* showing allelism to *immutans*. The F_2 generation of cs3630 cross to wild type showed that wild type could complement the yellow seed phenotype as all F_2 seed were brown. The cs3630 cross to *spotty* also showed that *spotty* could complement the yellow seed phenotype in the F_2 generation. The F_3 generation grown from the cs3630 cross to wild type produced the expected approximation of 3 brown seed producing plants: 1 yellow seed producing plant indicating the yellow seed allele is a single recessive allele. F_2 plants that were all green (but produced yellow seed) had seed collected from them individually and kept separate, and the F_3 generation grown from F_2 parent numbers 14, 15 and 16 produced F_3 individuals that all had all yellow F_4 seed. This suggested that the F_2 parent numbers 14, 15 and 16 were homozygous recessive for the yellow seed allele, but did not possess the *im* lesion as all of their offspring were not variegated.

Analysis of mutant chlorophyll and carotenoid concentrations indicated that the *im* alleles *spotty* and cs3633 show significant deviations in chlorophyll and carotenoid content (Figure 3). All other mutants had total chlorophyll content and a chlorophyll a/b ratio similar to wild type. The small standard deviations of the means indicated that the green tissue sampled was not partially variegated, as this would have produced large variations in chlorophyll and carotenoid concentrations on both a leaf area and fresh weight basis. More analysis of this phenomenon is underway (see below).

CONCLUSION AND FUTURE WORK

Little is known about how the mRNA splicing process occurs in the Kingdom Plantae; many models that have enjoyed support in animal systems give conflicting reports of support and dismissal in plants. The newly identified *im* alleles provide data that may allow for a model for plant systems of mRNA splicing to be produced that identifies nucleotide sequences in which differing degrees of affinity exists for splicing complexes. The *im* alleles suggest that null mutations in *im* may arise in the Introns of a nuclear gene by affecting the *im* mRNA splicing process. Of the *im* alleles sequenced, the point mutations caused definitive consequences of either Intron inclusion (e.g. V189), Exon skipping (e.g. cs3639), both Exon skipping and Intron inclusion may occur (e.g. cs3627), or activation of cryptic splice sites (e.g. V189, cs3630 and cs3157). Many alleles are predicted to be null by sequencing or Western analysis, but exhibit different phenotypes or varying severities of variegation. This suggests that the physiological process of variegation involves more factors than just null mutations in *im* (Figure 1), but light shift experiments have shown only mutants carrying the mutations in loci causing yellow seeds resist bleaching of emerging tissues (Figure 8). The suppression of the cs3630 *im* allele by the yellow seed locus warrants further investigation, as this could be an epistatic relationship between these two alleles or a true suppression of all *im* alleles. This will be tested by crossing the isolated yellow seed locus into another *im* allele to observe suppression of the phenotype. The discovery of the maternal effects of the yellow seed allele is confirmed by growing the crosses of cs3630 to wild type to the F_4 generation and allowing self-fertilization for each filial generation (Figure 9). The reciprocal cross was not necessary in this case because of the number of generations analyzed provides sufficient data; the filial generations produced a seed color phenotype based on their genetic composition of yellow seed alleles. In essence, the yellow seed phenotype appears to be maternally inherited and requires a reciprocal cross; however, it displays classical Mendelian ratio and behaves as a single nuclear mutation in the F_3 and F_4 generations.

The phenotypic variation in the *im* alleles grown under the same conditions cannot be explained by differences in IM protein concentration, as indicated by Western analysis. The observation that *spotty* green sectors are lighter than the green sectors of other mutants or of wild

type sections was supported by analysis of the chlorophyll concentrations. The *spotty* mutant has been determined to be carrying only the *im* mutation, and *spotty* is the only allele identified as a missense mutation that directly produces an early stop codon. How this phenomenon is related to the variation in variegation severity is not yet clear, but crosses of *spotty* to wild type will attempt to isolate any secondary mutation that may be causing the change in chlorophyll content and altered chlorophyll a/b ratios. The attempt to identify a non-null allele has not yet been successful, but the identification of the yellow seed phenotype as a suppression of *im* variegation will shine light on the process of variegation and the role *im* may play in this phenomenon.

FIGURES AND TABLES

cs3157

cs3633

cs3639

cs3641

wild type

spotty

cs3620

cs3630

cs3627

cs3628

wild type

spotty

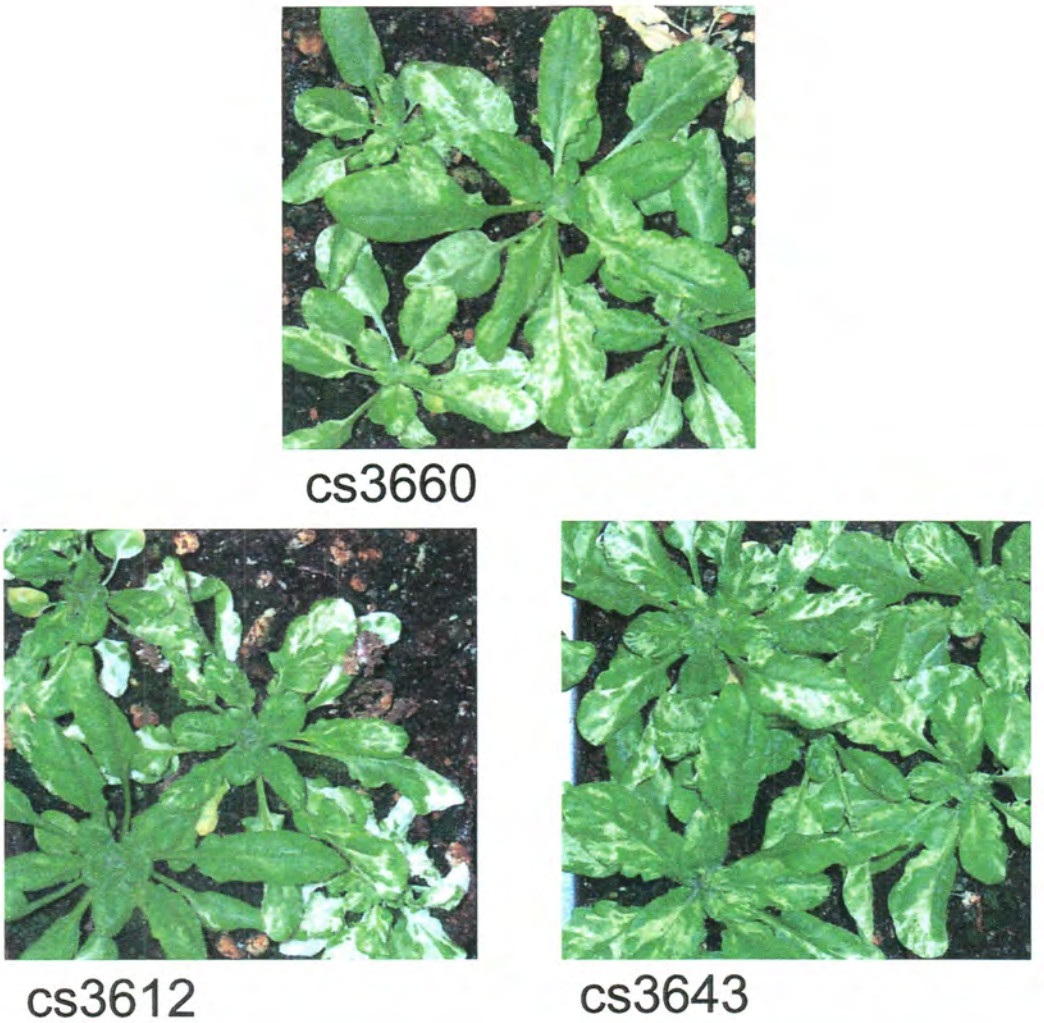

Figure 1. Alleles of *immutans* and wild type *Arabidopsis thaliana* Col. shown. Numbers by the pictures indicate the allele identity. All pictures were taken at the same magnification. Pictures were taken at the same plant ages and all plants grown under the same conditions and light intensities (see plant materials in Materials and Methods section).

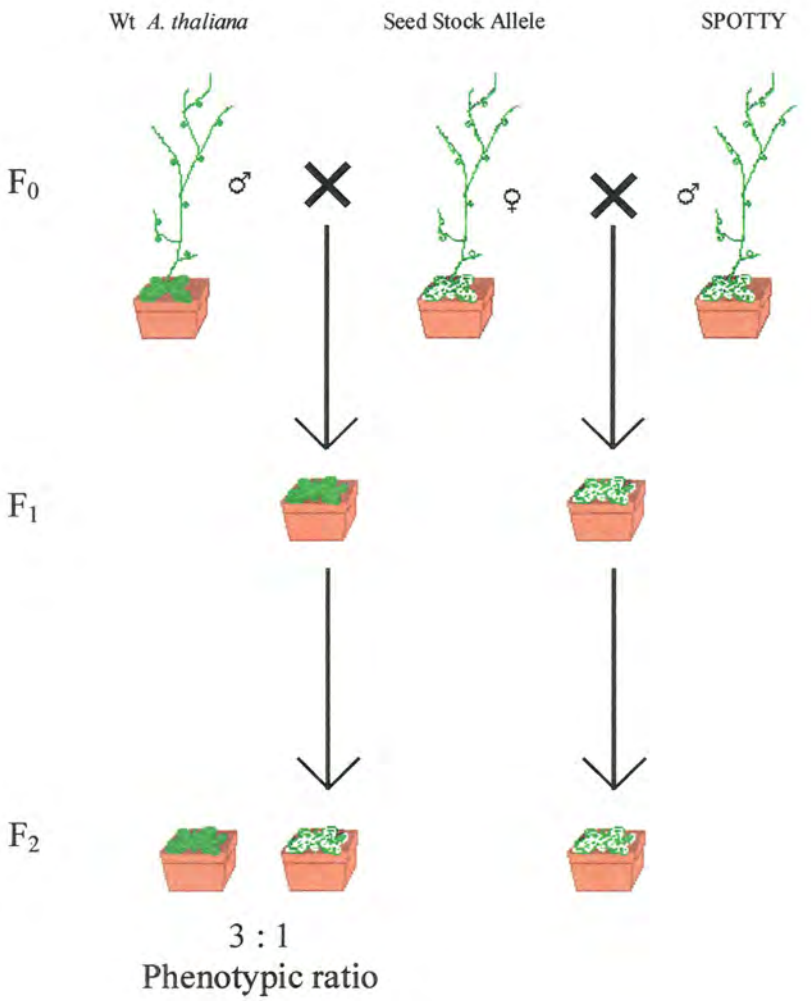

Figure 2. Graphic representation of crosses of *im* alleles to wild type and *spotty*. Both wild type and *spotty* were used as pollen donors (male) and other *im* alleles were used as pollen acceptors (female). Cross shown represents all known *im* alleles as recessive.

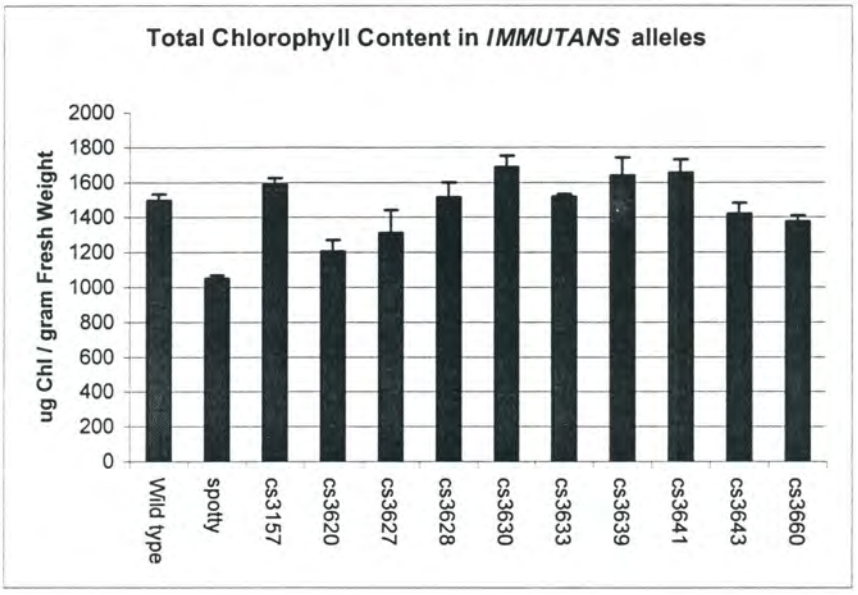

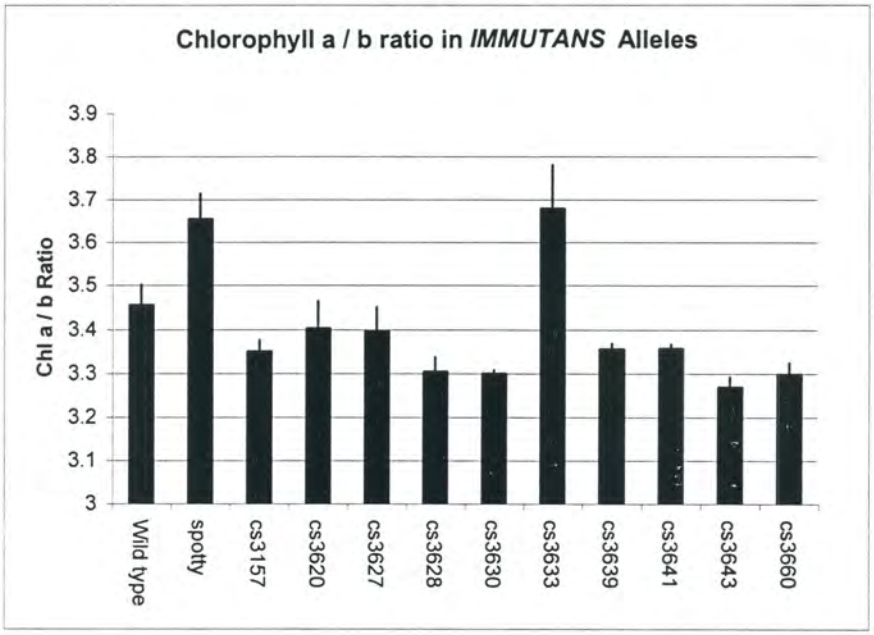

Figure 3. A and B. Pigment analysis of *im* mutants (wild type shown as a control). Pigments were extracted from 0.351 cm^2 leaf discs taken from all green leaf tissues. Data shows similar trends for calculations made on a leaf area basis. For each allele n = 3. Error bars indicate 1 standard deviation. Plants were grown as described in materials and methods section.

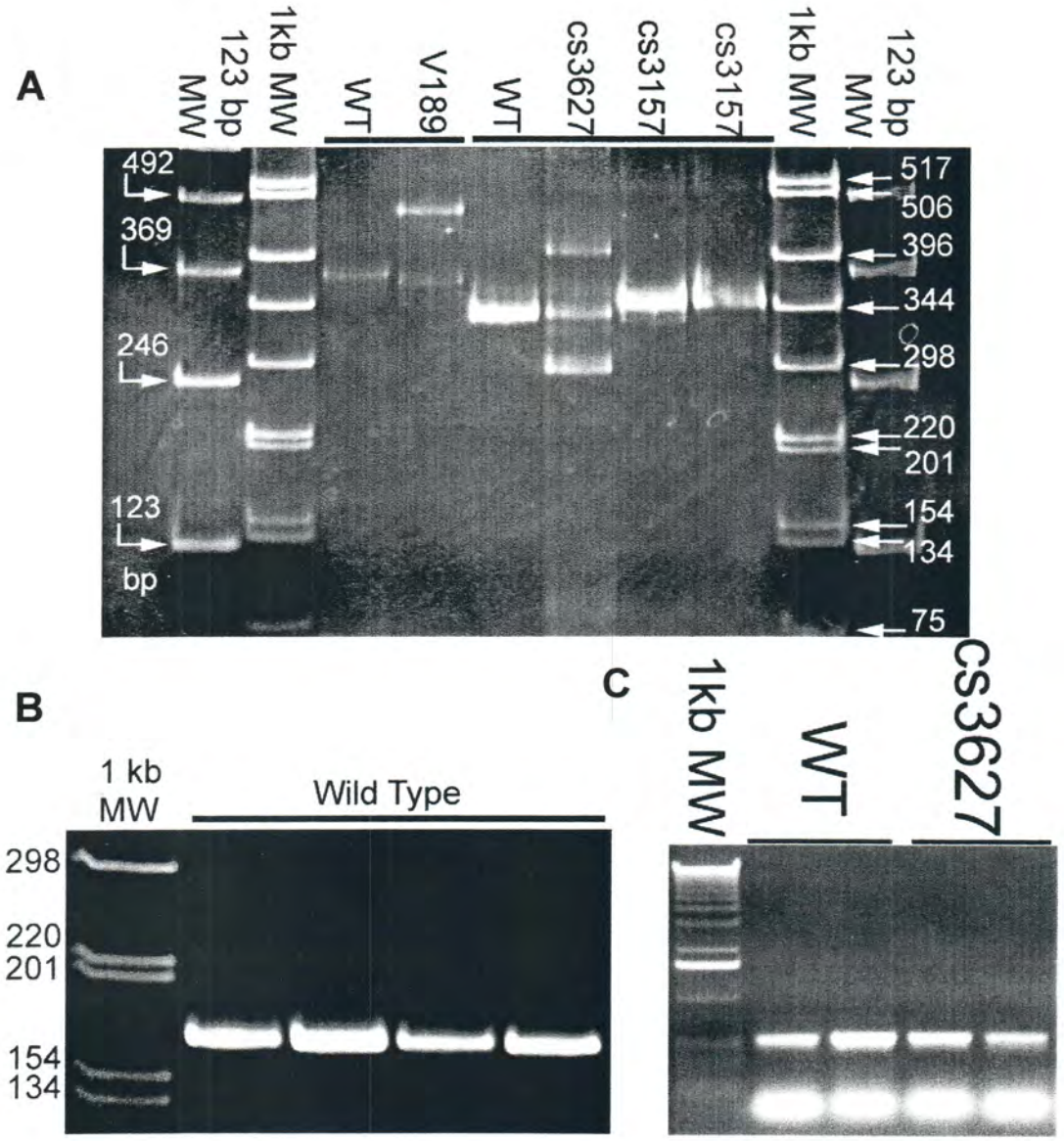

Figure 4. A. RT-PCR products electrophoresed on 12% polyacrylamide gels. B. PCR products amplified from wild type cDNA with primers IM5F and IM7R. C. Wild type (WT) and cs3627 PCR products amplified from cDNA with primers IM100A and DV0574.

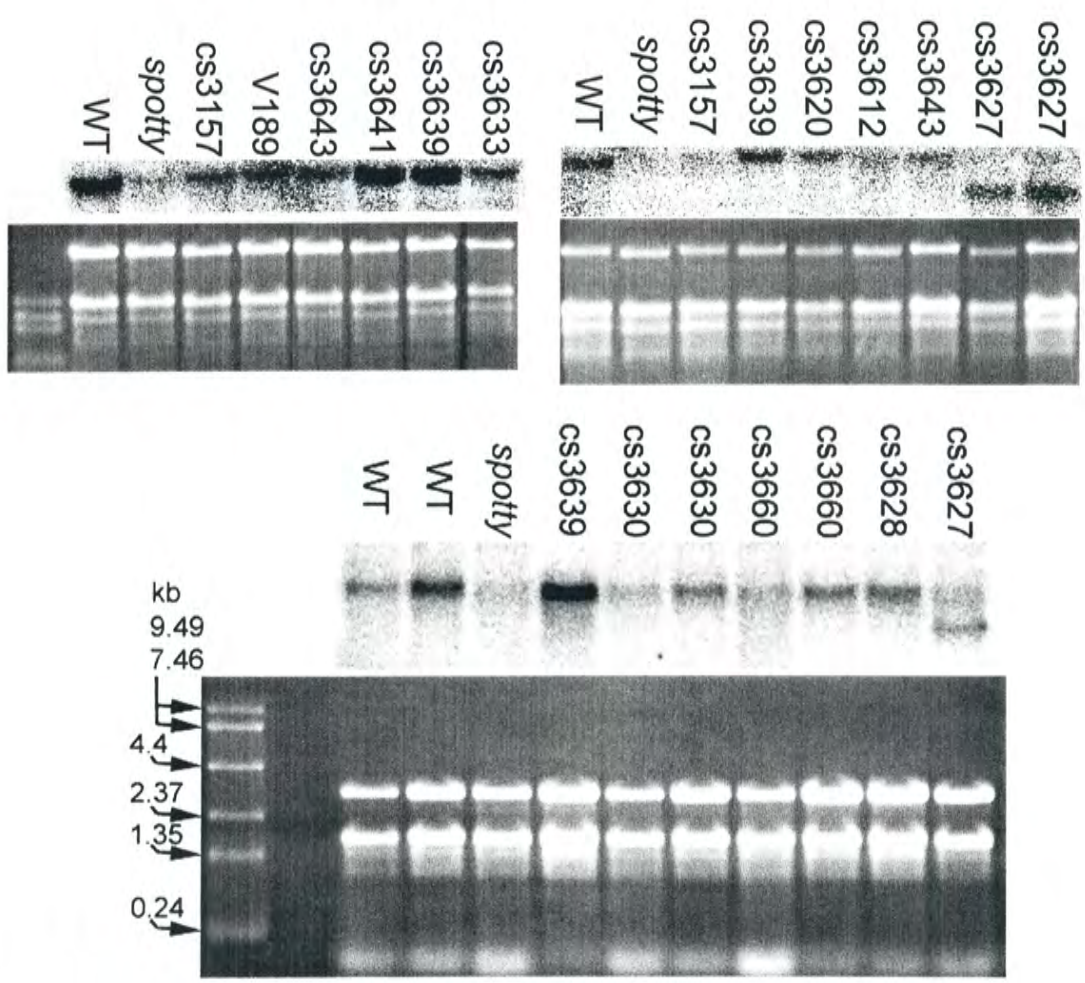

Figure 5. Northern blots of *im* alleles shown above rRNA gel.

Figure 6. Western blots of *im* alleles.

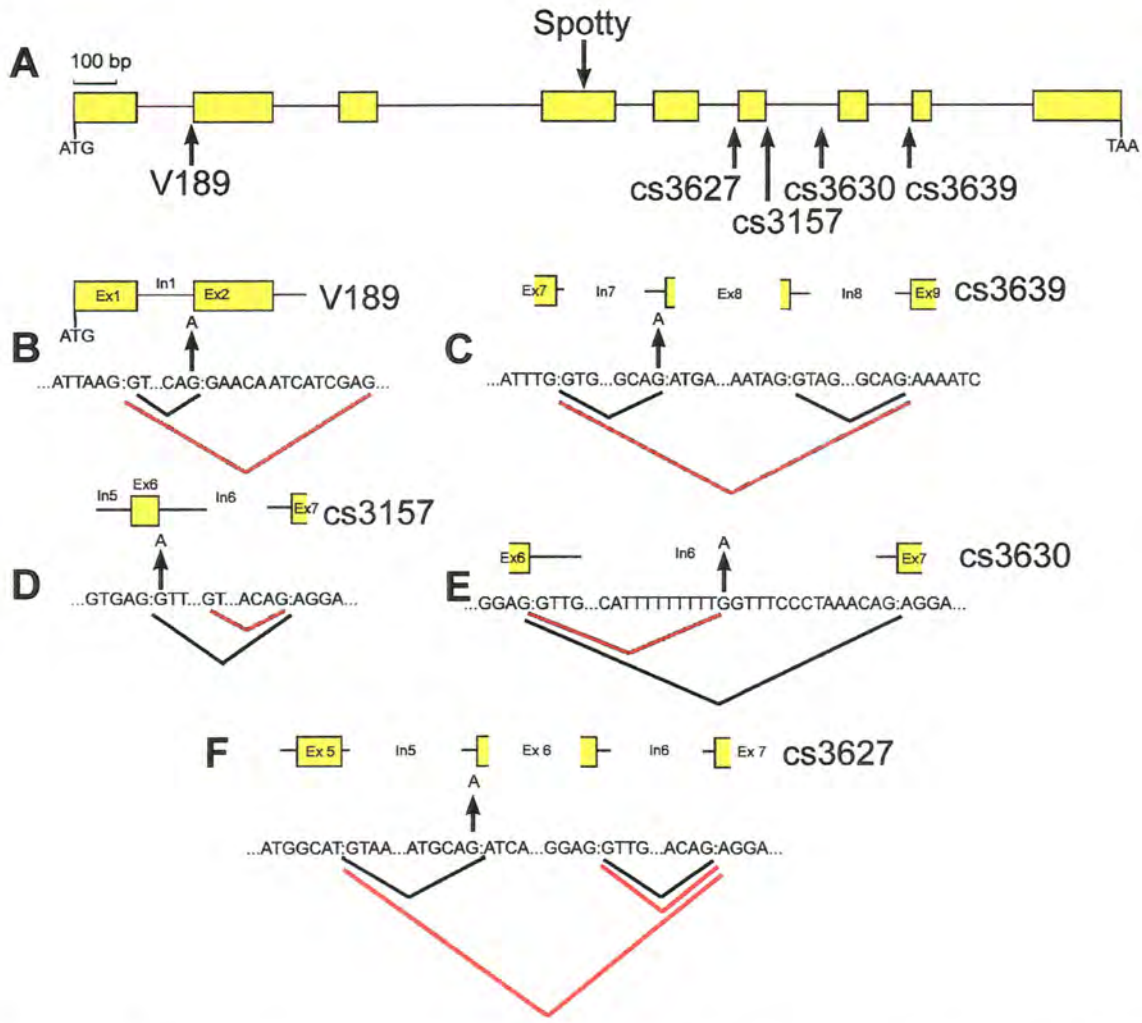

Figure 7. A. Graphic representation of *immutans* genomic DNA. Yellow boxes indicate Exons and lines indicate Introns. Arrows illustrate approximate location of indicated mutation. Scale bar = 100 bp. B, C, D, E, F. DNA sequences of indicated mutants showing the respective mutation. Black bars indicate wild type mRNA splicing patterns, and red bars indicate mutant splicing patterns.

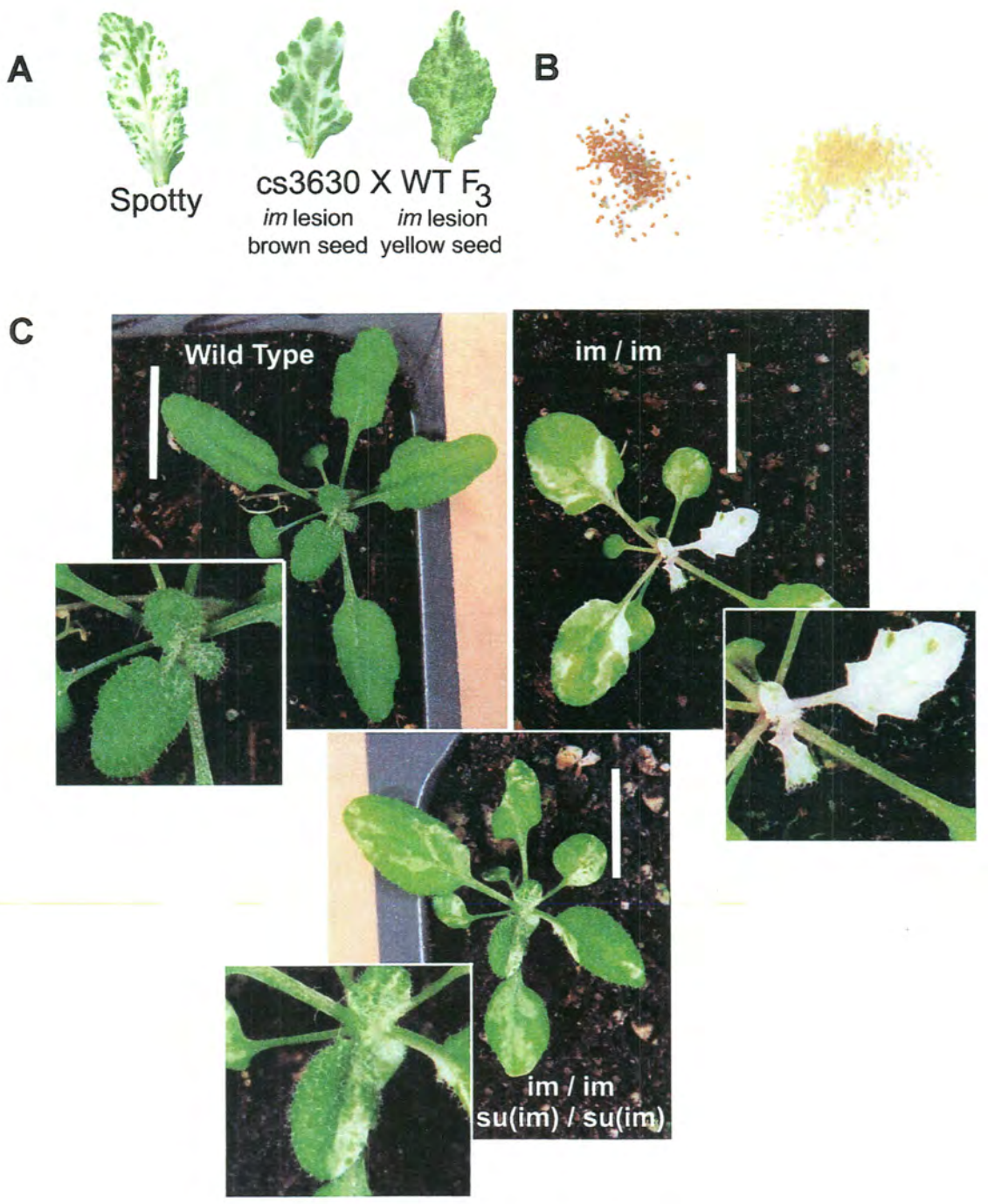

Figure 8. A. The suppression of the *im* allele cs3630 by the yellow seed phenotype. The far right leaf is from an F_3 plant (cs3630 crossed to wild type) that carries both the yellow seed allele and the *im* allele. The center leaf is from an F_3 plant (cs3630 crossed to wild type) that carries the *im* allele cs3630 only. The right leaf is from a *spotty* mutant of *im*. All plants were the same age and grown

under the same conditions. B. The yellow seed phenotype (right) shown contrasting the wild type (left) seed color. C. The Yellow seed allele acting as a suppressor of increased severity of variegation when plants are shifted to normal light conditions (100 μE m^{-1} sec^{-1}; see Materials and Methods section). Inset is close-up view of apical meristem. Top left is wild type, top right is *spotty*, bottom is double mutant *im* allele carrying yellow seed allele. White bar = 1 cm.

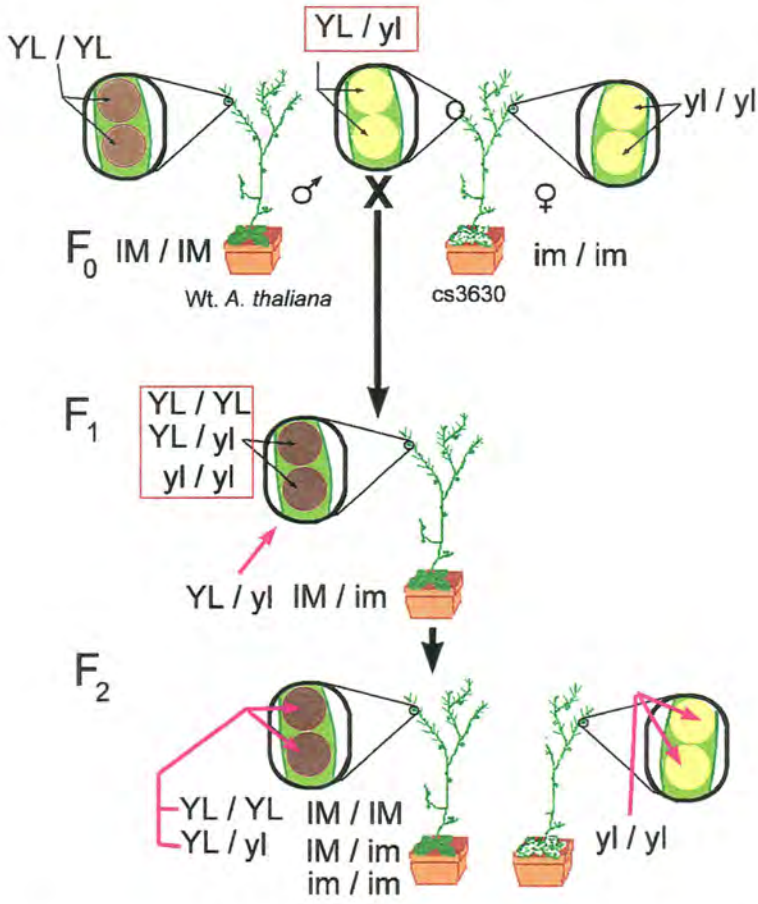

Figure 9. Schematic representation of a maternal effect gene (YL) in a di-hybrid cross. Circled and magnified are siliques that are showing the phenotype of the seed they contain. F_0 parental siliques are shown on the far left and right, but the silique resulting from the cross is shown in the middle. The red boxes indicate the genotypes possible in the seed, and these are of the next generation. Purple arrows show the action of the parental genotype on determining the phenotype of the next generation. This experiment of selfing the progeny of this cross has been carried out to the F_5 generation. Note that in the F_2 generation, 9/16 will be green plants that produce brown seed, 3/16

will be green plants that produce yellow seed, 3/16 will be variegated plants that produce brown seed, and 1/16 will be variegated plants that produce yellow seed. The use of "produce seed" here to denote color actually refers to the phenotype of the next generation, as usually seen in maternal effect genes.

Table 1. Alleles of *immutans*.

im allele[1]	Nature of mutation and method of generation	Location of mutation	*im* mRNA and protein levels[2]	Allelism to *im* determined by
im-1	Inversion; X-ray	Last half of genomic sequence	unknown	Crosses to wild type and other *im* alleles
spotty	G to A point mutation; early stop; EMS	Middle of Exon 4	<5% mRNA and no detectable IM protein	Crosses to wild type and other *im* alleles
V189	G to A point mutation; splicing; EMS	Last nucleotide in Intron 1	<5% mRNA and no detectable IM protein	Crosses to wild type and other *im* alleles
cs3157	G to A point mutation; splicing; X-ray	First nucleotide in Intron 6	<5% mRNA and no detectable IM protein	Crosses to wild type and other *im* alleles
cs3612	unknown; EMS	unknown	<5% mRNA and IM protein unknown	Not determined
cs3620	unknown; EMS	unknown	<5% mRNA and no detectable IM protein	Not determined
cs3627	G to A point mutation splicing; EMS	Last nucleotide in Intron 5	Multiple mRNAs and no detectable IM protein	Crosses to wild type and *spotty*
cs3628[3]	Unknown mutation; splicing; EMS	Exact location unknown, cDNA missing Exon 6	<5% mRNA and no detectable IM protein	Crosses to wild type and *spotty*
cs3630[3]	G to A point mutation; splicing; EMS	15th nucleotide from the end of Intron 1	<5% mRNA and no detectable IM protein	Crosses to wild type and *spotty*
cs3633	unknown; EMS	unknown	<5% mRNA and no detectable IM protein	Crosses to wild type and *spotty*
cs3639	G to A point mutation; splicing; EMS	Last nucleotide in Intron 7	Wild type mRNA levels and no detectable IM protein	Crosses to wild type and *spotty*

[1] *im* alleles *im-1*, *spotty* and cs3157 genomic DNA sequences were first identified by Wu et al, 1999.
[2] mRNA levels are estimates from Northern analysis.
[3] Carries yellow seed phenotype.

im allele[1]	Nature of mutation and method of generation	Location of mutation	*im* mRNA and protein levels[2]	Allelism to *im* determined by
cs3641	unknown; EMS	unknown	Wild type mRNA levels and no detectable IM protein	Not determined
cs3643[3]	unknown; EMS	unknown	<5% mRNA and no detectable IM protein	Crosses to wild type and *spotty*
cs3660[3]	G to A point mutation; splicing; EMS	Sequencing indicates mutation identical to cs3630	<5% mRNA and no detectable IM protein	Crosses to wild type and *spotty*

Table 2. Results of *im* allele crosses to wild type and *spotty*.

im allele	F_1 number and phenotype from cross to wild type	F_2 number and phenotype from cross to wild type	F_1 number and phenotype from cross to *spotty*	F_2 number and phenotype from cross to *spotty*
cs3627	21 plants all green	231 plants; 184 green, 47 variegated	6 plants all variegated	21 plants all vareigated
cs3628	10 plants all green	not complete	6 plants all variegated	not complete
cs3630	28 plants all green	294 plants; 241 green, 53 variegated; F_3: 160 plants; 136 brown seed, 24 yellow seed	9 plants all variegated	23 plants all variegated; F_3: 5 brown seed, 1 yellow seed, 17 died
cs3633	not complete	not complete	plants all variegated	not complete
cs3639	not complete	not complete	4 plants all variegated	not complete
cs3643	8 plants all green	not complete	9 plants all variegated	not complete
cs3660	14 plants all green	25 plants; 20 green, 5 variegated	6 plants all variegated	6 plants all variegated

LITERATURE SITED

Aluru, M., Hanhong, B., Dongying, W., and Rodermel, S. (2001). The *Arabidopsis immutans* mutation affects plastid differentiation and the morphogenesis of white and green sectors in variegated plants. Plant Physiol. Sept; 127: 67-77.

Ausubel, F., Brent, R., Kingston, R., Moore, D., Seidman, J., Smith, J., and Struhl, K. (1998). *Current Protocols in Molecular Biology*. Greene Publishing Associates/Wiley Interscience, New York, U. S. A.

Bennoun, P. (2001). Chlororespiration and the process of carotenoid biosynthesis. Biochim Biophys Acta. Aug 17;1506(2):133-42.

Carol, P. and Kuntz, M. (2001). A plastid terminal oxidase comes to light: implications for carotenoid biosynthesis and chlororespiration. Trends in Plant Science Jan; 6(1): 31-36.

Carol, P., Stevenson, D., Bisanz, C., Breitenbach, J., Sandmann, G., Mache, R., Coupland, G., and Kuntz, M. (1999). Mutations in the *Arabidopsis* gene *IMMUTANS* cause a variegated phenotype by inactivating a chloroplast terminal oxidase associated with phytoene desaturation. Plant Cell 11: 57-68.

Joet, T., Genty, B., Josse E-M., Kuntz, M., Cournac, L., Peltier, G. (2002). Involvement of a plastid terminal oxidase in plastoquinone oxidation as evidenced by expression of the arabidopsis thaliana enzyme in tobacco. J. Biol. Chem. [in press].

Josse, E-M., Simkin, A., Joël, G., Labouré, A-M., Kuntz, M., Carol, P. (2000). A plastid terminal oxidase associated with carotenoid desaturation during chromoplast differentiation. Plant Physiol. Aug; 123: 1427-1436.

Moran, R. 1982. Formulae for Determination of Chlorophyllous Pigments Extracted with *N, N*,-Dimethylformamide. Plant Physiol. 69:1376-1381.

Sagasser, M., Lu, G., Hahlbrock, K., and Weisshaar B. 2002. *A. thaliana* TRANSPARENT TESTA 1 is involved in seed coat development and defines the WIP subfamily of plant zinc finger proteins. Genes and Development 16:138-149.

Wetzel, C., Jiang, C-Z., Meehan, L., Voytas, D., and Rodermel, S. (1994). Nuclear-organelle interactions: the *immutans* variegation mutant of *Arabidopsis* is plastid autonomous and impaired in carotenoid biosynthesis. Plant J. 6(2): 161-175.

Wu D., Wright D., Wetzel C., Voytas D., and Rodermel S. (1999). The *IMMUTANS* variegation locus of *Arabidopsis* defines a mitochondrial alternative oxidase homolog that functions during early chloroplast biogenesis. Plant Cell 11: 43-56.

CHAPTER 3

GENERAL INTRODUCTION TO CAROTENOID BIOSYNTHESIS AND TOMATO FRUIT DEVELOPMENT

GENERAL INTRODUCTION

Tomato fruit ripening involves changes in color, flavor, texture and aroma. During fruit ripening, chloroplasts are converted into chromoplasts, and this conversion can proceed from etioplasts without the prior formation of chloroplasts. This process of development from normal chloroplasts is accompanied by chlorophyll degradation and the breakdown of thylakoid membranes (Chueng et al., 1993). While small immature fruits contain undifferentiated proplastids, mature green fruits develop chloroplasts that are identical in structure to green leaf chloroplasts (Chapter 4). All components of photosystem I and photosystem II that are necessary for photosynthetic activity (thylakoid membrane proteins and stromal enzymes) are contained in green fruit chloroplasts, and these proteins are diminished during ripening (Cheung et al., 1993). Chromoplasts are specialized for the storage of carotenoids and have various shapes of structures for carotenoid accumulation. These have been termed crystalline (carrot root and tomato fruit), globular (*Ranunculus* petals), fibrillar, membranous, and tubular (*Capsicum* and squash fruits, and many flower petals) (Frey-Wyssling and Schwegler, 1965; Rosso, 1968; Harris and Spurr, 1969). The shapes are dependent on the type of carotenoid that is accumulated and its concentration, the plant species, and the developmental stage of the cell (Frey-Wyssling and Schwegler, 1965; Rosso, 1968).

Tomato is classified as climacteric due to both an increase in respiration and ethylene production that occurs during the ripening process (Barry et al., 2000). Ethylene synthesis and perception are essential for tomato fruit ripening (Lanahan et al., 1994; Wilkinson et al., 1997; Barry et al., 2000). Inhibition of ethylene synthesis causes the inhibition of tomato fruit ripening (Theologis et al., 1993). The synthesis of ethylene is controlled at two steps: the formation of 1-aminocyclopropane-1-carboxylic acid (ACC) from *S*-adenosyl-L-Met and the conversion of ACC to ethylene (Barry et al, 2000). The enzyme, 1-aminocyclopropane-1-carboxylic acid synthase (ACS)

catalyzes the first step and ACC oxidase (ACO) catalyzes the second step. There are two types of ethylene regulation in higher plants (Barry et al, 2000). System 1 operates during vegetative growth and is responsible for producing the basal levels of ethylene in all tissues including non-ripening fruit. System 2 is functional during the ripening of climacteric fruit and during petal senescence. Two pathways regulate ripening-associated genes: an ethylene independent, but developmentally regulated pathway and an ethylene-dependent pathway. The ethylene independent pathway regulates the transcriptional activation of polygalacturonase (PG), ACO and phytoene desaturase (PDS), while the ethylene dependent pathway is responsible for the translatability of *PG*. (Theologis et al., 1993).

Carotenoids are C_{40} terpenoid compounds that are yellow, orange, and red pigments that exist high levels in the chloroplasts and chromoplasts (McGarvey and Croteau, 1995; Cunningham and Gantt, 1998). In chloroplasts, carotenoids have essential functions in photosynthesis and photoprotection. In some flowers and fruits, which have chromoplasts, carotenoids serve as attractants for pollinators as agents for seed dispersal (Bartley and Scolnik, 1995). Nuclear genes encode all the enzymes that control plant carotenoid biosynthesis, and the protein products are imported into plastids (Cunningham and Gantt, 1998). Transcriptional regulation is the major regulatory mechanism of carotenoid biosynthesis in flowers and fruits (Giuliano et al., 1993; Pecker et al., 1996; Ronen et al., 1999; Mann et al., 2000). Both the tomato and tobacco plant genomes contain two phytoene synthase (*PSY*) genes (Fraser et al., 1999; Busch et al., 2002). *PSY1* is up-regulated during fruit ripening, reaching a peak at the breaker (BR) stage, while *PSY2* transcripts are more abundant in mature leaves, and PSY2 is not active in tomato fruit carotenoid biosynthesis (Bartley and Scolnik, 1993; Giuliano et al., 1993; Fraser et al., 1999). Carotenoid synthesis begins in the tomato fruit when two molecules of geranylgeranyl diphosphate are condensed into phytoene, the first colorless carotenoid, by phytoene synthase 1 (PSY1) (Fraser et al., 1999). Phytoene is synthesized into the red pigment, *trans*-lycopene, by four consecutive desaturation reactions and an isomeration reaction forming carbon-carbon double bonds. Two enzymes in plants catalyze the desaturation reactions: two membrane-associated enzymes, phytoene desaturase (PDS) and ζ-

carotene desaturase (ZDS) (Beyer et al., 1989). Phytofluene and ζ -carotene are the first two products from the desaturation reaction by PDS. ZDS catalyzes the last two steps of desaturation to produce neurosporene and *cis*-lycopene. The isomeration reaction transforming *cis*-lycopene into *trans*-lycopene is catalyzed by the recently identified lycopene isomerase (CRTISO) (Park et al., 2002, Isaacson et al., 2002). *Trans*-lycopene is cyclized to synthesize either α- or β-carotene by lycopene ε-cyclase (LCYE), lycopene β-cyclase (LCYB) and BETA (Ronen et al., 2000). The mRNA levels of *LCYE*, *LCYB* and *BETA* decrease at the breaker stage to a non-detectable level at the red-ripe stage (Ronen et al., 1999 and 2000). During fruit ripening, the red pigment lycopene accumulates due to the up-regulation of the mRNA encoding lycopene-producing enzymes (*PSY1*, *PDS*, *ZDS, CRTISO*) and the down-regulation of the mRNA encoding lycopene cyclases (*LCYE*, *LCYB* and *BETA*) (Pecker et al., 1992; Corona et al., 1996; Pecker et al., 1996; Ronen et al., 2000, Park et al., 2002; Isaacson et al., 2002).

We are interested in the role of the tomato *ghost* (*gh*) gene in the regulation of carotenogenesis during chromoplast development. The *gh* mutant arose as a spontaneous recessive mutation in a commercial population (Rick et al., 1959), and *gh* is the result of a single nucleotide insertion that causes a translational frame shift creating an early stop codon (Josse et al., 2000, Rodermel, 2002). Tomato *gh* mutant leaves are white or variegated, and the fruits are usually white before reaching the ripe stage and turn orange with normal softening and aroma. The colorless carotenoid phytoene accumulates in the white leaves and fruits of *gh* plants (Mackinney et al., 1956). The carotenoid composition of *gh* green tissues is similar to that in the wild type, and green *gh* tissues also have normal chloroplasts. In contrast, the white tissues of *gh* leaves or fruits have plastids that lack organized membrane structures (Chapter 4) (Scolnik et al., 1987). Under normal illumination conditions *gh* fruits are white in their immature stage, proceed through a yellow intermediate stage equivocal to the turning stage in wild type fruits, and turn orange as development proceeds to ripening (Scolnik et al., 1987). However, when *gh* fruits are grown under low-light conditions, fruits are almost entirely green or variegated, with the green streaks or patches containing chlorophyll that later turn reddish (Rick et al., 1956).

The *Arabidopsis thaliana* mutant *immutans* (*im*) exhibits a variegated phenotype similar to *gh*. Tomato *gh* and the *A. thaliana immutans* (*im*) phenotypes arise from mutations in orthologous genes. Both the *im* and *gh* mutants show a retarded growth rate compared to wild type and accumulate the carotenoid precursor phytoene in chlorotic tissues (Scolnik et al., 1987; Wu et al., 1999; Aluru et al, 2001). *GH* (*IM*) encodes a plastid protein that acts as a terminal oxidase in the chloroplast alternative pathway of electron transport. There are two electron transport pathways that transfer electrons from plastoquinol in chloroplasts. The first pathway is the cytochrome pathway, and it is inhibited by cyanide and uses cytochrome b_6f oxidase as a plastoquinol oxidase. The second pathway is the alternative pathway, and it is inhibited by n-propyl galate (PG) and uses GH (IM) as a terminal oxidase. GH prevents plastoquinone from over-reduction by removing electrons and transferring then to O_2 (Wu et al., 1999; Carol et al., 1999; Carol and Kuntz, 2000; Cournac et al., 2000; Bennoun 2001; Joet et al., 2002). The physiological function of this alternative pathway is unclear, but stressors such as high light significantly increase both steady-state *im* mRNA levels and IM protein levels in *Arabidopsis* (Chapter 5).

In this study, we apply the *gh* mutant as a tool to examine the mechanisms of carotenoid biosynthetic regulation and tomato fruit ripening. The *gh* mutant is perturbed in carotenogenesis only, and both the ethylene biosynthesis gene transcription and the ethylene-controlled fruit ripening processes seem to be unaffected by a lack of GH (Chapter 4). Furthermore, *gh* mRNA accumulates in mutant fruit tissues during ripening suggesting that GH does not regulate its own transcription. As *gh* is inhibited at the PDS step of carotenoid biosynthesis, we were interested in the regulatory control of carotenogenesis by PDS and the possible involvement of GH in this process. We considered the transcriptional regulation model in which β-carotene production serves as a negative feedback regulator of PSY1 transcription (Römer et al., 2000). In the aforementioned study, the constitutive expression of the bacterial PDS (*crtI*) from *Erwina uredovora* (a phytoene desaturase that directly produces lycopene) in tomato produces an increase in the endogenous PDS and ZDS mRNA levels and a decrease of PSY1 mRNA level. Additionally, this expression of *crtI* in tomato causes a dramatic increase in β-carotene concentration but not in total carotenoid levels of the transgenic ripe

fruit. The researchers proposed the increased β-carotene is synthesized at the expense of lycopene levels. Based on this model, we expected the *gh* mutant to show a reciprocal effect in β-carotene production and the mRNA levels of PSY1, PDS and ZDS. We also measured the mRNA levels of the recently identified lycopene isomerase (CRTISO). We compared the carotenoid composition (with HPLC), steady state carotenogenic mRNA levels (with RT-PCR), the ultrastructure of plastids (with TEM) and cellular sizes (with LM) between wild type and *gh* mutant fruits. We found *gh* fruits accumulated low levels of carotenoids and were perturbed in carotenogenesis only, as ethylene biosynthesis and carotenoid sequestering transcription was unaffected in *gh*. The *gh* mutant fruit provides an excellent system to understand the regulation of carotenoid biosynthesis and the chloroplast-chromoplast conversion during fruit ripening.

The following manuscript in Chapter 4 was written to convey the results of analyzing the *gh* mutant in submission to a peer-reviewed journal for publication. I contributed to this manuscript the RT-PCR results, *gh* anatomical photographs and the first draft of the manuscript.

LITERATURE CITED

Bartley, G. and Scolnik, P. (1995). Plant carotenoids: pigments for photoprotection, visual attraction, and human health. Plant Cell 7: 1027-1038.

Bartley G. and Scolnik, P. (1993). cDNA cloning, expression during development, and genome mapping of PSY2, a second tomato gene encoding phytoene synthase. J. Biol. Chem. Dec 5;268(34): 25718-21.

Barry, C. S., Llop-Tous, M. I., and Grierson, D. (2000). The regulation of 1-aminocyclopropane-1-carboxylic acid synthase gene expression during the transition from system-1 to system-2 ethylene synthesis in tomato. Plant Physiol. July; 123: 979-986.

Beyer P, Mayer M, and Kleinig H. (1989). Molecular oxygen and the state of geometric isomerism of intermediates are essential in the carotene desaturation and cyclization reactions in daffodil chromoplasts. Eur. J. Biochem. Sep 1;184(1):141-50.

Busch, M., Seuter, R., Rüdiger, H. (2002). Functional analysis of the early steps of carotenoid biosynthesis in tobacco. Plant Physiol. 128:439-453.

Carol, P., Stevenson, D., Bisanz, C., Breitenbach, J., Sandmann, G., Mache, R., Coupland, G., and Kuntz, M. (1999). Mutations in the *Arabidopsis* gene *IMMUTANS* cause a variegated phenotype by inactivating a chloroplast terminal oxidase associated with phytoene desaturation. Plant Cell 11: 57-68.

Cheung, A., McNellis, T., and Piekos, B. (1993). Maintenance of Chloroplast Components during Chromoplast Differentiation in the Tomato Mutant *Green Flesh*. Plant Physiol. 101: 1223-1229.

Cournac, L., Josse, E., Joet, T., Rumeau, D., Redding, K., Kuntz, M., Peltier, G. (2000). Flexibility in photosynthetic electron transport: a newly identified chloroplast oxidase involved in chlororespiration. Philos. Trans. R. Soc. Lond. B. Biol. Sci. Oct 29;355(1402):1447-54.

Cunningham, Jr., F. and Gantt, E. (1998). Genes and enzymes of carotenoid biosynthesis in plants. Annu. Rev. Plant Physiol. Plant. Mol. Biol. 49: 557-583.

Fraser, P., Kiano, J., Truesdale, M., Wolfgang, S., and Bramley, P. (1999). Phytoene synthase 2 enzyme activity in tomato does not contribute to carotenoid synthesis in ripening fruit. Plant Mol. Biol. 40: 687-698.

Frey-Wyssling A, Schwegler F. (1965). Ultrastructure of the chromoplasts in the carrot root. J. Ultrastruct. Res. Dec;13(5):543-59.

Giuliano, G., Bartley, G., and Scolnik, P. (1993). Regulation of carotenoid biosynthesis during tomato fruit development. Plant Cell 5(4): 379-387.

Harris, W., and Spurr, A. 1969. Chromoplasts of tomato fruits. I and II. Am. J. Bot. 56: 369-389.

Isaacson, T., Ronen, G., Zamir, D., and Hirshberg, J. (2002). Clonong of *tangerine* from Tomato Reveals a Carotenoid Isomerase Essential for Production of β-Carotene and Xanthophylls in Plants. Plant Cell 14: 333-342.

Joet, T., Genty, B., Josse E-M., Kuntz, M., Cournac, L., and Peltier, G. (2002). Involvement of a plastid terminal oxidase in plastoquinone oxidation as evidenced by expression of the arabidopsis thaliana enzyme in tobacco. J. Biol. Chem. [in press].

Josse, E-M., Simkin, A., Joël, G., Labouré, A-M., Kuntz, M., and Carol, P. (2000). A plastid terminal oxidase associated with carotenoid desaturation during chromoplast differentiation. Plant Physiol. Aug; 123: 1427-1436.

Lanahan, M., Yen, H., Giovannoni, J., and Klee, H. (1994). The never ripe mutation blocks ethylene perception in tomato. Plant Cell Apr;6(4):521-30.

Mann, V., Harker, M., Pecker, I., and Hirschberg, J. (2000). Metabolic engineering of astaxanthin production in tobacco flowers. Nat. Biotechnol. Aug;18(8): 888-92.

McGarvey, D., and Croteau, R. (1995). Terpenoid metabolism. Plant Cell 7(7): 1015-1026.

Park, H., Kreunen, S., Cuttriss, A., DellaPenna, D., and Pogson, B. (2002). Identification of the Carotenoid Isomerase Provides Insight into Carotenoid Biosynthesis, Prolamellar Body Formation, and Photomorphogenesis. Plant Cell 14: 321-332.

Pecker, I., Gabbay, R., Cunningham, Jr, F., and Hirschberg, J. (1996). Cloning and characterization of the cDNA for lycopene beta-cyclase from tomato reveals decrease in its expression during fruit ripening. Plant Mol. Biol. Feb; 30(4): 807-19.

Pecker, I., Chamovitz, D., Linden, H., Sandmann, G., and Hirschberg, J. (1992). A single polypeptide catalyzing the conversion of phytoene to ζ-carotene is transcriptionally regulated during fruit ripening. Proc. Natl. Acad. Sci. U. S. A. June; 89: 4962-4966

Rick, C., Thompson, A., and Brauer, O. (1959). Genetics and development of an unstable chlorophyll deficiency in *Lycospersicon esculetum*. Am. J. Bot. 46(1): 1-11.

Ronen, G., Carmel-Goren, L., Zamir, D., and Hirschberg, J. (2000). An alternative pathway to β-carotene formation in plant chromoplasts discovered by map based cloning of *Beta* and *old-gold* color mutations in tomato. Proc. Natl. Acad. Sci. U. S. A. 97(20): 11102-11107.

Rodermel, S. (2002) Arabidopsis Variegation Mutants, The Arabidopsis Book, eds. C.R. Somerville and E.M. Meyerowitz, American Society of Plant Biologists, Rockville, MD, doi/10.1199/tab.0079, http://www.aspb.org/publications/arabidopsis/

Römer, S., Fraser, P., Kiano, J., Shipton, C., Misawa, N., Wolfgang, S., and Bramley, P. (2000). Elevation of the provitamin A content of transgenic tomato plants. Nat. Biotech. June; 18: 666-669.

Ronen, G., Cohen, M., Zamir, D., and Hirschberg, J. (1999). Regulation of carotenoid biosynthesis during tomato fruit development: expression of the gene for lycopene epsilon-cyclase is down regulated during ripening and is elevated in the mutant *Delta*. Plant J. 17(4): 341-351.

Rosso, S. (1968). The ultrastructure of chromoplast development in red tomato. J. Ultrastructure Res. 25: 307-322.

Scolnik, P., Hinton, P., Greenblatt, I., Giuliano, G., Delanoy, M., Spector, D., and Pollock, D. (1987). Somatic instability of carotenoid biosynthesis in the tomato *ghost* mutant and its effect on plastid development. Planta 171: 11-18.

Theologis, A., Oeller, P., Wong, L., Rottmann, W., and Gantz, D. (1993). Use of a tomato mutant constructed with reverse genetics to study fruit ripening, a complex developmental process. Dev Genet. 14(4):282-95.

Wilkinson, J., Lanahan, M., Clark, D., Bleecker, A., Chang, C., Meyerowitz, E., and Klee, H. (1997). A dominant mutant receptor from Arabidopsis confers ethylene insensitivity in heterologous plants. Nat. Biotechnol. May;15(5):444-7.

Wu D., Wright D., Wetzel C., Voytas D., and Rodermel S. (1999). The *IMMUTANS* variegation locus of *Arabidopsis* defines a mitochondrial alternative oxidase homolog that functions during early chloroplast biogenesis. Plant Cell 11: 43-56.

CHAPTER 4

THE TOMATO CHLOROPLAST TERMINAL OXIDASE *GHOST* IS REQUIRED FOR REGULATION OF CAROTENOID BIOSYNTHESIS AND CHROMOPLAST DEVELOPMENT

Jason E. Barr[1], Hanhong Bae[1,2], Steven R. Rodermel[1,3]

A manuscript for submission to Plant Physiology.

ABSTRACT

Tomato fruit synthesize and store large amounts of carotenoids in chromoplasts during fruit ripening. This process is controlled by a developmental program that includes an upregulation of expression of many genes for chromoplast proteins, especially genes involved in carotenogenesis. The *ghost* mutant of tomato exhibits a light-sensitive variegated phenotype in which the percentage of chlorotic tissue roughly reflects the growth illumination conditions. *gh* fruit are white when grown under normal light conditions and ripen through an intermediate yellow phase to a final orange state. *ghost* is the tomato ortholog of the *Arabidopsis immutans* mutant and is deficient in a chloroplast terminal oxidase. Wild type tomato fruit accumulate high levels of the *GH* transcript during ripening, suggesting that the GH protein plays a central role in carotenogenesis. The sizes of pericarp cells, chloroplast and chromoplast morphologies are significantly altered in the mutant, suggesting that GH is required for normal plastid differentiation and cell morphogenesis. These requirements might be mediated by plastid-to-nucleus signals. The patterns of transcript accumulation of ethylene-dependent and independent genes are similar during *gh* and wild type fruit ripening, with the exception that there is a global repression of carotenoid gene expression after the turning stage (yellow fruit) in the mutant pericarp tissue. The hypothesis that β-carotene provides a negative feedback control of phytoene

[1] Department of Botany, Iowa State University, Ames, IA 50011.
[2] Current address: USDA-ARS-Plant Sciences Institute, Bldg 001, Rm 342, 10300 Baltimore Ave., Beltsville, MD 20705
[3] Corresponding author email: rodermel@iastate.edu, phone (515) 294-8890

synthase 1 (*PSY1*) transcription is not supported by data obtained from the *gh* mutant, and another possible model of the transcriptional regulation of carotenogenesis is discussed.

INTRODUCTION

All the steps of higher plant carotenoid biosynthesis occur in plastids by imported nuclear gene products (Bartley and Scolnik, 1995; Cunningham and Gantt, 1998). In chloroplasts carotenoids serve as accessory pigments in photosynthesis; as structural components of pigment-protein complexes; and as photoprotective agents, where they protect the contents of the plastid from photooxidation by quenching excited triplet state chlorophyll and singlet oxygen (Demmig-Adams et al., 1996).

The first dedicated step of carotenogenesis is the conversion of geranylgeranyl diphosphate (GGDP) into phytoene, a noncolored C_{40} intermediate, by phytoene synthase, a soluble stromal enzyme (Figure 1). Colored carotenoids are derived from phytoene by a series of desaturation and cyclization reactions carried out by membrane-bound enzymes that are thought to be subunits of multimeric complexes (Bonk et al., 1997; Cunningham and Gantt, 1998). These enzymes are poorly characterized because they are membrane-bound and labile, and hence difficult to purify to homogeneity. Although considerable progress has been made in recent years in isolating higher plant genes for carotenoid biosynthetic enzymes and in studying the expression patterns of these genes (reviews, Cunningham and Gantt, 1998; Giuliano et al., 1993; Corona et al., 1996; Pecker et al., 1996; von Lintig et al., 1997; Ronen et al., 1999; Mann et al., 2000; Rodermel, 2001; Park et al., 2002, Isaacson et al., 2002), little is known about the regulation of the carotenoid biosynthetic pathway.

Genetic approaches are a powerful means of analyzing the factors that control metabolic pathways. Although a large number of carotenoid-deficient mutants have been isolated, the lesions in very few of these have been defined at the molecular level (reviewed in Rodermel, 2002). One reason for this is the lethality of albinos. Another is that in most species it is difficult to clone genes for which only a mutant phenotype is known. We became interested in the control of carotenoid biosynthesis as a

consequence of our studies on the *immutans* (*im*) variegation mutant of *Arabidopsis thaliana* (Wetzel et al., 1994. Meehan et al., 1996; Wu et al., 2000; Aluru et al., 2001; Rodermel 2002). *immutans* has green and white leaf sectors due to the action of a nuclear recessive gene. Whereas cells in the green sectors contain chloroplasts, cells in the white sectors are heteroplastidic and contain vacuolated plastids that lack internal lamellar structures, as well as rare, normal-appearing chloroplasts (Wetzel et al., 1994). Sectoring in *im* is sensitive to growth illumination and temperature, with elevated light or temperature resulting in enhanced white sector formation. The white *immutans* sectors accumulate phytoene, indicating that the mutant is defective in the phytoene desaturase (PDS) step of carotenogenesis. *immutans* plants are fully viable.

We and others have recently cloned *IM* and found that it codes for a chloroplast membrane protein that bears homology to the mitochondrial alternative oxidase (AOX) (Wu et al., 1999; Carol et al., 1999). AOX functions in the inner membrane of mitochondria as an alternate terminal oxidase to cytochrome c oxidase, transferring electrons from ubiquinol to molecular oxygen (Vanlerberghe and McIntosh, 1994). IM has quinol oxidase activity *in vitro* (Cournac et al., 2001), and thus by analogy to AOX, our working hypothesis is that IM functions as a terminal oxidase in plastid membranes, transferring electrons from the plastoquinone pool to oxygen (Aluru et al., 2001). According to this scenario, IM functions as a component in a redox chain responsible for carotenoid desaturation: electrons are transferred from phytoene to PQ via PDS, and thence from PQ to oxygen via IM (Wu et al., 1999; Carol et al., 1999). Consistent with the phenotype of *immutans*, we suggested that IM might be essential early in chloroplast biogenesis when there are discontinuities between the synthesis and assembly of components of the photosynthetic apparatus, and plastids have more or less of various photosynthetic components (Wetzel et al, 1994). IM might act during this stage as a "safety valve" (Niyogi, 2000), allowing the detoxification of excess electrons that might occur, for example, if a functional PSII were in place, but not a functional PSI. In the absence of IM and downstream electron sinks in nascent thylakoid membranes, it would thus be anticipated that phytoene would accumulate because of an over-reduced PQ pool and an inability to regenerate

plastoquinone (Wu et al., 1999; Aluru et al., 2001). Under these conditions, carotenoid biosynthesis would cease, and without colored (photoprotective) carotenoids, the contents of the plastid would become photooxidized (white sectors). On the other hand, the PQ pool would not be over-reduced in *immutans* cells whose developing thylakoids contained sufficient downstream electron sinks. Hence, carotenoid accumulation would occur in these plastids, allowing the biogenesis of normal chloroplasts to proceed (green sectors).

We have recently found that *IM* expression is ubiquitous in *Arabidopsis* tissues and during development, and that multiple types of plastids, tissues and organs are affected in the mutant (Aluru et al., 2001). These observations suggest that IM function is not limited to carotenogenesis, but rather, that the protein plays a more general role in plastid metabolism, plant physiology and plant development. Support for this notion comes from experiments in *Chlamydomonas* showing that IM might be the elusive terminal oxidase of chlororespiration (Cournac et al., 2001). We have also found that IM might be an important factor that regulates plant responses to stress (Rizhsky et al., in press; Barr and Rodermel, unpublished). The role of IM as an alternate electron sink is just beginning to be understood.

The *ghost* (*gh*) variegation mutant of tomato arose as a spontaneous recessive mutation in a commercial population (Rick et al., 1959). The phenotype of *gh* is similar to that of *im*, and recent studies have shown that *im* and *gh* define genes in orthologous proteins (Josse et al., 2000; Rodermel 2002). *Arabidopsis* lacks an abundant chromoplast population, and thus the finding that GH and IM are orthologs provides an opportunity to use the ripening of tomato fruit as a model system to understand IM function. During ripening, undifferentiated proplastids in immature fruit develop into chloroplasts in mature green (MG) fruit. The chloroplasts are then converted into carotenoid-accumulating chromoplasts as the fruit progresses through the turning (TU), breaker (BR) and finally red-ripe (RR) stages of development. During the chloroplast-to-chromoplast developmental process, chlorophyll is degraded and thylakoid membranes are dismantled (Harris and

Spurr, 1969; Cheung et al., 1993), and newly-synthesized carotenoids become sequestered within specific lipoprotein structures (Pozueta-Romero et al., 1997; Vishnevetsky et al., 1999). Although the function of carotenoids in chromoplasts is poorly understood, they appear to serve as attractants for pollinators as agents for seed dispersal (Bartley et al., 1995). Tomato is a climacteric fruit, and development from the MG stage requires the synthesis of ethylene (Lanahan et al., 1994; Wilkinson et al., 1997; Barry et al., 2000). Whereas some genes that are expressed differentially during the ripening process depend on ethylene for their expression, others do not and are presumably expressed in response to developmental factors.

In this paper we use fruit ripening in *ghost* as a model to address the function of GH in carotenogenesis and chromoplast development: how is the regulation of carotenogenesis altered in the mutant, and how are plastid and fruit development affected? On the basis of our findings we develop a hypothesis to explain how the carotenoid pathway is regulated when PDS activity is altered. These studies are of more than academic interest. Vitamin A is derived from provitamin A (β-carotene) in the human diet, and thus knowledge about the regulation of carotenogenesis assumes a practical urgency because vitamin A deficiency has been identified by the U.N. as one of the most severe malnutrition problems in the developing world. Our studies should thus facilitate genetic engineering approaches to enhance the provitamin A content of staples that are used in developing countries, such as rice, maize, and cassava. The development of "golden rice" is a significant advance in this direction (Beyer et al., 2002).

MATERIALS AND METHODS

Plant Material

The *gh* mutant arose as a spontaneous recessive mutation in *Lycopersicon esculentum* Mill (Rick et al., 1959). Heterozygous *gh*/+ tomato seeds (provided by the C. M. Rick Tomato Genetics Resource Center, Department of Vegetable Crops, University of California, Davis) were germinated in pots 20 cm high and 20 cm in diameter in the greenhouse. The plants were watered daily and fertilized every

7 days. Seeds were collected from the heterozygotes and germinated in a growth chamber under low light conditions (22°C continuous light, 80 μmol m^{-2} sec^{-1}) to promote the recovery of viable (variegated) *gh/gh* seedlings. Higher light intensities generate lethal, albino plants. After 4-6 weeks, variegated (*gh/gh*) and green (+/+ or +/*gh*) progeny were transferred to the greenhouse and grown to maturity for another several months. Fruit from these plants were used for subsequent analyses. Seeds from the green progeny were collected and lines that did not segregate variegated plants after two generations were classified as wild type (+/+) ("wild type" controls). Whereas most analyses were conducted on plants growing in the greenhouse under ambient illumination conditions (designated "normal light", or NL, conditions), some experiments were performed on plants grown in the greenhouse under thermal screen shade cloth (Aluminet®, Hummert International, St. Louis, MO) (designated "low light", or LL, plants). Wild type fruits from NL-grown plants were harvested at four stages of development: mature green, breaker, turning and red-ripe (attained approximately 6, 7, 8 and 9 weeks after fertilization, respectively). Fruit from NL- and LL-grown *gh* plants were harvested at three stages of development: white, yellow, and orange for the NL samples, and green, yellow, and orange for the LL samples. In some experiments, three and four month-old wild type flowering plants were watered before fertilization with 200 mL of 1.0×10^{-7} M norflurazon (NF) (Sigma, St. Louis, MO). The application was continued daily during the entire fruit developmental period.

Analysis of mRNA Expression

Pericarp tissue was dissected from tomato fruit, immediately frozen in liquid nitrogen and stored at -80°C until use. For RNA isolation, the pericarp samples were ground to a fine power in a mortar and pestle in liquid nitrogen, and total cell RNAs were isolated using the RNeasy Plant Mini Kit (Qiagen Inc., Valencia, CA). The samples were electrophoresed on 3% formaldehyde-1% agarose gels and blotted onto GeneScreen Plus® Hybridization Transfer Membranes (NEN™ Life Science Products, Boston, MA). Probes included a full-length *GHOST* cDNA (Rodermel, 2002), and PCR amplification products for *ACS6* (aminocyclopropane-1-carboxylic acid synthase; gi508608) (Barry et al., 2000) and *PAP* (plastid-associated protein; gi2632089) (Pozueta-Romero et al., 1997). The PCR amplifications

were from tomato genomic DNA using gene-specific primers, and included an initial denaturation of 3 min at 94°C, followed by 30 cycles of 1 min at 94°C, 1 min at 58°C, 1 min at 72°C, and a final 10-min extension at 72°C. The PCR products were electrophoresed in 0.8% agarose gels and purified using the QIAEX II Gel Extraction System (Qiagen Inc., Valencia, CA). The fragments were ^{32}P-labeled by random priming (Ausubel et al., 1998). Hybridization and washing of the membranes were performed as described (Wetzel et al., 1994). All RNA gel blot analyses were repeated with at least two different RNA samples.

In addition to RNA gel blots, mRNA expression was studied using RT-PCR (procedures described in Wetzel and Rodermel, 1998). In brief, total cell RNAs were isolated as described above and RNA quality was assessed on stained 3% formaldehyde-1% agarose gels. To remove genomic DNA contamination, the RNAs were treated with RNase-free DNase (Life Technologies, Rockville, MD), and RNA quality was re-checked by electrophoresis on 3% formaldehyde-1% agarose gels. The Superscript™ first-strand cDNA synthesis for RT-PCR kit (Life Technologies, Rockville, MD) was used to generate first-strand cDNAs and the cDNAs were used as templates for PCR amplification. This kit includes a control RNA and primers for the RT assay. The PCR primers included: *PSY1* (X60441; upstream 5'-GAAGGAATGCGTATGG-3', downstream 5'-GGTCTCGGTTTCGTCGTA-3'); *PDS* (X59948; upstream 5'-TTGTGTTTGCCGCTCCAGTGGATAT-3', downstream 5'-GCGCCTTCCATTGAAGCCAAGTAT-3'); *ZDS* (AF195507; upstream 5'-GCGTTCGAGGCAATTGAAGC-3', downstream 5'-CCATGCTATCGATGTAGTCC-3'); *CRTISO* (AF416727; upstream 5'-GATCGCCAAATCCTTAGCAA-3', downstream 5'-GCCCTGGGAAGAGTGTTTTT-3'); *LCYB* (X86452; upstream 5'-GGCTTCTCTAGATCTCTTGTTCAG-3', downstream 5'-GTTCAGGTAGAAACAATCGAGACG-3'); *BETA* (AF254793, upstream 5'-CATTTTCTACGAGCTCCACCTCCCTCC-3', downstream 5'-TTTGGCCACATCTAGAGTGGTGAAGGG-3'); *CHYB* (Y14809; upstream 5'-AAGGACCTTTTGAGCTGAACGAC-3', downstream 5'-ACTTCTCTGAGTGATGAAGCGAATG-3').

Linearity of PCR amplification was determined for each gene by using a 0.125, 0.25, 0.5, 1.0, 2.0 µL dilution series of the wild-type cDNAs from mature green, turning, and red ripe fruits and 15, 18, 20, 22 or 25 PCR cycles per dilution. 22 cycles fell within the linear range for all genes except PSY and was thus used in all analyses except PSY, for which 15 cycles were selected. PCR of *PDS*, *ZDS*, *CRTISO*, *LCYB*, *LCYE*, *BETA* and *CHYB* included an initial denaturation of 3 min at 94°C, followed by 22 cycles of 1 min at 94°C, 1 min at 58°C, 1 min at 72°C, and a final 10-min extension at 72°C. PCR of *PSY1* was carried out as described above but with 15 PCR cycles. All genes were amplified in individual reactions that included an equal amount of an internal control consisting of the neomycin phosphotransferase gene (*NPTII*) and *NPTII*-specific primers. NPTII was isolated by PCR amplification from the pBI121L vector. The PCR products were separated by electrophoresis on 1.5% agarose gels, blotted onto a nitrocellulose membrane, and probed with the corresponding ^{32}P-labeled PCR fragment generated from genomic DNA by procedures described above for the generation of probes for the RNA gel blot analyses. RT-PCR was repeated at least 3 times with different RNA extractions from separate plants.

Microscopy

The transmission electron microscopy (TEM) and light microscopy (LM) were performed as previously described (Wetzel et al., 1994; Aluru et al., 2001). In brief, tomato fruit pericarp samples were collected and fixed with 3% glutaraldehyde (w/v) and 2% paraformaldehyde (w/v) in 0.1 M cacodylate buffer (pH 6.5) for 48 h at 4 °C. Samples were rinsed 3 times (10 min wash) in 0.1 M cacodylate buffer followed by post-fixation in 1% osmium tetroxide in 0.1 M cacodylate buffer (pH 6.5) for 1 hour at room temperature. The samples were then dehydrated in a graded ethanol series, cleared with ultrapure acetone, infiltrated and embedded using Spurr's exoxy resin (Electron Microscopy Sciences, Ft. Washington, PA). Resin blocks were polymerized for 48 hours at 70 °C. Thick and ultrathin sections were made using a Reichert Ultracut S ultramicrotome (Leeds Precision Instruments, Minneapolis, MN). Samples from this step were used for LM, and for TEM, the ultrathin sections were collected onto copper grids and counter-stained with 5% uranyl acetate in 100%

methanol for 20 min followed by Satos' lead stain for 20 min. Images were captured using a Jeol 1200EX scanning and transmission electron microscope (Japan Electron Optic Laboratories, Akishima, Japan)

Extraction and HPLC analysis of carotenoids

A 10 g sample of minced tomato pericarp tissues (pooled from more than one fruit) was combined with 4 g celite, 1 g solid $CaCO_3$ to neutralize organic acids, and 50 mL methanol and tetrahydrofuran (1:1 by vol) containing 0.1 g butylated hydroxytoluene (BHT)/L and ethyl β-apo-8'-carotenoate (Fluka, Milwaukee, WI) as an internal standard. Carotenoids were extracted from the plant tissue by homogenizing for 1 min using a Brinkman (Westbury, NY) homogenizer. The resulting suspension was filtered through No. 1 and 42 Whatman filter papers in a Buchner funnel under vacuum (Lessin et al., 1997). The filter cake was resuspended with 50 mL methanol and tetrahydrofuran (1:1 by vol), homogenized for 1 min, and filtered through the same filter papers. The extraction of the filter cake with methanol and tetrahydrofuran was then repeated. The combined methanol and tetrahydrofuran filtrates were transferred to a separatory funnel. The carotenoids were extracted by adding 50 mL petroleum ether (containing 0.1 g BHT/L) and 50 mL of NaCl solution (100 g/L) followed by careful shaking. The lower aqueous/methanol/THF phase was collected and the upper petroleum ether phase was transferred to a 200-mL volumetric flask. The aqueous/methanol/THF phase was extracted two more times with 50 mL aliquots of petroleum ether. The petroleum ether layers were transferred to the same 200-mL volumetric flask, which was then brought to volume with additional petroleum ether. A 4-mL aliquot was evaporated to dryness under vacuum. The dried lipid extract was reconstituted in 1 mL of methyl-*tert*-butyl ether (MTBE) followed by 1 mL of methanol. The reconstituted extract was filtered through a 0.2 µm nylon syringe filter (Alltech, Deerfield, IL), and a 25-µL aliquot was injected into the HPLC system. The components included a 717 Plus autosampler with temperature control set at 5°C, two 510 solvent-delivery systems, and the 996 photodiode array detector (Waters Corporation, Milford, MA). The system operated with Millennium^{32} Software Version 3.05.01 (Waters Corporation). Carotenoids were separated on a 5-µm C_{30} Carotenoid Column (4.6 x

250 mm; Waters Corporation) eluted by using a linear mobile-phase gradient from 100% methanol (containing 1 g ammonium acetate/L) to 100% MTBE over 55 min. The flow rate was 2.0 mL/min. Solvents were HPLC grade; the methanol, MTBE, and ammonium acetate were purchased from Fisher Scientific (Chicago, IL). Internal standard calibration curves were generated for β-carotene (Fluka), lycopene (Sigma, St. Louis, MO) and lutein (Kemin Foods, Des Moines, IA), which were the only commercially available carotenoid standards relevant to the study. All tomato samples were extracted and analyzed in triplicate.

RESULTS

Morphology of *ghost*

When *ghost* plants are germinated and maintained in the greenhouse, they have pale cotyledons and the first true leaves that emerge are completely chlorotic. However, when the mutants are germinated under low light conditions in a growth chamber, then shifted to the greenhouse 4-6 weeks later (i.e., NL, or normal light-grown plants, see Materials and Methods), the true leaves are white and/or variegated (Figure 2C). Fruit from these plants are initially all-white, but then turn uniformly yellow and finally all-orange (Figure 2B). These observations are in accord with the earliest reports on the mutant (Rick, 1959). However, when *gh* plants are grown under shade cloth in the greenhouse (i.e., LL, or low light-grown plants), the true leaves are nearly all-green, and the emerging fruit are green with dark-green streaks (Figures 2B). These fruit progress to an intermediate yellow stage, then turn orange with streaks of red. The patterns of fruit development in *gh* contrast with the progression of LL- and NL-grown wild type fruit from the mature green, to the breaker, turning, and finally red-ripe stages (Figure 2B).

Anatomy of *gh* fruit

ghost fruit are smaller than normal at all stages of development (Figures 2A and 2B). This observation prompted us to ask whether the *gh* mutation also influences fruit anatomy. To investigate this question, we performed light microscopy on tissue sections of fruit from WT and *ghost* plants that

were grown under normal light conditions. Figure 3 shows that the morphology of the pericarp tissue of the green and red WT fruit is similar (e.g., cell sizes are roughly the same). In contrast, cells in the white fruit of the mutant are generally smaller than those in the orange fruit. Because the anatomy of *gh* orange fruit resembles that of WT red fruit, the anatomical profiles suggest that GH affects pericarp differentation, especially early in fruit development. The mutation does not appear to affect the anatomy of the epidermis (skin), since development in both WT and *gh* fruit is accompanied by a decrease in the thickness of the epidermis.

One question that arose during the course of our investigations was whether the yellow and orange colors of *ghost* fruit represent pericarp and/or skin phenotypes. Rick (1959) suggested that the yellow color of *ghost* fruit is due to the presence of a non-carotenoid, alkali-soluble pigment in the fruit epidermis, which he did not identify . Scolnik and co-workers (1987) agreed with this conclusion. To further examine this question, we dissected skin and pericarp tissues from *gh* orange and WT red fruit. Figure 2A shows that the skin colors of the two types of fruit are the same (yellow), but that the pericarp colors differ (yellow /orange versus red). We conclude that fruit coloration is a combination of the skin and pericarp colors.

Plastid development is impaired in *ghost* fruits

IMMUTANS affects the differentiation of multiple plastid types in *Arabidopsis*, including chloroplasts, amyloplasts and etioplasts (Aluru et al., 2001). Although previous reports have shown that chloroplast development is affected in *gh* (Scolnik et al., 1987), we wanted to determine whether GHOST influences chromoplast development. Figure 4 shows the results of transmission electron microscopy (TEM) of thin sections of WT and *gh* fruit tissues. Confirming earlier studies (e.g., Rosso, 1968; Harris and Spurr, 1969; Camara et al., 1982), we found mature green fruit of WT plants have typical chloroplasts (Figure 4A), but that as chloroplasts are converted into chromoplasts, the thylakoid membranes degrade and osmiophilic globules and undulating membrane structures accumulate (Figure 4B). Plastids in *gh* white fruit lack organized internal membrane structures and

instead accumulate osmiophilic (perhaps phytoene-accumulating) bodies (Figure 4C). In *gh* orange fruit, the plastids are similar to those in the white fruit (Figure 4D), with the exception that rudimentary lamellar structures are observed. We conclude that chromoplasts in WT red and gh orange fruit have different morphologies, and that GHOST affects chromoplast development.

Expression pattern of genes involved in fruit ripening

Tomato fruit ripening involves changes in gene transcription, and control is mediated through ethylene-independent and ethylene-dependent pathways (Barry et al., 2000). To assess whether these pathways are influenced by GH, we examined the expression of representative genes by RNA gel blot and RT-PCR analysis using four stages of wild type fruit development (MG, BR, TU, and RR) and three *gh* fruit stages (WH, YL, and OR) (Figure 5). For these studies we chose *ACS6* and *PAP* as representative ethylene-dependent response genes. We also wanted to look at *GH* itself; it is not known whether this gene is responsive to ethylene. Finally, we wanted to assess how GH influences the expression of genes involved in carotenogenesis. Of the carotenoid biosynthetic genes examined, none are ethylene-responsive. The expression of all these genes has been examined in WT plants (Fraser et al., 1999; Ronen et al., 1999; Ronen et al., 2000; Cuningham and Gantt, 2001)

Figure 4A reveals that in both WT and *gh* fruits, the abundance of *ACS6* mRNA gradually declines during ripening to an undetectable level at the fully ripe stage. By contrast, *PAP* and GH mRNAs are up-regulated during ripening in both *gh* and WT, although *GH* transcript levels in *gh* are reduced in all *gh* fruits relative to the wild type fruits. The *gh* mRNA has a nonsense codon midway though the gene, and thus it is possible that these decreases are a consequence of nonsense codon mediated mRNA decay (van Hoof, A and PJ Green, 1996). *Lhcb* mRNA was not detected in any fruit developmental stage by northern blot analysis, even in the mature green stage of WT fruit. This result is surprising, but in accord with a previous study (Cheung et al., 1993). By contrast, mRNAs for other photosynthetic genes decrease during ripening (Piechulla et al., 1987).

Figure 4B shows the impact of GH on the expression of genes for carotenoid biosynthesis during *gh* and WT fruit ripening. We used RT-PCR for these analyses since the levels of mRNAs from these genes are too low to be detected by RNA gel blot analysis. Induction of *PSY1* transcription is found in both the WT turning and in *gh* yellow fruits, and this increase continues for wild type red-ripe fruits but decreases in *gh* orange fruits. A similar pattern was observed for *CRTISO*. The transcription of the desaturases, *PDS* and *ZDS*, increased during the ripening of WT fruit, but decreased progressively during the ripening of the *gh* fruit. Transcripts of the lycopene cyclases, *LCYB* and *LCYE,* decreased in both *gh* and wild type, whereas the *BETA* lycopene cyclase exhibited maximal transcript levels in the wild type turning and *gh* yellow fruit. The β-carotene hydroxylase (*CHYB*) increased slightly during both WT and *gh* development, but fell late in development in the *gh* orange fruit.

Overall, the data in Figure 5 reveal that the expression patterns of ethylene-dependent and ethylene-independent genes is generally not influenced by GH, with the notable exception of late in *gh* fruit development (orange stage), when there is a massive decrease in the accumulation of mRNAs from carotenoid genes. mRNA levels of carotenoid biosynthetic genes are also significantly lower in *gh* than in WT fruit at all stages of development, suggesting that superimposed on the orange stage-specific suppression there is a more general repression of carotenogenesis gene transcription in the mutant fruit.

Carotenoid composition of *gh* fruit

To explore the impact of GH on the regulation of carotenoid accumulation, we performed HPLC analysis on pericarp tissue from the terminal stages of fruit development in the WT and *gh* plants, i.e., from the red-ripe and orange fruit stages, respectively. Table 1 reveals that the major carotenoid in wild type fruit is *trans*-lycopene. By contrast, the *gh* orange fruit accumulate phytoene and have a 14-fold decrease in lycopene (Table 1).

DISCUSSION

GH is required for plastid differentiation and tissue morphogenesis

Recent studies in the *immutans* mutant of *Arabidopsis* revealed that IM is expressed ubiquitously in *Arabidopsis* tissues and organs and that it appears to be required for the development of multiple plastid types, including chloroplasts, amyloplasts and etioplasts (Aluru et al., 2001). In addition, IM appears to be required for normal tissue morphogenesis inasmuch as leaf anatomy is radically altered in the mutant. These studies also showed that the green *im* sectors have significantly higher than normal photosynthetic rates and elevated chlorophyll *a/b* ratios. It was concluded that the changes in structure and photosynthetic function of the green leaf sectors are part of an adaptive mechanism that attempts to compensate for a lack of photosynthesis in the white leaf sectors, while maximizing the ability of the plant to avoid photodamage.

In this report we found that GH, the tomato homolog of IM, affects the morphogenesis of pericarp tissue during tomato fruit ripening. The smaller than normal cells found in the pericarp of white, immature *gh* fruit might be a consequence of photooxidation. During the early ripening process, green fruit are normally formed whose cells contain chloroplasts (mature green stage). By analogy to the proposed function of IM in carotenogenesis in chloroplasts (Wu et al., 1999), a lack of GH during chloroplast biogenesis in the fruit might result in an inability to form photoprotective carotenoids, resulting in photooxidation of the contents of the developing plastid under high light illumination conditions. Support for this interpretation is provided by our finding that *gh* fruit turn green under low light illumination (Figure 2). In other experiments we found that photooxidation produces smaller than normal cells (Meehan et al., 1996). In these experiments, flow cytometry was used to analyze the sizes of cell-sorter purified white cells from *immutans* and norflurazon-treated wild type *Arabidopsis*. The white cells from both treatments were, on average, about 50% smaller than normal. If photooxidation represents a block in plastid development and cell differentiation, then this block can be overcome in *gh* since the pericarp cells in the terminal stages of ripening (orange) are normal-sized.

Regardless of the mechanism by which the white cells are generated in *gh* fruit, the fact that pericarp tissue anatomy is perturbed suggests that GH is required for normal tissue morphogenesis early in fruit ripening. A considerable body of evidence supports the notion that the transcription of nuclear genes for many plastid and mitochondrial proteins is controlled by the developmental state of the plastid (the "plastid signal" hypothesis) (reviewed in Rodermel, 2001). In addition to plastid signals that regulate the transcription of genes for organellar proteins, it has been proposed that plastid signals control tissue and organ developmental programming. Identification of this type of plastid-to-nucleus signaling pathway(s) has come from an examination of a handful of nuclear gene-induced pigment mutants whose white leaf tissues have abnormal plastids and altered palisade and/or spongy mesophyll cell layer organizations; usually, pigment mutants have normal leaf anatomies. These mutants include *dag* of *Antirrhinum*, *dcl* of tomato, and several *Arabidopsis* mutants, including *cla*1, *cue*1, and *pac* (reviewed in Rodermel, 2001). Because the products of the genes defined by these mutations reside in the plastid, it has been argued that these proteins are not independently required for plastid development and leaf morphogenesis, but that the effects on mesophyll cell differentiation are a consequence of incomplete chloroplast differentiation. We have previously suggested that *immutans* should be added to this list of mutants, because of the alterations in its leaf anatomy (Aluru et al., 2001). The present data show that the ortholog of this protein in tomato affects the morphogenesis of other tissues, as well. Our current working hypothesis is that GH is required for the transmission of a plastid-to-nucleus "developmental" signal that regulates normal pericarp morphogenesis.

In addition to tissue morphogenesis, plastid differentiation is affected in *gh*. As discussed above, normal chloroplasts do not develop during the mature green stage of ripening, perhaps because a lack of GH causes plastid photooxidation. Chromoplast differentiation is also affected in *gh*, since chromoplasts in the terminal stages of ripening in the mutant (orange) and wild type (red ripe) differ morphologically. This suggests that chromoplast development is blocked at the orange stage in the

mutant. Consistent with this notion, the expression patterns of most mRNAs from ethylene-dependent and ethylene-independent genes are similar in the mutant and wild type during early ripening (Figure 5), but at the orange stage carotenoid gene expression appears to be specifically repressed. One possibility is that GH is required for the transmission of a plastid signal that causes the suppression of carotenoid gene transcription. Regardless, our data are consistent with the idea that GH is necessary for the normal progression of the chromoplast developmental program, and that without GH, this program is blocked.

We do not know the nature of this block, but it is not likely due to a failure of plastids to survive photooxidation in the mature green stage, nor to the photooxidative destruction of a chloroplast factor that is required for chromoplast development. In support of this idea, we have treated wild type tomato plants with norflurazon at the time of flowering and have generated white (photooxidized) fruit that are capable of developing into red-ripe ripe fruit (Figure 7). This suggests that photooxidized plastids are capable of developing into chromoplasts. The variety of plastid-types that can give rise to chromoplasts is remarkable, and includes proplastids, chloroplasts, amyloplasts, and etioplasts (e.g., in tomato placed in darkness at the time of flowering). This plasticity is consistent with the notion that developmental programs for different plastid-types are normally coordinated but not linked processes. As an example, plastids in the *green flesh* mutants have characteristics of both chloroplasts and chromoplasts (Cheung et al., 1993).

The increases in *GH* mRNA expression during ripening of wild type fruit are consistent with earlier findings (Josse et al., 2000; Rodermel, 2002). One possibility is that *GH* expression is developmentally-regulated and that its induction is a reflection of its involvement in the desaturation steps of carotenogenesis. Consistent with this notion is the finding that phytoene accumulates in the mutant fruit (Table 1). It is also possible that GH, like IM, might have a more general role in plastid metabolism (Aluru et al., 2001). For instance, it might be part of a global antioxidant system that appears to be upregulated during fruit ripening in response to increased oxidative pressure (Jimenez

et al., 2002). In accord with this idea, we have found that IM mRNAs and proteins are expressed in response to stress in tobacco and *Arabidopsis* (Barr and Rodermel, unpublished).

Transcriptional regulation in *gh* provides evidence for a *trans*-lycopene model of carotenoid biogenesis regulation

Our mRNA results revealed that the levels of mRNAs from all carotenoid biosynthetic genes in the orange fruit were reduced when compared to WT red-ripe fruit. Also accompanying these changes were reductions in all intermediates of the carotenoid pathway, except phytoene, which increased. Previous studies have suggested that the major control point of the carotenoid biosynthetic pathway resides at the PSY step. Part of this regulation is thought to involve negative feedback of *PSY* transcription by the levels of β-carotene (Römer et al., 2000). Our data do not support this notion, since we found that decreased β-carotene in the *gh* orange fruit were accompanied by decreased (rather than increased) *PSY* mRNAs.

An alternative model of regulation posits that *trans*-lycopene levels play a central role in regulating carotenogenesis, and that this occurs via the regulation of transcript levels of *PDS* and *ZDS* in positive fashion. The phenomenon of *trans*-lycopene control was first described in transgenic rice expressing the bacterial genes *crtB* (for the phytoene synthase step) and *crtI* (which catalyzes all four desaturation steps) in an effort to enhance the β-carotene levels of rice endosperm ("golden rice") (Beyer et al., 2002). This study reported that the expression of the bacterial *LCYB* (β-lycopene cyclase) was unnecessary to observe an increase in β-carotene content in the endosperm. This was attributed to the endogenous *LCYB* being induced and both transcript and protein levels accumulating to high levels (Beyer et al., 2002). Accompanying the changes in the transgenic plants were increases in *PDS* and *ZDS* mRNAs. To test the hypothesis that the changes in *PDS, ZDS* and *LYCB* expression were due to increased lycopene levels, the researchers treated daffodil flower petals (the flower petals contain chromoplasts and accumulate high amounts of carotenoids derived from lycopene) with CPTA (2-(chlorophenlythio- triethylamine hydrochloride). This compound blocks the

activity of lycopene cyclases and causes an accumulation of *trans*-lycopene. The treatment with CPTA caused an increase in phytoene and *trans*-lycopene, as well as an increase in *PDS* and *ZDS* transcript levels, supporting their hypothesis.

In our studies we found overall lower levels of *trans*-lycopene in *gh* orange versus red WT fruit and also lower levels of *PDS* and *ZDS* transcripts. This is consistent with the *trans*-lycopene hypothesis (illustrated in Figure 7). It is worth noting, however, that the pool sizes of the various carotenoid intermediates are not constant when comparing the WT red versus *gh* orange fruit. For instance, the ratio of lycopene/β-carotene decreases from 18:1 in the red fruit to 4.75:1 in the orange fruit. In this step of the pathway both LCYB and BETA mRNAs are decreased in the orange fruit, i.e., flux from lycopene to β-carotene is not constant in the two sets of fruit. It will be of interest to determine how flux through this step of the pathway is controlled.

In addition to the present work, several recent studies also support the idea that lycopene plays a central role in regulating flux through the carotenoid biosynthetic pathway. The *Beta* mutant in tomato causes the constitutive expression of a lycopene β-cyclase, and the resulting uncontrolled activity causes an increase in β-carotene content of the fruit but not an increase in the total carotenoid levels. In the ripening *Beta* fruit, the transcription of *PDS* decreased in correlation with the decrease in lycopene content in the orange, pink and red stages of fruit ripening (Ronen et al., 2000). The *Delta* mutant in tomato causes the constitutive expression of the lycopene ε-cyclase, and this uncontrolled increase in activity causes a dramatic increase in the levels of δ-carotene, which is an intermediate in the synthesis of lutein (Ronen et al., 1999). Again, the decrease in lycopene content correlated with a decrease in *PDS* transcription.

In conclusion, both the formation of lycopene and its use as a substrate for the lycopene cyclases is an important branching point in the carotenogenic pathway. The recent identification of the tomato lycopene isomerase *CRTISO* indicates the importance in formation of the *trans*-lycopene isomer, and

the expression of *CRTISO* follows the pattern of *GH*, *PDS* and *ZDS* during fruit ripening. The data obtained from the *gh* mutant agrees with the *trans*-lycopene model of regulation of carotenoid biosynthesis, but also indicates that the regulation of carotenogenesis is a more complicated process than previously thought and possibly contains multiple regulatory steps.

References

Aluru, M., Hanhong, B., Dongying, W., and Rodermel, S. (2001). The *Arabidopsis immutans* mutation affects plastid differentiation and the morphogenesis of white and green sectors in variegated plants. Plant Physiol. Sept; 127: 67-77.

Ausubel, F., Brent, R., Kingston, R., Moore, D., Seidman, J., Smith, J., and Struhl, K. (1998). *Current Protocols in Molecular Biology*. Greene Publishing Associates/Wiley Interscience, New York, U. S. A.

Barry, C. S., Llop-Tous, M. I., and Grierson, D. (2000). The regulation of 1-aminocyclopropane-1-carboxylic acid synthase gene expression during the transition from system-1 to system-2 ethylene synthesis in tomato. Plant Physiol. July; 123: 979-986.

Bartley G. and Scolnik, P. (1993). cDNA cloning, expression during development, and genome mapping of PSY2, a second tomato gene encoding phytoene synthase. J. Biol. Chem. Dec 5;268(34): 25718-21.

Bartley, G. and Scolnik, P. (1995). Plant carotenoids: pigments for photoprotection, visual attraction, and human health. Plant Cell 7: 1027-1038.

Bennoun, P. (2001). Chlororespiration and the process of carotenoid biosynthesis. Biochim Biophys Acta. Aug 17;1506(2): 133-42.

Beyer P, Mayer M, and Kleinig H. (1989). Molecular oxygen and the state of geometric isomerism of intermediates are essential in the carotene desaturation and cyclization reactions in daffodil chromoplasts. Eur. J. Biochem. Sep 1;184(1):141-50.

Beyer, P., Al-Babili, S., Xudong, Y., Lucca, P., Schaub, P., Welsch, R., and Potrykus, I. (2002). Golden Rice: Introducing the β-Carotene Biosynthesis Pathway into Rice Endosperm by Genetic Engineering to Defeat Vitamin A Deficiency. J Nutr. 2002 Mar;132(3):506S-10S.

Bonk M, Hoffmann B, Von Lintig J, Schledz M, Al-Babili S, Hobeika E, Kleinig H, Beyer P. (1997). Chloroplast import of four carotenoid biosynthetic enzymes in vitro reveals differential fates prior to membrane binding and oligomeric assembly. Eur. J. Biochem. Aug 1;247(3):942-50.

Breitenbach, J., Zhu, C., and Sandmann, G. (2001). Bleaching herbicide norflurazon inhibits phytoene desaturase by competition with the cofactors. J. Agric. Food Chem. Nov;49(11):5270-2.

Camara, B., Bardat, F., Moneger, R. (1982). Sites of biosynthesis of carotenoids in Capsicum chromoplasts. Eur. J. Biochem. Oct;127(2):255-8.

Carol, P. and Kuntz, M. (2001). A plastid terminal oxidase comes to light: implications for carotenoid biosynthesis and chlororespiration. Trends in Plant Science Jan; 6(1): 31-36.

Carol, P., Stevenson, D., Bisanz, C., Breitenbach, J., Sandmann, G., Mache, R., Coupland, G., and Kuntz, M. (1999). Mutations in the *Arabidopsis* gene *IMMUTANS* cause a variegated phenotype by inactivating a chloroplast terminal oxidase associated with phytoene desaturation. Plant Cell 11: 57-68.

Cheung, A., McNellis, T., and Piekos, B. (1993). Maintenance of Chloroplast Components during Chromoplast Differentiation in the Tomato Mutant *Green Flesh*. Plant Physiol. 101: 1223-1229.

Corona, V., Aracri, B., Kosturkova, G., Bartley, G., Pitto, L., Giorgetti, L., Scolnik, P., and Giuliano, G. (1996). Regulation of a carotenoid biosynthesis gene promoter during plant development. Plant J. Apr;9(4):505-12.

Cournac, L., Josse, E., Joet, T., Rumeau, D., Redding, K., Kuntz, M., Peltier, G. (2000). Flexibility in photosynthetic electron transport: a newly identified chloroplast oxidase involved in chlororespiration. Philos. Trans. R. Soc. Lond. B. Biol. Sci. Oct 29;355(1402):1447-54.

Cunningham, Jr., F. and Gantt, E. (1998). Genes and enzymes of carotenoid biosynthesis in plants. Annu. Rev. Plant Physiol. Plant. Mol. Biol. 49: 557-583.

Cunningham, Jr., F. and Gantt, E. (2001). One ring or two? Determination of ring number in carotenoids by lycopene cyclases. Proc. Natl. Acad. Sci. U. S. A. Feb; 98(5): 2905-2910.

Demmig-Adams B, Gilmore AM, Adams WW 3rd. (1996). Carotenoids: in vivo function of carotenoids in higher plants. FASEB J. Mar;10(4):403-12.

Fraser, P., Bramley, P., and Seymour, G. (2001). Effect of the *Cnr* mutation on carotenoid formation during tomato fruit ripening. Phytochemistry 58: 75-79.

Fraser, P., Romer, S., Shipton, C., Mills, P., Kiano, J., Misawa, N., Drake, R., Wolfgang, S., and Bramley, P. (2002). Evaluation of Transgenic Tomato Plants Expressing an Additional Phytoene Synthase in a Fruit-Specific Manner. Proc. Natl. Acad. Sci. U. S. A. 99(2): 1092-1097.

Fraser, P., Kiano, J., Truesdale, M., Wolfgang, S., and Bramley, P. (1999). Phytoene synthase 2 enzyme activity in tomato does not contribute to carotenoid synthesis in ripening fruit. Plant Mol. Biol. 40: 687-698.

Giuliano, G., Bartley, G., and Scolnik, P. (1993). Regulation of carotenoid biosynthesis during tomato fruit development. Plant Cell 5(4): 379-387.

Harris, W., and Spurr, A. 1969. Chromoplasts of tomato fruits. I and II. Am. J. Bot. 56: 369-389.

Isaacson, T., Ronen, G., Zamir, D., and Hirshberg, J. (2002). Clonong of *tangerine* from Tomato Reveals a Carotenoid Isomerase Essential for Production of β-Carotene and Xanthophylls in Plants. Plant Cell 14: 333-342.

Jimenez, A., Creissen, G., Kular, B., Firmine, J., Robinson, S., Verhoeyen, M., and Mullineaux, P. (2002). Changes in oxidative processes and components of the antioxidant system during tomato fruit ripening. Planta Mar;214(5):751-8.

Joet, T., Genty, B., Josse E-M., Kuntz, M., Cournac, L., and Peltier, G. (2002). Involvement of a plastid terminal oxidase in plastoquinone oxidation as evidenced by expression of the arabidopsis thaliana enzyme in tobacco. J. Biol. Chem. [in press].

Josse, E-M., Simkin, A., Joël, G., Labouré, A-M., Kuntz, M., and Carol, P. (2000). A plastid terminal oxidase associated with carotenoid desaturation during chromoplast differentiation. Plant Physiol. Aug; 123: 1427-1436.

Lanahan, M., Yen, H., Giovannoni, J., and Klee, H. (1994). The never ripe mutation blocks ethylene perception in tomato. Plant Cell Apr;6(4):521-30.

Park, H., Kreunen, S., Cuttriss, A., DellaPenna, D., and Pogson, B. (2002). Identification of the Carotenoid Isomerase Provides Insight into Carotenoid Biosynthesis, Prolamellar Body Formation, and Photomorphogenesis. Plant Cell 14: 321-332.

Pecker, I., Chamovitz, D., Linden, H., Sandmann, G., and Hirschberg, J. (1992). A single polypeptide catalyzing the conversion of phytoene to ζ-carotene is transcriptionally regulated during fruit ripening. Proc. Natl. Acad. Sci. U. S. A. June; 89: 4962-4966

Pecker, I., Gabbay, R., Cunningham, Jr, F., and Hirschberg, J. (1996). Cloning and characterization of the cDNA for lycopene beta-cyclase from tomato reveals decrease in its expression during fruit ripening. Plant Mol. Biol. Feb; 30(4): 807-19.

Piechulla, B. and Gruissem, W. (1987). Diurnal mRNA fluctuations of nuclear and plastid genes in developing tomato fruits. EMBO J. Dec 1;6(12):3593-9.

Pozueta-Romero, J., Rafia, F., Houlne, G., Cheniclet, C., Carde, J., Schantz, M., and Schantz, R. (1997). A ubiquitous plant housekeeping gene, PAP, encodes a major protein component of bell pepper chromoplasts. Plant Physiol. Nov;115(3):1185-94.

MacKinney, G., Rick, C., and Jenkins, J. (1956). The phytoene content of tomatoes. Proc. Natl. Acad. Sci. U. S. A. 42: 404-408.

Mann, V., Harker, M., Pecker, I., and Hirschberg, J. (2000). Metabolic engineering of astaxanthin production in tobacco flowers. Nat. Biotechnol. Aug;18(8): 888-92.

McGarvey, D., and Croteau, R. (1995). Terpenoid metabolism. Plant Cell 7(7): 1015-1026.

Meehan L, Harkins K, Chory J, and Rodermel SR. 1996. *Lhcb* transcription is coordinated with cell size and chlorophyll accumulation: studies on fluorescence-activiated, cell-sorter-purified single cells from wild-type and *IMMUTANS Arabidopsis thaliana.* Plant Physiol. 112:953-963.

Niyogi, KK. (2000). Safety valves for photosynthesis. Curr. Opin. Plant Biol. Dec;3(6):455-60.

Rick, C., Thompson, A., and Brauer, O. (1959). Genetics and development of an unstable chlorophyll deficiency in *Lycospersicon esculetum.* Am. J. Bot. 46(1): 1-11.

Rizhsky, L., Hallak-Herr, E., Van Breusegem, F., Rachmilevitch, S., Barr, J., Rodermel, S., Inzé,D., and Mittler, R. (2002). Characterization of double antisense plants with suppressed expression of ascorbate peroxidase and catalase. [in press].

Rodermel S. (2001). Pathways of plastid-to-nucleus signaling. Trends in Plant Science. Oct;6(10):471-478.

Rodermel, S. (2002) Arabidopsis Variegation Mutants, The Arabidopsis Book, eds. C.R. Somerville and E.M. Meyerowitz, American Society of Plant Biologists, Rockville, MD, doi/10.1199/tab.0079, http://www.aspb.org/publications/arabidopsis/

Römer, S., Fraser, P., Kiano, J., Shipton, C., Misawa, N., Wolfgang, S., and Bramley, P. (2000). Elevation of the provitamin A content of transgenic tomato plants. Nat. Biotech. June; 18: 666-669.

Ronen, G., Carmel-Goren, L., Zamir, D., and Hirschberg, J. (2000). An alternative pathway to β-carotene formation in plant chromoplasts discovered by map based cloning of *Beta* and *old-gold* color mutations in tomato. Proc. Natl. Acad. Sci. U. S. A. 97(20): 11102-11107.

Ronen, G., Cohen, M., Zamir, D., and Hirschberg, J. (1999). Regulation of carotenoid biosynthesis during tomato fruit development: expression of the gene for lycopene epsilon-cyclase is down regulated during ripening and is elevated in the mutant *Delta*. Plant J. 17(4): 341-351.

Rosso, S. (1968). The ultrastructure of chromoplast development in red tomato. J. Ultrastructure Res. 25: 307-322.

Simkin, A., Breitenbach, J., Kuntz, M., and Sandmann, G. (2000). In vitro and in situ inhibition of carotenoid biosynthesis in Capsicum annuum by bleaching herbicides. J. Agric. Food Chem. Oct;48(10):4676-80.

Scolnik, P., Hinton, P., Greenblatt, I., Giuliano, G., Delanoy, M., Spector, D., and Pollock, D. (1987). Somatic instability of carotenoid biosynthesis in the tomato *ghost* mutant and its effect on plastid development. Planta 171: 11-18.

Seymour, G., Fray, R., Hill, P, and Tucker, G. (1993). Down-regulation of two non-homologous endogenous tomato genes with a single chimaeric sense gene construct. Plant Mol. Biol. Oct;23(1):1-9

Smolke, C.D., Martin, V.J., and Keasling, J.D. (2001). Controlling the metabolic flux through the carotenoid pathway using directed mRNA processing and stabilization. Metab. Eng. Oct;3(4):313-21.

Theologis, A., Oeller, P., Wong, L., Rottmann, W., and Gantz, D. (1993). Use of a tomato mutant constructed with reverse genetics to study fruit ripening, a complex developmental process. Dev Genet. 14(4):282-95.

van Hoof, A and Green, PJ. 1996. Premature nonsense codons decrease the stability of phytohemagglutinin mRNA in a position dependent manner. Plant J. 10: 415-424.

Vanlerberghe, G., and McIntosh, L. (1994). Mitochondrial electron transport regulation of nuclear gene expression. Studies with the alternative oxidase gene of tobacco. Plant Physiol. Jul;105(3):867-74.

von Lintig, J., Welsch, R., Bonk, M., Giuliano, G., Batschauer, A., and Kleinig, H. (1997). Light-dependent regulation of carotenoid biosynthesis occurs at the level of phytoene synthase expression and is mediated by phytochrome in Sinapis alba and Arabidopsis thaliana seedlings. Plant J. Sep;12(3):625-34.

Vishnevetsky, M., Ovadis, M., and Vainstein, A. (1999). Carotenoid sequestration in plants: the role of carotenoid-associated proteins. Trends Plant. Sci. Jun;4(6):232-235.

Wetzel, C., Jiang, C-Z., Meehan, L., Voytas, D., and Rodermel, S. (1994). Nuclear-organelle interactions: the *immutans* variegation mutant of *Arabidopsis* is plastid autonomous and impaired in carotenoid biosynthesis. Plant J. 6(2): 161-175.

Wilkinson, J., Lanahan, M., Clark, D., Bleecker, A., Chang, C., Meyerowitz, E., and Klee, H. (1997). A dominant mutant receptor from Arabidopsis confers ethylene insensitivity in heterologous plants. Nat. Biotechnol. May;15(5):444-7.

Wu D., Wright D., Wetzel C., Voytas D., and Rodermel S. (1999). The *IMMUTANS* variegation locus of *Arabidopsis* defines a mitochondrial alternative oxidase homolog that functions during early chloroplast biogenesis. Plant Cell 11: 43-56.

FIGURES AND TABLES

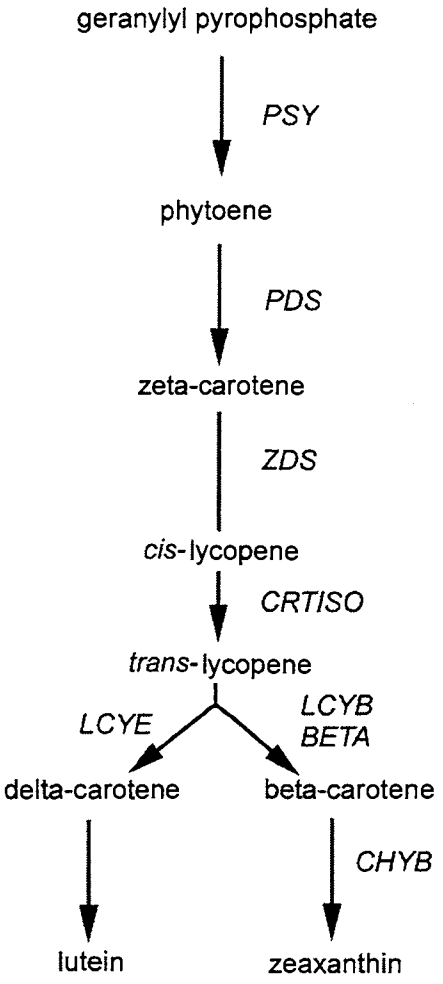

Figure 1. The carotenoid biosynthetic pathway in plants. Carotenoid synthesis begins in the tomato fruit when two molecules of geranylgeranyl diphosphate are condensed into phytoene, the first colorless C_{40} carotenoid, by phytoene synthase 1 (PSY1) (Fraser et al., 1999). Phytoene is synthesized into the red pigment, *trans*-lycopene, by four consecutive desaturation reactions and an isomeration reaction forming carbon-carbon double bonds catalyzed by phytoene desaturase (PDS), ζ-carotene desaturase (ZDS) and the newly identified lycopene isomerase (CRTISO). *Trans*-lycopene is cyclized to form either α- or β-carotene by lycopene ε-cyclase (LCYE), lycopene β-cyclase (LCYB) and BETA (Ronen et al., 2000).

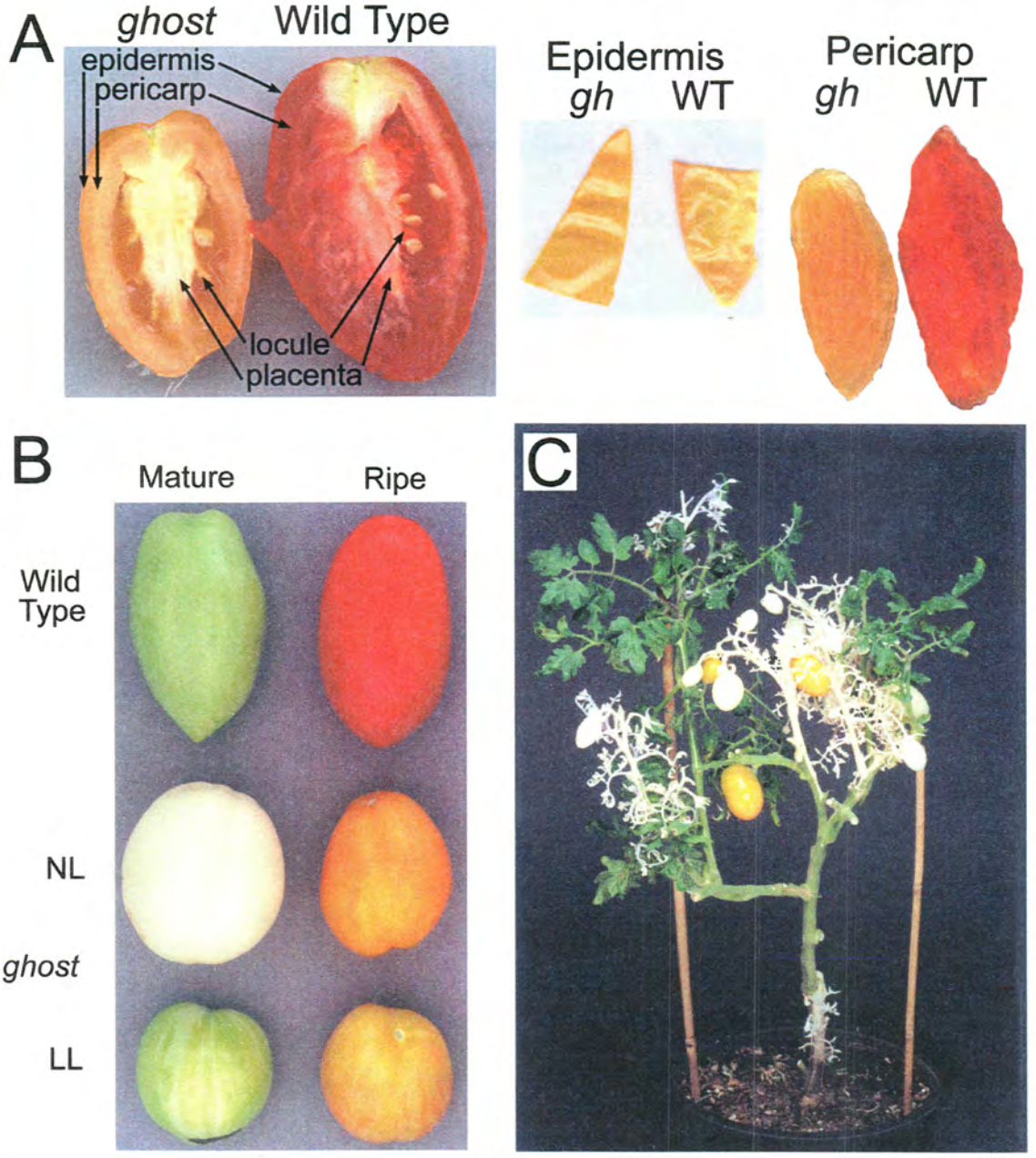

Figure 2. **A**. At left are wild type and *ghost* fruits sectioned through the center. At center are wild type (WT) and *ghost* (*gh*) skins dissected from ripe fruits. At right are wild type (WT) and *ghost* (*gh*) pericarps dissected from ripe fruits. **B**. Tomato fruit at two stages: mature (Left column) and ripe (right column). Top is wild type, center is *ghost* grown in normal light (NL) in greenhouse conditions, and bottom is *ghost* grown at low light (LL), which is 80 µmol m^{-2} sec^{-1}. **C**. *ghost* tomato mutant with white and orange fruit.

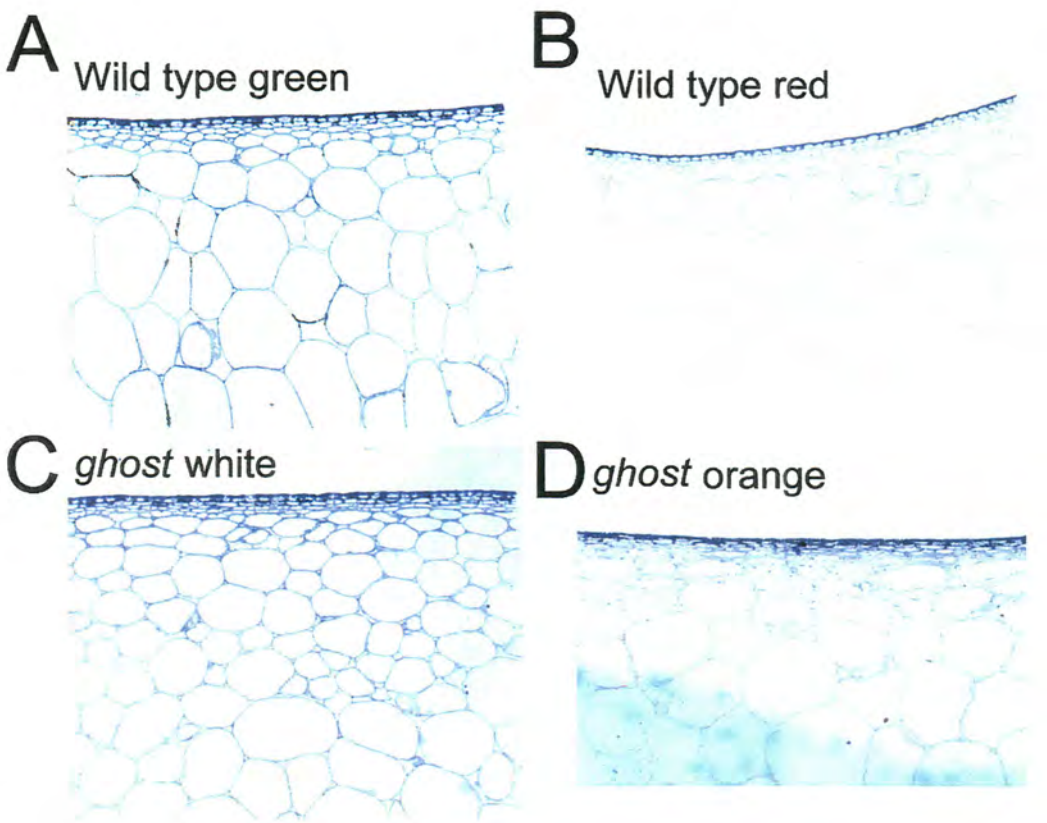

Figure 3. Morphology of *ghost* and wild type tomato. Light Microscopy of fruit sections. All images are at the same magnification (100X). Top left, Wild type mature green fruit. Top right, Wild type red-ripe fruit. Bottom left, *ghost* white fruit. Bottom right, *ghost* orange fruit.

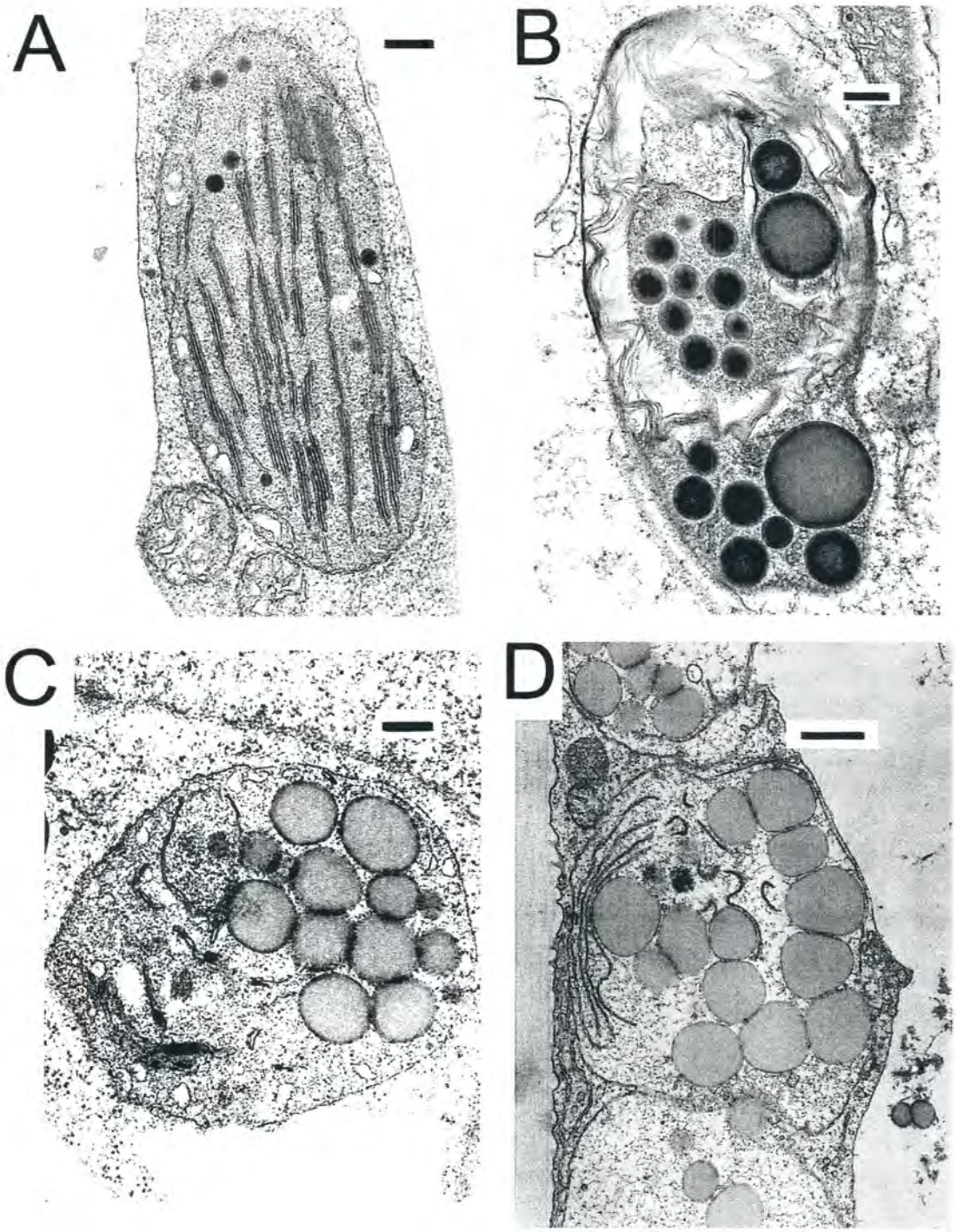

Figure 4. Ultrastructure of *ghost* and wild type tomato. Transmission electron microscopic analysis of plastids from fruit pericarp. A, Wild type mature green fruit. B, Wild type red-ripe fruit. C, *ghost* white fruit. D, *ghost* orange fruit. Scale bar = 200 nm.

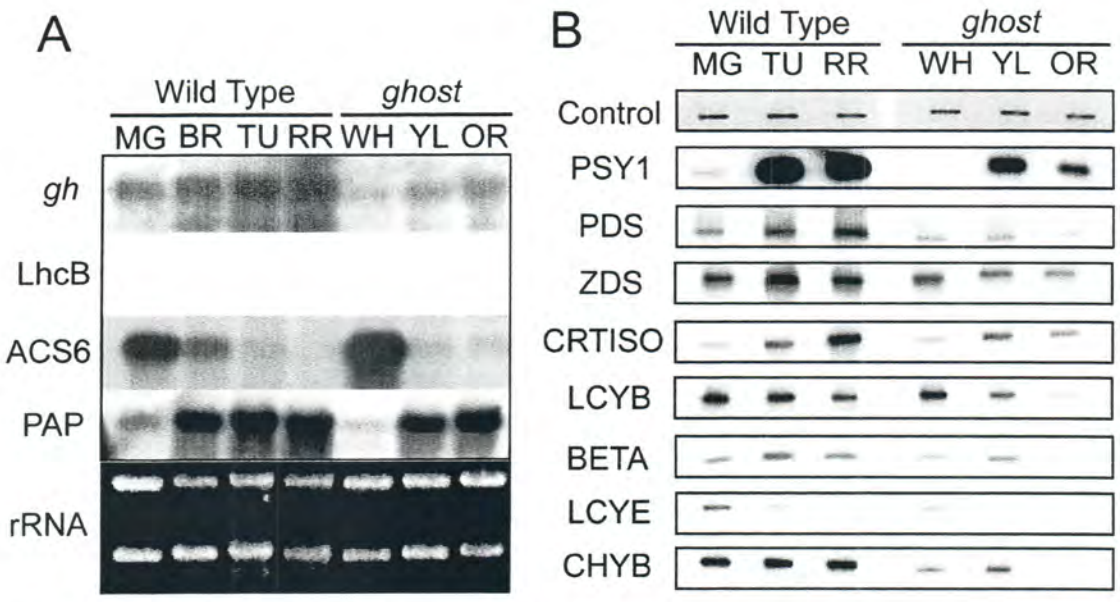

Figure 3. A. Steady state mRNA levels of *GH*, *Lhcb* (chlorophyll A/B binding protein), *ACS6* (1-aminocyclopropane-1-carboxylic acid synthase), and *PAP* (plastid-lipid associated protein) in wild type and *ghost* mutant tomato fruits during ripening. Total RNA was isolated from pericarp tissues, and 5 µg total RNA was loaded per lane (rRNA shown at bottom as a loading control). Representative blots are shown. **B**. RT-PCR products from amplification of carotenoid biosynthetic genes were blotted onto nitrocellulose membranes and hybridized to radiolabeled DNA probes. Control shows the PCR amplification of the NPTII gene added to the PCR reaction mix. Gene abbreviations are: PSY1 (phytoene synthase 1), PDS (phytoene desaturase), ZDS (ζ-carotene desaturase), CRTISO (lycopene isomerase), LCYB (lycopene β-cyclase), BETA (lycopene β-cyclase), CHYB (β-carotene hydroxylase), LCYE (lycopene ε-cyclase). In both A and B, the four ripening stages of wild type fruits that were used are: mature green (MG), breaker (BR), turning (TU), and red-ripe (RR). The three ripening stages of *ghost* fruits that were used are: white (WH), yellow (YL), and orange (OR) fruits.

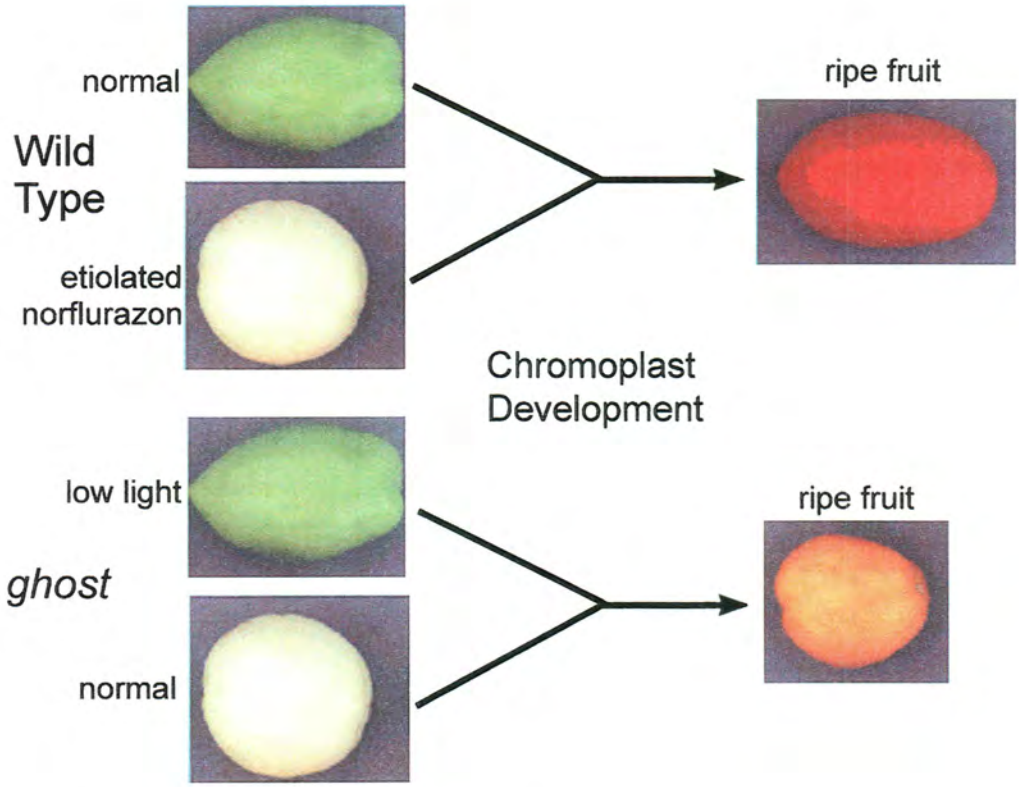

Figure 4. Graphic representation of chromoplast development from different mature fruit states. Norflurazon treatment of wild type fruits and growth conditions of *ghost* fruit described in methods section. Fruits shown are representative of treatments, and images are at the same magnification.

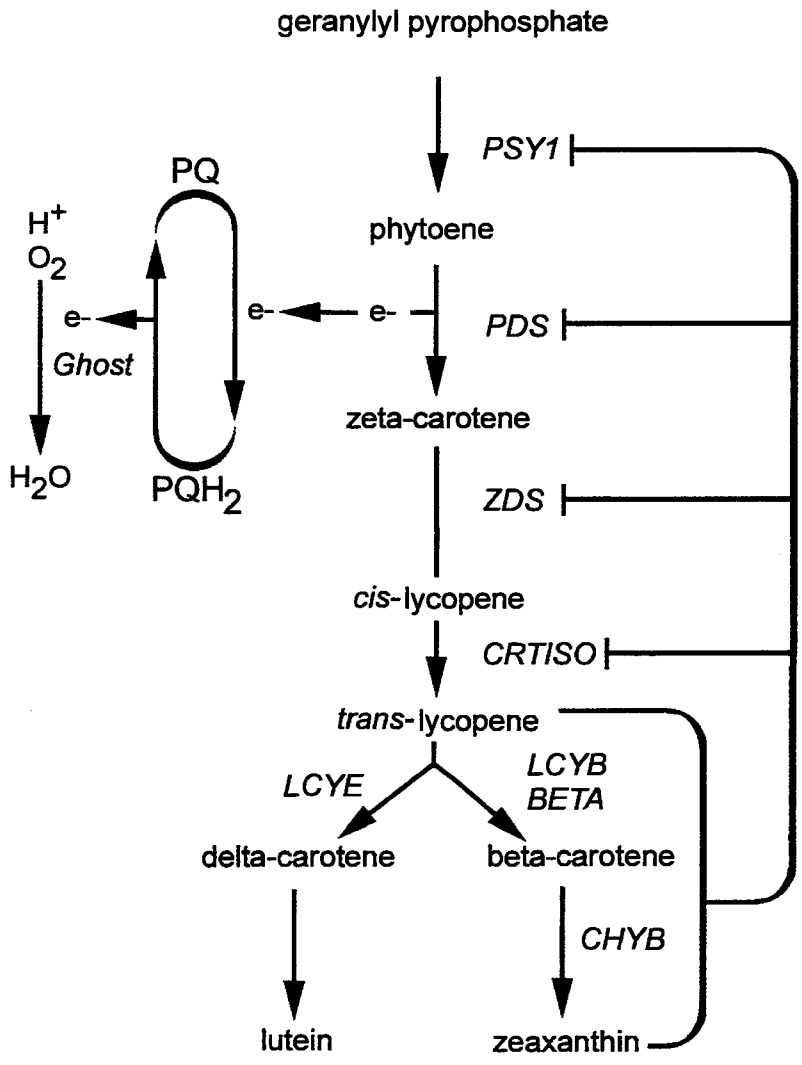

Figure 5. Carotenoid biosynthetic pathway in tomato fruit. Electrons from desaturation reactions are transferred to the plastoquinone pool. GH oxidizes the plastoquinone pool by transferring the electrons to molecular oxygen. During fruit ripening, *PSY1* transcription is developmentally induced and phytoene is produced at high levels. Subsequent PDS activity begins to reduce the plastoquinone pool, and this stimulates the transcription of the phytoene desaturases and isomerase (*CRTISO*), which produces saturating amounts of *trans*-lycopene. In the *ghost* mutant, the wild type pattern of developmental transcriptional changes of *PSY1*, *LCYE*, *BETA* and *LCYB* are still observed. PDS and ZDS transcripts decline during *gh* fruit development. The *trans*-lycopene hypothesis is shown in grey. The grey bars indicate the transcriptional effects of *trans*-lycopene or other products of carotenoid biosynthesis on *PSY1*, *PDS*, *ZDS*, and *CRTISO* mRNA levels.

Carotenoid	Wild Type	ghost	Ratio of WT / ghost
phytoene	0.2672	2.0019	0.133473
phytofluene	0.1493	0.2678	0.557506
zeta-carotene	0.052	0.0619	0.840065
neurosporene	0	0.0105	--
all-*trans*-lycopene	2.7498	0.1835	14.9853
13-*cis*-lycopene	0.0465	0.0114	4.0789
gamma-carotene	0.0419	0	--
beta-carotene	0.1531	0.0407	3.761671
lutein	0.0317	0.0102	3.107843

Table 1. Carotenoid content from HPLC analysis of wild type red ripe and *ghost* orange ripe fruits. The values (arbitrary units) have been corrected for an internal standard. Excepting lycopene, values are summations of all detected isomers.

CHAPTER 5

THE CHLOROPLAST TERMINAL OXIDASE *IMMUTANS* IS TRANSCRIPTIONALLY AND TRANSLATIONALLY RESPONSIVE TO LIGHT STRESS

ABSTRACT

Increases in light energy cause formation of reactive oxygen species (ROS) and photo-oxidative damage in plant cells. ROS scavenging mechanisms, such as carotenoids and enzymatic pathways, exist to detoxify these ROS species before damage is caused to the chloroplast. The *Arabidopsis thaliana* mutant *immutans* is devoid of a chloroplast terminal oxidase that functions to oxidize plastoquinone by removing electrons and reducing molecular oxygen to water. This mutant exhibits light-sensitive variegation by which increases in light intensity cause random patches of white, photo-oxidized lesions to be formed in growing tissues. IM is related to carotenoid biosynthesis and may have a role in preventing ROS damage in chloroplasts. Previous studies in tobacco (*Nicotiana tabacum*) show that antisense APX and CAT double mutants do not exhibit the leaf lesions that are present in the single mutants alone. The double mutant's less severe phenotype correlated with an increase in *IM* mRNA levels. High light treatment of *A. thaliana* show that both *IM* mRNA and protein levels will increase in response to a 5 hour treatment of high light but decrease by 24 and 48 hours of treatment. This implicates IM in the ROS scavenging mechanism response to high light.

INTRODUCTION

Light energy is a crucial component of photosynthesis and plant biology. The light energy is absorbed by light harvesting pigments, chlorophyll and carotenoids, and used to create a proton-motive force across the thylakoid membrane by reducing the lumen pH. Light energy is used to excite electrons from chlorophylls and are passed among electron carriers in the photosystems, cytochrome b_6/f and plastoquinone pools (called the Z-scheme), and during this transport, protons are translocated across the thylakoid membrane (Figure 1). This electrochemical gradient is used to synthesize adenosine triphosphate (ATP) from adenosine diphosphate (ADP) and inorganic phosphate (P_i) upon proton translocation to the stroma via ATP synthase activity.

Too much light energy can be harmful for plants as it may damage the photosynthetic components in excess amounts. Light energy can cause singlet chlorophylls to excite to form triplet chlorophylls. Triplet chlorophylls are usually quenched by carotenoids, but electrons may also be

passed to molecular oxygen generating reactive oxygen species (ROS) (Jespersen et al., 1997; Kliebenstein et al., 1998; Van Breusegem et al., 1999; Smirnoff 2000). ROS are short-lived superoxides, oxygen radicals and peroxides, and these molecules will react with proteins, lipids and nucleic acids. The ROS damage is rapid and can render chloroplasts chlorotic, devoid of organized internal membrane structures, and inhibit nuclear transcription of photosynthetic genes (Rodermel 2001). This process of light-induced damage is termed photo-oxidation and can be induced via herbicides such as norflurazon (a carotenoid synthesis inhibitor) or be present in light sensitive mutants such as the *Arabidopsis thaliana* mutant *immutans*. *immutans* is devoid of a chloroplast terminal oxidase that functions to oxidize plastoquinone by removing electrons and reducing molecular oxygen to water. This mutant exhibits light-sensitive variegation by which increases in light intensity cause random patches of white, photo-oxidized lesions to be formed in growing tissues (Chapter 2). Interestingly, photo-oxidation can be counteracted in the plant cell by ROS scavengers. These ROS scavengers are systems of chemicals, such as ascorbate and glutathione, and proteins such as ascorbate peroxidase (APX), superoxide dismutase (SOD), catalase (CAT) and glutathione reductase (GR) that absorb ROS and safely dissipate the excess energy (Jespersen et al., 1997; Kliebenstein et al., 1998; Van Breusegem et al., 1999; Smirnoff 2000).

A recent study of tobacco (*Nicotiana tabacum*) mutants has shown that antisense RNA techniques can reduce CAT and APX activity (Appendix). These mutants display leaf lesions indicative of photo-oxidative damage. However, double mutants in both APX and CAT do not display more severe leaf lesions, and transcription of the chloroplast terminal oxidase (*IM*) is induced. To examine if *IM* is related to high light treatments, an experiment to determine the steady state transcriptional and protein levels of *IM* was conducted. If IM is related plant tolerance of high light stress, as in tobacco, *IM* transcripts and IM protein levels should increase markedly over the non-treated plants. The high light treatment should reduce transcription of the chlorophyll a/b binding protein (CAB), which would be indicative of photo-oxidative damage (Wetzel et al., 1994).

MATERIALS AND METHODS

Wild type *Arabidopsis thaliana* Col. were germinated on soil and grown in a growth chamber (22°C constant light 70 µmol m^{-2} sec^{-1}) for 2 weeks. Plant for high light treatment were transferred to another growth chamber for the high light treatment (22°C constant light 750 µmol m^{-2} sec^{-1}), and control plants were removed from the growth chamber and replaced. Plant tissues were sampled for Northern and Western analysis as described in Chapter 2; tissue was sampled at 2, 5, 24 and 48 hours post-treatment with high light. Northern and Western analysis was conducted as described in Chapter 2. High light treatment was repeated twice to confirm results, and both Northern and Western blots from each treatment were repeated three times to confirm results.

RESULTS AND DISCUSSION

Photo-oxidative damage of chloroplasts due to high light may illicit many nuclear transcriptional events, such as the transcription of APX and SOD, to recover from ROS damage (Jespersen et al., 1997; Kliebenstein et al., 1998; Van Breusegem et al., 1999; Smirnoff 2000). The treatment of wild type *Arabidopsis thaliana* Col. with high light (750 μmol m^{-1} sec^{-1}) caused the temporary reduction in CAB transcription indicative of light stress as detected by Northern analysis (Figure 2). The treatment also increased the steady-state *IM* mRNA levels, indicating *IM* mRNA transcription or stability is responsive to light environment in *Arabidopsis*. IM is implicated in cartotenogenesis but is not an enzyme in the carotenoid biosynthetic pathway (Wetzel et al., 1994, Wu et al., 1999). Carotenoids are ROS scavenging compounds in addition to light-harvesting pigments. IM could be active in the assistance of carotenogenesis via phytoene desaturase (PDS), which becomes active via flavinylation and membrane association (Busch et al, 2002; see Chapter 3 for more on carotenoid biosynthesis). In this model, IM activity assists carotenogenesis by facilitating electron transport from PDS to plastoquinone and finally to molecular oxygen forming water (Wu et al., 1999). In high light situations, carotenoid turnover increases, and this demand for carotenogenesis may require increases in IM to perform this role of assisting PDS. This model does not explain the presence of *IM* in roots and etiolated tissues, as detected by *IM* promoter: β-glucuronidase (IM:GUS) fusion plants and Northern analysis (Aluru et al., 2001). Alternatively, IM may reduce the amount of electrons present in the plastoquinone pool independent of PDS, as the plastoquinone pool may be over-reduced by other chloroplast activities (i.e. the increased activity in photosystem II in high light). In this model, IM plays an important role in diverting excess electrons from the photosynthetic electron transport chain, which is a role that is similar to the mitochondrial alternative oxidase (AOX). AOX is homologous to IM and oxidizes ubiquinone and removes excess electrons from the mitochondrial electron transport chain (Maxwell et al., 1999). Western analysis of plants treated for 5 hours shows a marked increase in IM levels, but IM levels are closer to untreated levels at the 24 hour time point in correlation with Northern data (Figure 3). Clearly, IM responds to light stress by increasing mRNA and protein levels, but more experiments are necessary to determine if IM truly does affect the redox state of the plastoquinone pool.

FIGURES AND TABLES

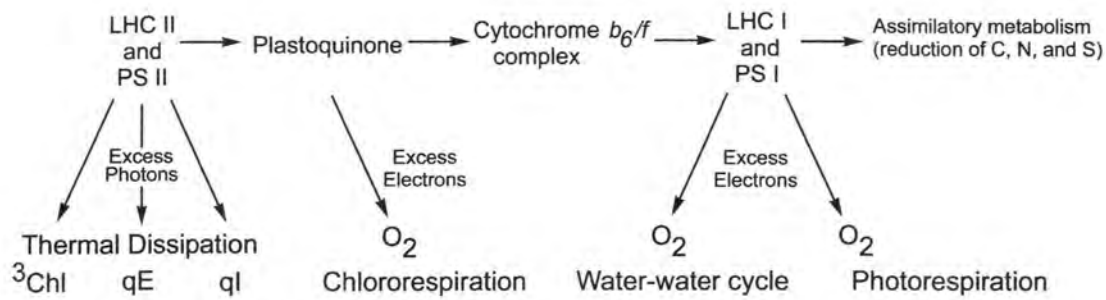

Figure 1. Scheme in which photo-oxidative damage can occur.

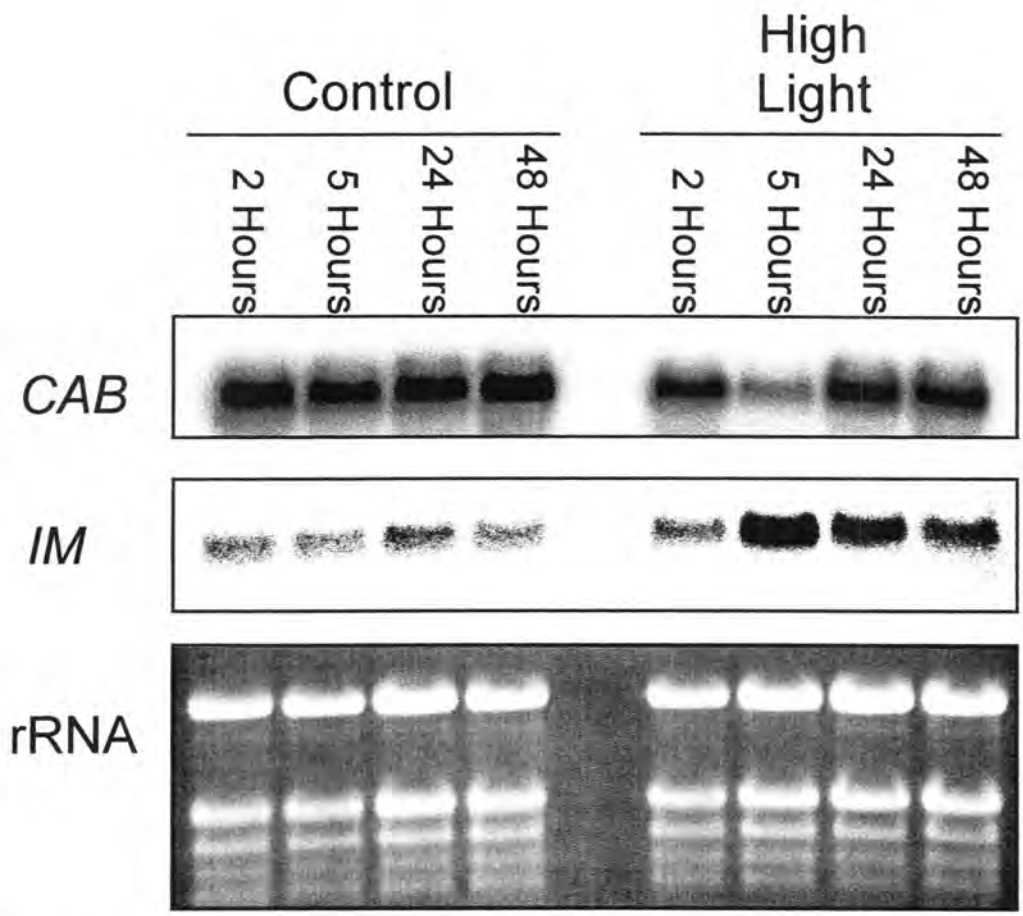

Figure 2. Representative Northern blots of total RNA isolated from control (normal light conditions: 22°C constant light 70 µmol m^{-1} sec^{-1}) and treated plants (high light conditions : 22°C constant light 750 µmol m^{-1} sec^{-1}).

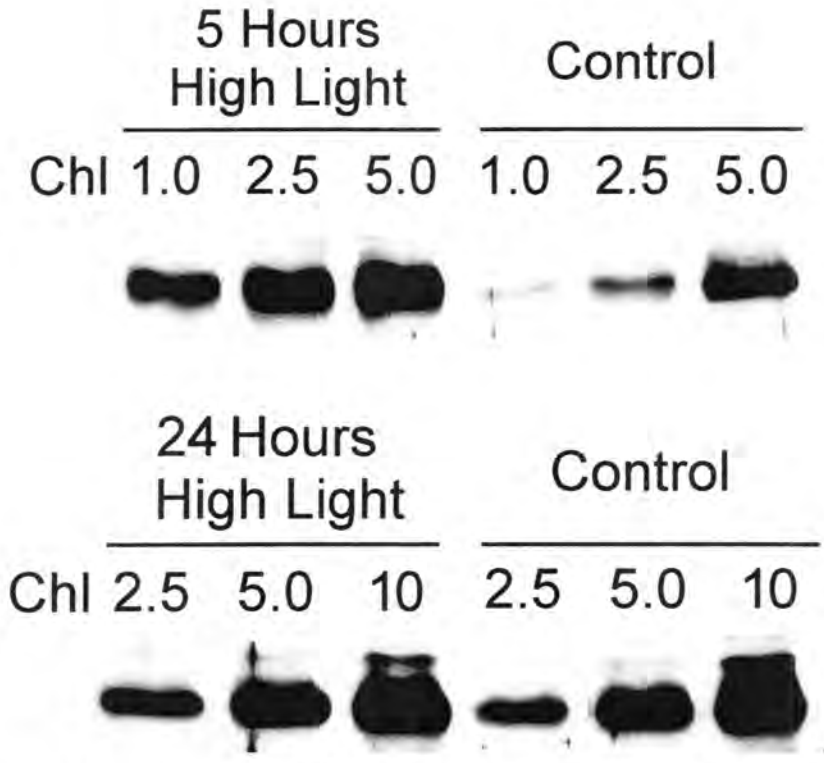

Figure 3. Representative Western blots of chloroplasts isolated from control (normal light conditions: 22°C constant light 100 µmol m^{-1} sec^{-1}) and treated plants (high light conditions : 22°C constant light 750 µmol m^{-1} sec^{-1}). Gels were loaded on a per chlorophyll basis.

LITERATURE CITED

Aluru, M., Hanhong, B., Dongying, W., and Rodermel, S. (2001). The *Arabidopsis immutans* mutation affects plastid differentiation and the morphogenesis of white and green sectors in variegated plants. Plant Physiol. Sept; 127: 67-77.

Busch, M., Seuter, A., and Rüdiger, H. 2002. Functional analysis of the earl steps of carotenoid biosynthesis in tobacco. Plant Physiol. Feb, 128: 439-453.

Jespersen, H., Kjærsgård, I., Østergaard, L., and Welinder, K. 1997. From sequence analysis of three novel ascorbate peroxidases from *Arabidopsis thaliana* to structure, function and evolution of seven types of ascorbate peroxidase. Biochem. J. 326: 305-310.

Kliebenstein, D., Monde, R-A., and Last, R. 1998. Superoxide Dismutase in Arabidopsis: an eclectic enzyme family with disparate regulation and protein localization. Plant Physiol. 118: 637-650.

Maxwell, D.P., Wang, Y., and McIntosh, L. 1999. The alternative oxidase lowers mitochondrial reactive oxygen production in plant cells. PNAS Jul 6; 96(14):8271-6.

Rodermel, S. 2001. Pathways of plastid-to-nucleus signaling. Trends Plant Sci. 2001 6(10):471-8.

Smirnoff, N. 2000. Ascorbate biosynthesis and function in photoprotection. Philos Trans R Soc Lond B Biol Sci. Oct 29;355(1402):1455-64.

Van Breusegem, F., Slooten, L., Stassart, J-M., Moens, T., Botterman, J., Van Montagu, M., and Inzé, D. 1999. Overproduction of *Arabidopsis thaliana* FeSOD confers oxidative stress tolerance to transgenic maize. Plant Cell Physiol. 40(5): 515-523.

Wetzel, C., Jiang, C-Z., Meehan, L., Voytas, D., and Rodermel, S. (1994). Nuclear-organelle interactions: the *immutans* variegation mutant of *Arabidopsis* is plastid autonomous and impaired in carotenoid biosynthesis. Plant J. 6(2): 161-175.

Wu D., Wright D., Wetzel C., Voytas D., and Rodermel S. (1999). The *IMMUTANS* variegation locus of *Arabidopsis* defines a mitochondrial alternative oxidase homolog that functions during early chloroplast biogenesis. Plant Cell 11: 43-56.

CHAPTER 6

GENERAL CONCLUSION

SUMMARY

New alleles of *immutans* will help elucidate the nature of variation seen in *im* mutants and provide a non-null mutant for further studies and further the study of the mechanism by which *im* variegation occurs. Current *im* alleles have given evidence that a general model of pre-mRNA splicing mechanisms in plants can be generated from or, if such a model exists, these mutants may test its accuracy. Additionally, the yellow seed phenotype has correlated with a less severe phenotype in subsequent generations and provides resistance to increased bleaching in light shift experiments. The yellow seed allele, now isolated in a wild type background, can be confirmed a suppressor of *im* by crossing it to other *im* mutants, such as *spotty*. Suppressor alleles of *im* will provide a clue into the mechanisms of variegation caused by *im*, possibly defining the physiological defects in *im*, and explain the generation of "bi-phenotypic" variegation (i.e. one plant genotype can produce two plant phenotypes). The characterization of suppressor mutants, such as the yellow seed allele, clearly is germane to the understanding of variegation processes and the function of IM in this process.

The further characterization of carotenoid biosynthesis implicates GH(IM) in plastid developmental processes, and IM was first suspected to be a key factor in chloroplast biogenesis and has been implicated in general plastid synthesis (see Chapter 2). However, with the bi-phenotypic variegation of the null mutants, it is difficult to argue that IM is necessary for this process to occur; yet IM is necessary for chloroplast biogenesis to occur in high light intensities, as the null mutant is completely albino when grown under these conditions (see Chapter 2). Carotenoid biosynthesis has been a recent focus of study, as carotenoids are important compounds for food coloring and human nutrition. Little is known about regulation of the carotenogenic pathway, and reports generally indicate the regulation level being at transcription (see Chapter 3). However, some reports favor translational control of the pathway (see Chapter 3). It is necessary to understand the control and

effects of the carotenoid biosynthesis pathway if scientists are to be successful in engineering plants that develop higher concentrations of desired carotenoids, such as lutein (a vitamin A precursor), and create transgenic plants that have enhanced nutritional attributes. Data are presented herein that implicate GH(IM) is necessary to maintain continual upregulation of transcription of the carotenogenic pathway in ripening tomato, where chromoplasts are developmentally progressing into chromoplasts. This process may be analogous to the development of chloroplasts from proplastids in the apical meristem, where a defect in GH(IM) causes bi-phenotypic variegation. Further studies in *ghost* may be to overexpress GH in tomato plants to study its effects on chromoplast development and carotenogenesis as well as developing or isolating new mutants that are affected in the regulation of carotenogenesis in the chromoplast. Additionally, it would be interesting to explore controlled expression experiments in which *im* or *gh* cDNA was transgenically expressed with either inducible promoters (i.e. promoters responsive to hormone treatment) or organ-specific promoters (i.e. CAB in tomato would target GH to leaves only, allowing production of orange tomato fruit without the side-effects of variegation). These experiments would allow analysis of expressing *IM*(*GH*) in a developmentally specific way to dissect the point during which it is necessary.

ACKNOLEDGEMENTS

I would like to thank Dr. Steven Rodermel for the outstanding support and encouragement that exceeds above and beyond all known bounds previously defined in society. His acceptance of my enthusiasm towards the sciences has enabled me to achieve many personal goals such as the completion of this thesis, and, as I was an undergraduate-graduate combined student, his patience and teaching has been greatly appreciated. It is through the kind instruction of teachers like Dr. Rodermel that the intellectual ranks of society are renewed for many generations. I would like to thank Linda Wild, Interdepartmental Genetics Coordinator, and many other persons in professorial, administrative and secretarial positions at Iowa State University too numerous to mention who have been of great assistance and understanding of my unique program an providing advice in my studies and experiments. I would also like to thank my friends and family for support, and I would like to extend my greatest and most sincere thanks to my wife, Kelli, for her undying support, understanding of my long hours in the laboratory and patience at suppertime.

APPENDIX

Characterization of double antisense plants with suppressed expression of ascorbate peroxidase and catalase.

Ludmila Rizhsky[1], Elza Hallak-Herr[2], Frank Van Breusegem[3], Shimon Rachmilevitch[2], Jason E. Barr[4], Steven Rodermel[4], Dirk Inzé[3] and Ron Mittler[4,*]

[1]Department of Biology, Technion - Israel Institute of Technology, Technion City, Haifa 32000, Israel. [2]Department of Plant Sciences, The Hebrew University of Jerusalem, Jerusalem 91904, Israel. [3]Department of Genetics, University of Gent, K.L. Ledeganckstraat 35, B-9000 Ghent, Belgium. [4]Department of Botany, Plant Sciences Institute, Iowa State University, Room 353 Bessey Hall, Ames IA 50011 USA.
* To whom correspondence should be addressed. E-mail: rmittler@iastate.edu; Phone 1-515-294-7455; Fax: 1-515-294-1337

Abbreviations: APX, ascorbate peroxidase, AS, antisense; ASC, ascorbate; CAT, catalase; dAS, double antisense; GPX, glutathione peroxidase; GR, glutathione reductase; GSH, glutathione; MDA, monodehydroascorbate; PR, pathogen-related; RbcS, ribulose-1,5-bisphosphate carboxylase/oxygenase small subunit; ROI, reactive oxygen intermediates; SOD, superoxide dismutase.

The plant genome is a highly redundant and dynamic genome. Here, we show that double antisense plants lacking the two major hydrogen peroxide-detoxifying enzymes, ascorbate peroxidase (APX) and catalase (CAT), activate an alternative/ redundant defense mechanism that protects them from hydrogen peroxide toxicity. A similar mechanism was not activated in single antisense plants that lacked APX or CAT, paradoxically rendering these plants more sensitive to oxidative stress compared to double antisense plants. The reduced susceptibility of double antisense plants to hydrogen peroxide toxicity correlated with suppressed photosynthetic activity, the induction of metabolic genes belonging to the pentose phosphate pathway, and the induction of a chloroplastic homolog of mitochondrial alternative oxidase. Suppression of photosynthetic activity appeared to be critical for lowering the sensitivity of plants to oxidative stress because antisense plants with reduced expression of ribulose-1,5-bisphosphate carboxylase/oxygenase protein, that had suppressed photosynthetic activity, were less sensitive to oxidative stress than wild type plants. Our results suggest that a coordinated induction of metabolic and defense genes, coupled with the suppression of photosynthetic activity, can compensate for the lack of APX and CAT. In addition, our findings demonstrate that the plant genome has a high degree of plasticity and will respond differently to different stressful conditions, namely, lack of APX, lack of CAT, or lack of both APX and CAT.

Words in Abstract: 217

INTRODUCTION

Whereas molecular oxygen has a relatively low reactivity towards most cellular components, partially reduced forms of atmospheric oxygen, globally named "reactive oxygen intermediates" (ROI), may react with many cellular substances potentially leading to the oxidative destruction of cells (Asada and Takahashi, 1987). ROI are formed in plant cells as byproducts of many metabolic reactions. For example, hydrogen peroxide (H2O2) is produced through the catalytic activity of glycolate oxidase in peroxisomes during photorespiration, and superoxide (O2-) is generated by leakage of electrons from chloroplastic or mitochondrial electron transport systems. While under normal growth conditions the formation of ROI occurs at a low rate, many stresses that disrupt the biochemical and physiological homeostasis of cells cause a dramatic increase in the rate of ROI production (Allen, 1995; Asada and Takahashi, 1987; Dat et al., 2000; Mittler, 2002). Recent studies suggested that ROI may play an important role in plant cells as signaling molecules involved in the regulation of gene expression during stress or pathogen infection (Karpinski et al., 1999; Knight and Knight, 2001; Kovtun et al., 2000; Hirt, 2000; Grant et al., 2000; Pei et al., 2000).

Plants, as well as most aerobic organisms, contain complex enzymatic and nonenzymatic mechanisms capable of detoxifying O2- and H2O2. Superoxide radicals are scavenged through the catalytic activity of superoxide dismutase (SOD), whereas H2O2 is removed through the catalytic action of ascorbate peroxidase (APX), glutathione peroxidase (GPX), and catalase (CAT). Non-enzymatic scavenging of ROI involves ascorbic acid, glutathione, á-tocopherol, and carotenoids (Asada and Takahashi, 1987; Foyer and Halliwell, 1976). The importance of ROI scavenging for the growth and defense of plants was recently demonstrated using transgenic tobacco plants with reduced CAT or APX expression. These were found to be hypersensitive to treatments that involved the accumulation of ROI, including high light, ozone, application of the O2- generating herbicide paraquat, salt stress, pathogen infection, and low CO2 combined with high light (Willekens et al., 1997; Orvar and Ellis, 1997; Mittler et al., 1999). In addition, mutants deficient in the biosynthesis of the antioxidant ascorbic acid were shown to be hypersensitive to environmental stresses (Conklin et al., 1996).

ROI appear to play a central role in the defense of plants against pathogens. During many plant-pathogen interactions ROI are produced by plant cells at a very high rate and are thought to activate plant defenses, including programmed cell death (Delledonne et al., 2001; Hammond-Kosack, and Jones, 1996; Dangl et al., 1996). In contrast, the activity and expression of APX and CAT is suppressed during this response (Clark et al., 2000; Durner and Klessig, 1995; Mittler et al., 1998). Thus, the plant simultaneously produces more ROI and diminishes its own capability to scavenge H2O2.

The studies described above point to a complex mode of regulation controlling the steady state level of ROI in cells. Depending upon the physiological condition encountered by plants, i.e., biotic or abiotic stress, they may alter the balance between ROI production and ROI removal to enhance (biotic), or suppress (abiotic), the cellular level of ROI. Balancing ROI production and ROI scavenging is therefore crucial for many different aspects of plant metabolism. In addition, due to the potential toxicity of ROI, a high degree of redundancy is expected to occur between different ROI scavenging mechanisms.

We previously reported that plants with suppressed APX or CAT are limited in their capability to balance their intracellular level of ROI (Mittler et al., 1999). However, APX and CAT might be functionally redundant and compensate for the lack of each other. We therefore generated double antisense plants lacking both APX and CAT. To our surprise, at least under a defined set of environmental conditions, these appeared to be less sensitive to oxidative stress than single antisense plants lacking APX or CAT.

RESULTS

Characterization of Double Antisense Plants with Suppressed Expression of APX and CAT

All crosses between antisense APX (*apx I*; AS-APX; Orvar and Ellis, 1997), antisense CAT (*cat 1*; AS-CAT; Willekens et al., 1997), and wild type (WT) plants, as well as the isolation of double antisense (dAS) plants are described in Methods. We compared the growth of WT, AS-APX, AS-CAT,

and dAS plants under three different light intensities: low (75 µmol photons m-2 sec-1), moderate (150-200 µmol photons m-2 sec-1), and high (600-800 µmol photons m-2 sec-1), using a continuous light source, at 22-240C. At low light there was no apparent difference between the different plants (not shown). At moderate light AS-CAT plants developed lesions on their leaves while WT, AS-APX, and dAS plants did not (Figure 1A). At high light all antisense plants, including dAS, developed lesions, while WT plants did not (not shown). We therefore focused our studies on plants that grow at moderate or low light. RNA blot analysis was performed on leaf samples obtained from the different plants grown at moderate light. As shown in Figure 1B, dAS plants that had suppressed expression of APX and CAT did not appear to induce stress response genes such as cytosolic CuZnSOD (SOD) or cytosolic glutathione reductase (GR). In contrast, AS-APX plants induced CAT, GR, and SOD in an apparent attempt to compensate for the reduced APX expression, and AS-CAT plants induced APX and PR-1 (PR-1a), developed lesions, and had a reduced expression of ribulose-1,5-bisphosphate carboxylase/oxygenase small subunit (rbcS), and glucose-6-phospate dehydrogenase (G6PDH; Figures 1A and 1B). The response of AS-APX and AS-CAT plants indicated that they were subjected to oxidative stress. However, at least under moderate light, dAS plants appeared not to be subjected to a similar level of stress.

To confirm that the suppression of CAT and APX expression, evident by a reduction in the steady state level of transcripts encoding APX and CAT (Figure 1B), resulted in a reduction in APX and CAT activities, we measured these activities in the different plants grown under moderate light. As shown in Figure 2A, the activity of CAT was suppressed in AS-CAT plants and the activity of APX was suppressed in AS-APX plants. In contrast, the activity of APX was enhanced in AS-CAT plants and the activity of CAT was enhanced in AS-APX plants. These results were in good agreement with the steady state level of transcripts encoding APX and CAT in the different plants (Figure 1B). In contrast to AS-APX and AS-CAT plants, both CAT and APX activities were suppressed in dAS plants. To expand our analysis of plants grown under moderate light we measured the level of the antioxidants ascorbic acid (ASC) and glutathione (GSH) in dAS plants. The overall level of these antioxidants as well as the size of their reduced pool can provide an indication to the degree of oxidative stress encountered by plants (Herouart et al., 1993; Noctor and Foyer, 1998). As shown in Figure 2B, the levels of reduced ASC and GSH in dAS plants were similar to those of WT plants. In contrast, ASCAT and AS-APX plants had high levels of ASC and GSH, suggesting that these plants were exposed to oxidative stress. The levels of oxidized ASC (DHA) and GSH (GSSG) were maintained at 15-20% of their corresponding pools in all plants (not shown). This result is in accordance with the presence of an ASC and GSH regenerating enzymes in the different plants, postulated to be sufficient for maintaining the antioxidant pools at a reduced level (Polle, 2001). Measurements of overall H2O2 levels in leaf tissues of the different plants, grown under moderate light, did not reveal dramatic differences between dAS plants and the other plants (Figure 2B). However the concentrations of H2O2 at the different cellular compartments of the different plants, that may be critical for the activation of different signal transduction pathways, are not known, and it is possible that grinding of plant tissue to measure H2O2 results in measurements that do not reflect the true *in vivo* level of this compound (Mittler, 2002).

To further characterize the phenotype of dAS plants, and examine their resistance to oxidative stress, we subjected plants to stress imposed by treatment with the superoxide generating agent paraquat, at the three different light conditions, and assayed plants for cell death by measuring ion leakage. At high and moderate light there was no apparent difference between the different antisense plants, including dAS (not shown), however, at low light AS-CAT plants were more sensitive to paraquat treatment compared to AS-APX or dAS plants (Figure 3). Thus, although the expression of CAT and APX was suppressed in dAS plants they appeared to be less sensitive than AS-CAT plants to this treatment.

Suppression of Photosynthetic Activity in Double Antisense Plants

Measurements of photosynthetic activity and dark respiration were performed on the different plants grown at low light intensity using a saturating light experimental design. Plants were clamped with a Li-Cor LI-6400 apparatus and the light intensity within the measuring chamber was changed to 2000 µmol photons m-2 sec-1. The rate of CO2 assimilation was then measured every minute over

the course of 15 min. As shown in Figure 4A, the maximal photosynthetic activity of dAS plants was lower than that of WT or AS-CAT and AS-APX plants. No significant differences in stomatal conductance were detected between the different plants during the course of the experiment (not shown).

Dark respiration, i.e., CO2 emission in the dark, measured at the start and at the end of the experiment described above is shown in Figure 4B. Interestingly, compared to AS-CAT and AS-APX plants, dAS plants did not have a high rate of dark respiration following the high light treatment. The behavior of dAS plants was therefore comparable to that of WT plants, suggesting that they were not affected in a similar manner by the high light treatment as AS-CAT or AS-APX plants. However, the nature of the enhanced dark respiration and its relation to oxidative stress is unknown.

Additional measurements performed on WT and dAS plants grown at moderate light intensity, however, using the same light intensity used for the growth conditions as a light source for the measurements, confirmed that dAS plants had about 50% lower photosynthetic activity compared to WT plants (WT, 8.2, SE=1.4 ; dAS, 4.7, SE=0.9; n=5; μmol CO2 cm-2 sec-1). The decreased photosynthetic activity of dAS plants did not appear to be a result of a lower number of stomata, because stomata counting indicated that dAS plants had a high number of stomata (80 mm-2, SE=9.6, n=10) compared to WT (53 mm-2, SE=4.2, n=8) or AS-APX (55 mm-2, SE=4.8, n=10) plants, and an equivalent number of stomata to AS-CAT plants (76 mm-2, SE=7.2, n=10), all measured on leaf number 4 of the different plants.

The suppression of photosynthetic activity in dAS plants may result from the inability of these plants to use ambient CO2 levels for photosynthesis. To examine this possibility we compared the degree of increase in photosynthetic activity between the different plants upon changing the CO2 concentrations from ambient (350ppm) to near saturating (2200ppm). This analysis was performed at saturating light as described for Figure 4A. As shown in Figure 4C, there was no difference between the fold increase in photosynthetic activity of dAS plants and WT plants. In contrast, AS-CAT plants appeared to significantly benefit from the increase in O2 levels, possibly due to the suppression of photorespiration in these plants at high CO2 levels (Willekens et al., 1997). The results presented in Figure 4C suggest that the mode of suppression of photosynthetic activity in dAS plants is different from that observed in AS-CAT and ASAPX plants. Thus, at least some of the suppression in photosynthetic activity, observed in AS-CAT and AS-APX plants (Figure 4A), could be prevented by increasing the level of 10 CO2, whereas the photosynthetic activity of dAS plants appeared not to be affected in a similar manner by this increase (Figure 4C).

Profiling Gene Expression in Double Antisense Plants

To understand the basis of dAS resistance we performed a filter array analysis of gene expression in plants grown under moderate light. We screened about 500 different stress response and metabolic genes in an attempt to identify a gene(s)/pathway(s) that may be specifically expressed in dAS plants and provide a possible explanation to the enhanced tolerance of these plants. An example of our filter array hybridization is shown in Figure 5A. Based on this analysis the only pathway that appeared to be specifically affected in dAS plants was the pentose phosphate pathway. Thus, as shown in Table 1, at least three transcripts encoding enzymes belonging to this pathway, i.e., transaldolase, transketolase, and ribulose-5-phosphate isomerase, were induced in dAS plants (2-3 fold induction in pentose phosphate pathway genes was also observed by RNA blots; not shown). The pentose phosphate pathway was previously linked to the defense of animal cells against oxidative stress (Pandolfi et al., 1995). It is therefore possible that it plays a similar role in dAS plants enhancing the supply of NADPH for ROI removal. A number of other genes were also induced in dAS plants but their induction did not appear to be specific to dAS plants. The expression level of these genes, as well as that of other ROI-related genes, not shown in Figure 1B, is shown in Table 1. These results suggest that other defense enzymes with an H2O2 detoxification activity such as thylakoid/stromal APX, GPX, or thioredoxin peroxidase were not induced in dAS plants. Interestingly, the level of transcripts encoding cytosolic monodehydroascorbate (MDA) reductase was induced in dAS plants (Table 1). Although MDA reductase was also induced in AS-CAT plants, the combined induction of MDA reductase and transcripts belonging to the pentose phosphate pathway

may indicate that in dAS plants these two mechanisms cooperate to enhance the non-enzymatic scavenging of H2O2 by ascorbic acid.

Measuring the Level of Different Proteins Involved in Photosynthesis in dAS Plants

We performed protein gel blots comparing WT and dAS plants to examine whether the decrease in photosynthetic activity in dAS plants is a result of a decrease in the level of proteins involved in photosynthesis. This analysis was performed on plants growingunder low or moderate light. As shown in Figure 5B, we could not detect a decrease in these proteins in dAS plants. Similar results were obtained with AS-CAT and AS-APX plants grown under low light (not shown). However, in AS-CAT plants grown under moderate light there was a decrease in the level of certain photosynthetic proteins including RbcS (not shown; see Figure 1B for a decrease in rbcS transcripts in AS-CAT plants grown under moderate light). Because many of the different components of the photosynthetic apparatus are linked, a reduction in the level of any one of these components may lead to an overall suppression of photosynthetic activity. For example, it was found that even a moderate decrease in the activity of chloroplastic aldolase resulted in the inhibition of photosynthesis in potato (Haake et al., 1998). A comprehensive proteomic and metabolomic analysis may therefore be required to identify a specific protein(s) or metabolite(s) that may account for the suppression in photosynthetic activity in dAS plants.

Induction of Chloroplastic Alternative Oxidase in dAS plants

A defense function against ROI stress was recently suggested for mitochondrial alternative oxidase (mitAOX; Maxwell et al., 1999). However, this gene was mainly induced in AS-CAT plants and not in dAS plants (Table 1; Dat et al., unpublished). A homolog of mitAOX was recently reported to exist in chloroplasts (Carol et al., 1999; Wu et al., 1999). It has been shown that this enzyme (designated IMMUTANTS, or chlAOX) has quinol oxidase activity (Josse et al., 2000), suggesting that it diverts electrons flowing from photosystem II (PSII) to photosystem I (PSI) at the plastoquinone pool and use these to reduce O2 into water. Because the majority of ROI production in chloroplasts occurs at PSI using electrons supplied by PSII (Asada, 1999), chlAOX might lower the rate of ROI production in chloroplasts by reducing the flow of electrons from PSII to PSI. As shown in Figure 6A, chlAOX was specifically induced in dAS plants at low light. At moderate light it was also induced in AS-CAT plants, and at high light it was induced in all plants, including WT plants.

The induction of chlAOX in WT plants at high light support a role for this enzyme in preventing the formation of ROI in chloroplasts during high light stress. To test whether chlAOX is also induced in other plants in response to high light stress we examined its induction in Arabidopsis. As shown in Figure 6B, in Arabidopsis chlAOX was induced following a 5 hour high light stress treatment. This induction was observed at the transcript as well as the protein level and coincided with a reduction in the steady state level of transcripts encoding the chlorophyll a/b binding protein (Cab). The findings presented in Figure 6 support a role for chlAOX in preventing ROI related damage during high light stress in plants.

Decreased Sensitivity of Antisense Plants with Suppressed Photosynthetic Activity to Oxidative Stress

Because a decrease in photosynthetic activity was associated with the dAS phenotype (Figure 4A), we tested whether plants with reduced photosynthetic activity are less sensitive to oxidative stress. For this analysis we used antisense tobacco plants with reduced expression of *rbcS* (Jiang and Rodermel, 1995). We subjected 3-week-old *rbcS* antisense (AS-RbcS) and control (WT) plants grown under low light conditions to oxidative stress imposed by paraquat, and compared the degree of cell death induced by this treatment in the different plants. As shown in Figure 7A, AS-RbcS plants had a reduction of about 20-25% in their photosynthetic activity. Prior to paraquat application we tested the expression level of PR-1 by RNA blot analysis to confirm that these plants were not subjected to any additional stress and/or had an induced systemic acquired resistance response (Figure 7B). As shown in Figure 7C, compared to WT plants AS-RbcS plants were less sensitive to oxidative stress induced by paraquat and had a decreased level of cell death in response to this treatment.

Response of dAS plants to pathogen infection

Reactive oxygen intermediates play a key role in the defense of plants against pathogen attack (Hammond-Kosack and Jones, 1996). Accordingly, plants with reduced CAT or APX expression are hyper-responsive to pathogen attack and activate the hypersensitive response (HR) upon infection with low titers of bacteria that do not induce the HR in WT plants (Mittler et al., 1999). Our findings, that under certain environmental conditions dAS plants are less sensitive to oxidative stress compared to AS-CAT or AS-APX plants, prompted us to examine the response of dAS plants to pathogen infection. Because growth of plants at moderate light resulted in the induction of PR gene expression in ASCAT plants, we infected plants with bacteria and measured cell death and PR-1 induction in plants grown under low light conditions. For these studies we used a bacterial pathogen that induces the HR in tobacco but cannot propagate within tobacco leaves (Mittler et al., 1999). As shown in Figure 8, dAS plants were similar to AS-CAT and ASAPX plants in their response to bacterial infection. Thus, they activated HR-cell death upon infection with a low titer of bacteria similar to AS-CAT and AS-APX plants (Figure 8A), and they induced PR-1 expression in a similar manner to that of WT, AS-CAT, or AS-APX plants (Figure 8B). The differences observed between dAS plants and AS-CAT 15 or AS-APX plants in their response to various abiotic conditions (Figures 1-3) were therefore not reflected in the response of these plants to pathogen infection.

DISCUSSION

At least 3 central players are involved in the removal of H2O2 in plants: APX, CAT, and GPX. In a previous study Willekens et al., (1997) reported that a deficiency in CAT resulted in the induction of APX and GPX, suggesting that these enzymes were induced to compensate for CAT suppression. Here we show that CAT deficiency is also accompanied by an induction in mitochondrial AOX and MDA reductase, two additional enzymes involved in ROI protection (Table 1; Murthy and Zilinskas, 1994; Maxwell et al., 1999). In addition, we show that APX deficiency results in the induction of CAT, SOD, and GR (Figure 1B, Table 1). Taken together these findings suggest a high degree of redundancy in ROI detoxifying mechanisms in plants. Interestingly, compared to plants with suppressed APX or CAT, a decrease in both APX and CAT did not result in the induction of similar ROI scavenging mechanisms in dAS plants (Figure 1B, Table 1). Moreover, dAS plants, with reduced APX and CAT, should have been more sensitive to
ROI stress compared to AS-APX or AS-CAT. However, at least under low or moderate light, dAS plants did not appear to be subjected to the same degree of oxidative stress as AS-CAT or AS-APX plants (Figures 1-3). It is possible that dAS plants induced an unknown ROI scavenging mechanism that protected them from ROI-induced damage. Alternatively, they might have suppressed the rate of ROI production, thereby lowered their intracellular level of ROI. The suppression of photosynthetic activity in dAS plants may account for such a response (Figure 4). The photosynthetic apparatus is one of the major sources of ROI production in photosynthetic tissues, and suppression of photosynthetic activity was shown to accompany the defense response of certain plants to adverse physical conditions (Mittler et al., 2001). It is unlikely that the suppression of photosynthetic activity in dAS plants was a result of an oxidative damage to the photosynthetic apparatus because such damage would have been accompanied by the induction of ROI scavenging mechanisms (Table 1; Figure 1B). Furthermore, measurements of variable fluorescence at low and moderate light failed to detect damage to PSII in dAS plans (not shown), and enhanced CO2 levels did not result in an increase in photosynthetic activity that was higher than that observed in WT plants (Figure 4C).

To test the possibility that suppression of photosynthetic activity might have enhanced the tolerance of dAS plants to oxidative stress we tested the response of plants with suppressed photosynthetic activity, i.e., AS-RbcS plants (Jiang and Rodermel, 1995), to oxidative stress. The suppression of photosynthetic activity in these plants is a result of a reduction in RbcS protein and is unlikely to involve changes in ROI metabolism. The enhanced tolerance of AS-RbcS plants to oxidative stress induced by paraquat (Figure 7) supported the hypothesis that suppression of photosynthetic activity plays an important role in protecting dAS plants against oxidative stress. Our results may therefore reveal another aspect of the defense response of plants to oxidative stress: the

suppression of a cellular pathway that enhances ROI production, i.e., the photosynthetic apparatus, in order to balance the overall level of ROI in cells.

Preventing the formation of ROI in chloroplasts is likely to protect plant tissue from oxidative stress. Our findings that chlAOX is induced in dAS plants at low light, and in WT tobacco and Arabidopsis plants at high light (Figure 6), may suggest that this enzyme plays an active role in suppressing the production of ROI in these plants. It has been suggested that chlAOX can intercept electrons flowing from PSII to PSI, and reduce oxygen into water (Carol et al., 1999; Wu et al., 1999; Josse et al., 2000; Cournac et al., 2000). Thus, the activity of this enzyme might decrease the overall rate of ROI production in chloroplasts by reducing the flow of electrons to PSI and the reduction of oxygen to ROI by PSI during stress (Asada and Takahashi, 1987). Chloroplastic AOX is essential for chloroplast biogenesis, and leaves of mutants lacking this enzyme bleach when exposed to high light during germination (Wetzel et al., 1994). These findings, as well as the induction of chlAOX in wild type tobacco and Arabidopsis plants at high light, may suggest that this enzyme plays a defense role against ROI production, similar to mitochondrial AOX (Maxwell et al., 1999). It is thus possible that two different mechanisms, aimed at lowering the rate of ROI production, are specifically activated in dAS plants: suppression of photosynthetic activity (Figure 4), and induction of chlAOX (Figure 6). The combined action of these mechanisms may attenuate the rate of ROI production in dAS plants and enable them to survive in the absence of APX and CAT.

In addition to the mechanisms that suppress ROI production, at least two different mechanisms may cooperate in dAS plants to actively detoxify H_2O_2: the pentose phosphate pathway, and MDA reductase (Table 1). The pentose phosphate pathway was found to be indispensable for the removal of ROI in mammalian cells and yeast (Pandolfi et al., 1995; Juhnke et al., 1996). In addition, the expression of transcripts encoding enzymes of the pentose phosphate pathway was found to be induced in plants in response to stress (Fahrendorf et al., 1995; Moehs et al., 1996). It was suggested that during stress the pentose phosphate pathway serves as a key source for the supply of reduced NADPH for ROI removal (Pandolfi et al., 1995; Juhnke et al., 1996). Because dAS plants had an enhanced expression of MDA reductase (Table 1), it is possible that the enhanced supply of NADPH via the pentose phosphate pathway in these plants is used for enhancing the regeneration of ASC by this enzyme. Ascorbic acid can react non-enzymatically with hydrogen peroxide in a reaction similar to that catalyzed by APX, resulting in the oxidation of ASC to monodehydroascorbate (MDA; Foyer and Halliwell, 1976; Asada and Takahashi, 1987; Noctor and Foyer, 1998). The rapid reduction of MDA to ASC by MDA reductase may therefore facilitate the non-enzymatic detoxification of H_2O_2 by ASC in dAS plants, and enhance the detoxification of H_2O_2 in the absence of APX and CAT. Although the steady state level of ASC was not significantly higher in dAS plants compared to control plants (Figure 2B), it is possible that the rate of regeneration of MDA to ASC is higher in dAS plants. Thus, using the same pool size of ASC as WT plants, the non-enzymatic scavenging of H_2O_2 may be higher in dAS plants due to a high turnover rate of ASC oxidation and ASC reduction. Further studies, including a comprehensive metabolomic analysis are required to address this possibility.

The importance of APX and CAT to the defense of plants against oxidative stress should not be undermined by our results. Under high light conditions, or in response to pathogen infection, when ROI production is significantly enhanced, the redundant mechanism(s) activated in dAS plants appeared not to be sufficient to prevent tissue damage or HR activation. Thus, dAS plants grown under high light conditions developed lesions similar to AS-APX and AS-CAT plants, while wild type plants did not (not shown), and dAS plants activated the HR in a similar manner to AS-CAT and AS-APX upon challenge with a low titer of bacteria (Figure 8). Nevertheless, identifying redundant mechanisms or alternative strategies for ROI protection may allow, through genetic manipulations, to enhance the tolerance of plants and crops to adverse environmental conditions. For example, it may be beneficial to transiently reduce the photosynthetic activity of crops during periods of environmental stress. This type of manipulation may protect plants from ROI production that is associated with the photosynthetic apparatus during stress. Alternatively, overexpression of chlAOX during stress may protect plant tissues from oxidative stress.

The reason for the plasticity observed in the activation of redundant ROI defense mechanisms between the different antisense plants, i.e., AS-CAT, AS-APX, and dAS, is not known.

Because APX and/or CAT expression was most likely suppressed in antisense plants immediately upon germination, due to the use of the 35ScaMV promoter, it is possible that early events in gene expression were affected in a different manner in plants that lacked APX, CAT, or APX and CAT. An early change in gene expression might affect a number of critical systems in plants, including events associated with chloroplast biogenesis. The constitutive induction of chlAOX in dAS plants may provide some evidence for an early effect on gene expression in these plants, because this gene was found to be essential for chloroplast biogenesis during early stages of germination (Wetzel et al., 1994).

The differences observed between the response of AS-CAT and AS-APX plants to moderate light (Figures 1-3; Table 1) suggest that under these conditions at least two different signal transduction pathways are activated in these plants. Thus, AS-CAT plants activate a cell death pathway resulting in the formation of lesions, whereas AS-APX plants do not form lesions (Figure 1A). In addition, the defense mechanisms activated in AS-APX plants appear to be different from those activated in AS-CAT plants (Figure 1B; Table 1). The induction of cell death and mitAOX in AS-CAT plants suggest that in these plants a signal transduction pathway that involves the mitochondria is activated. The mitochondrion was suggested to be involved in controlling the activation of programmed cell death (PCD) in plants (Lam et al., 2001). In addition, peroxisomes, were CAT is localized (Willekens et al., 1997), are thought to be one of the cellular sites of nitric oxide synthesis (NO; Corpas et al., 2001). Because NO is a key regulator of PCD and defense response activation in plants (Klessig et al., 2000; Delledonne et al., 2001), it is possible that the lack of CAT in peroxisomes of AS-CAT plants activated a signal transduction pathway that triggered PCD. In contrast, AS-APX plants that lack the cytosolic isoform of APX, but contain CAT, do not activate PCD or mitAOX expression. Interestingly, the response of dAS plants to growth at moderate light is very different from that of AS-APX or AS-CAT plants (Figures 1-3). It is possible that in dAS plants, that lack APX and CAT, the two different pathways activated in the single antisense plants are simultaneously activated, however, their integration results in a completely different outcome. Thus, these plants suppress photosynthesis and activate different defense mechanisms including chlAOX. Future studies using array technology and knockout or antisense Arabidopsis plants lacking APX and/or CAT may identify the specific components of the different signaling pathways activated in these plants. These studies are underway in our laboratories.

METHODS

Plant Material

The production and characterization of transgenic tobacco plants expressing antisense RNA for APX (*apx I*; AS-APX; Orvar and Ellis, 1997), CAT (*cat 1*; AS-CAT; Willekens et al., 1997), or *rbcS* (AS-RbcS; Jiang and Rodermel, 1995) was previously reported. Crosses were performed between AS-APX and AS-CAT plants, between their corresponding controls (Orvar and Ellis, 1997; Willekens et al., 1997; referred herein as WT), and between AS-CAT and AS-APX and wild types. Progenies of all crosses were selfed and their seedlings germinated and examined by RNA and protein blots for the expression of APX and CAT. Blots were performed on leaves of similar size and age from the different plants, subjected to the same light intensity. At least 3 different plants from each of the groups studied, i.e., WT, AS-APX, AS-CAT, and dAS were selected and propagated by shoot cuttings and seeds to generate a large number of plants. These were again tested by RNA and protein blots prior to analysis. All experiments were performed in triplicates and repeated at least twice.

Growth Conditions and Photosynthetic Measurements

Growth of plants and experiments were conducted under controlled environmental conditions at 22-24oC. Continuous illumination was provided by cool-white fluorescent lamps (75 or 150-200 µmol m-2 sec-1), or cool-white fluorescent lamps plus sodium vapor lamps (600-800 µmol m-2 sec-1). Photosynthetic activity, dark respiration, and stomatal conductance of leaves was measured with a Licor LI-6400 apparatus using the following measuring cell (6 cm2) parameters: 24oC, 0, 75, 150, 600, or 2000 µmol photons m-2 sec-1, 350 or 2200 ppm CO2, and an air flow of 300 µl/sec, as

previously described (Mittler et al., 2001). Stomata were counted with an epifluorescene microscope (CARL Zeiss, Germany).
Arabidopsis (*Arabidopsis thaliana* ecotype Colombia) plants were grown for weeks at 220C, 70 µmol m-2 sec-1. High light stress was imposed by shifting of plants to 700 µmol m-2 sec-1 at 220C for 48 hours. Control and high light treated plants were sampled at different times and analyzed by RNA and protein blots as described below. For the detection of chlAOX protein, chloroplasts were isolated from the different plants (Wu et al., 1999) and loaded on gels based on equal levels of chlorophyll or protein.

Bacterial Infections
Fully expanded leaves of 3-week-old plants were inoculated with *Pseudomonas syringae* pv *phaseolicola* (NPS3121) according to Mittler et al., (1999). Mock-infected plants were infiltrated with water. Mock and pathogen-infected plants were kept at 22-24oC under continuous illumination (75 µmol m-2 sec-1). At different times after infection leaves were sampled, photographed, and analyzed for HR cell death and expression of the PR protein, PR-1, as described below by measurements of ion leakage and RNA blots. 23
Additionally, bacteria were extracted from infected leaves and plated, to assay for viability and *in planta* growth. In accordance with previous reports *P.s. phaseolicola* (NPS3121) was unable to grow *in planta* in tobacco (Mittler et al., 1999).

Paraquat Treatment and Cell Death Measurements
Fully expanded leaves of 3 to 4-week-old plants were infiltrated with different concentrations of paraquat (methyl viologen, Sigma; Mittler et al., 1999). Plants were incubated at 24oC under continuous illumination (75 µmol m-2 sec-1), sampled and assayed for cell death as described below.

Measurement of Ion Leakage from Leaf Discs.
Cell death was assayed by measuring ion leakage from leaf discs. For each measurement, five leaf discs (9-mm diameter) were floated abaxial side up on 5 ml of double distilled water for 3 h at room temperature. Following incubation, the conductivity of the bathing solution was measured with a conductivity meter (Consort); referred to as value A. The leaf discs were then returned to the bathing solution, introduced into sealed tubes and incubated with the bathing solution at 95oC for 25 min. After cooling to room temperature the conductivity of the bathing solution was again measured; referred to as value B. For each measurement ion leakage was expressed as % leakage, i.e., (value A/ value B)x100.

RNA and Protein Blots and Biochemical Measurements.
Immunodetection RbcL, RbcS, D1, PsaH, and LHCP was performed by protein blot analysis of total leaf protein with a chemiluminescence detection system (Mittler et al., 1998). Total RNA was isolated as previously described (Mittler et al., 1998) and subjected to RNA gel blot analysis (Mittler et al., 1999). A probe for 18S rRNA was used to ensure equal loading of RNA. The level of ASC and GSH was determined in frozen plant tissue as previously described (Mittler and Tel-Or, 1991; Mittler et al., 1991). Hydrogen peroxide levels were measured by infiltrating leaves with 50 µM H2DCF-DA (sigma) in a 20 mM K2HPO4, pH 6.5 buffer. Leaf discs (2X6 cm) were prepared from plants 30 min after infiltration and immediately grounded in 400 µl ice-cold 20 mM K2HPO4, pH 6.5 buffer. The extracts were cleared by filtration and centrifugation (Karpinski et al., 1999) and assayed using a Hitachi F-2000 fluorescence spectrophotometer at 488 nm excitation and 520 nm emission. Control experiments in which H2O2 (0.1-10 mM) was infiltrated into leaves, prior (30 min), or with H2DCF-DA were also performed for calibration.

Filter Array Hybridization
Clones for the production of filter arrays were ordered from the tomato EST library at Clemson University, or isolated by a differential display screen from stressed tobacco tissue, following paraquat application (Vranova, et al., in preparation). Filter arrays were prepared from the clones by spotting PCR products in triplicates on nylon membranes at the Hadassah Medical School DNA Facility of the

Hebrew University, and at the Ghent laboratory. Filters were hybridized with radiolabeled cDNAs prepared from total RNA isolated from the different plants (pooling RNA from 3-5 plants per sample) using oligo dT and SuperscriptTM reverse transcriptase (GibcoBRL) as suggested by the manufacturer. Hybridization conditions were as follows: 60oC, 5XSSC ,5X Denhart, 0.5% SDS, 100 µg/ml salmon sperm DNA, overnight. Washing conditions were as follows: 60oC, 2XSSC, 0.1% SDS, for 20 minutes, followed by 0.2XSSC, 0.1% SDS, 60oC for 20 min. Following hybridization and washes the signals were assayed with a phosphoimager (Fuji BAS1000) and analyzed with TINATM software (Raytest). A number of control "housekeeping" genes, animal-specific genes (as negative controls), and empty spots (for background) were also spotted on the membrane. These were used to normalize the intensity of signals between the different filters and calculate the changes in gene expression presented in Table 1. When pertinent, the expression level of specific genes was verified by RNA blots.

ACKNOWLEDGMENTS

We thank Dr. Brian E. Ellis for providing seeds for AS-APX plants. We also thank Dr. Itzhak Ohad for his help in performing variable fluorescence measurements, and Drs. Rachel Nechushtai, Barbara A. Zilinskas, and Gadi Schuster for gifts of antibodies. This work was supported by the Israeli Academy of Science, The Biotechnology Council Iowa State University, U.S. Dept. of Energy (grant no DE-FG02-94ER20147 to S.R.), and The Fund for the Promotion of Research at the Technion.

FIGURE LEGENDS

Figure 1. Molecular Characterization of Double Antisense Plants. **(A)** Photographs of leaves from wild type (WT), APX antisense (AS-APX), CAT antisense (AS-CAT), and APX and CAT antisense (dAS) plants, showing the formation of lesions on leaves of AS-CAT plants but not on leaves of dAS plants that lack both APX and CAT. Leaves of similar developmental age and size were photographed from 5-6 week old plants grown under moderate light intensity (150 µmol photons m-2 sec-1). **(B)** RNA gel blot analysis performed with RNA obtained from the leaves shown in (A). The expression of the stress response genes SOD, GR and/or PR-1 is shown to be induced in AS-APX and AS-CAT plants but not in dAS plants.

Figure 2. Biochemical Characterization of Double Antisense Plants. **(A)** Measurements of CAT and APX activities in WT, AS-APX, AS-CAT, and dAS plants. The measurements of APX and CAT activities are in good agreement with the level of transcripts encoding CAT and APX in the different plants shown in Figure 1B. Results are mean and standard deviation of 3 independent measurements. **(B)** Ascorbate (ASC), glutathione (GSH), and H2O2 levels in WT, AS-APX, AS-CAT, and dAS plants. Results shown are mean and standard deviation of 3 independentmeasurements. Leaves of similar developmental age and size were sampled and analyzed from 4 week old plants grown under moderate light intensity (150 µmol photons m-2 sec-1).

Figure 3. Induction of Cell Death by Paraquat in AS-CAT Plants. Wild type (WT), APX antisense (AS-APX), CAT antisense (AS-CAT), and APX and CAT antisense (dAS) plants were treated with 10-6 M paraquat at a low light intensity (75 µmol photons m-2 sec-1) and assayed for cell death at different times following paraquat application by measuring ion leakage from leaf discs. Data shown is mean and standard deviation of 3 independent measurements.

Figure 4. Measurements of Photosynthetic Activity and Dark Respiration in the Different Antisense Plants. **(A)** Measurements of photosynthetic activity in 3-4 week old control and antisense plants grown at low light (75 µmol photons m-2 sec-1) and subjected to saturating light for 15 min. Leaves of similar developmental age and size were clamped with a LI-6400 photosynthetic measuring apparatus, subjected to saturating light (2000 µmol photons m-2 sec-1), and assayed for their rate of CO2 assimilation. Double antisense plants (dAS) are shown to have a low photosynthetic activity compared to WT or AS-APX and AS-CAT plants. 29 **(B)** Rates of dark respiration, i.e., CO2 emission, measured at the beginning (75 µE) and at the end (2000 µE) of the experiments shown in (A). Dark

respiration was measured with a LI-6400 photosynthetic measuring apparatus. **(C)** Fold-increase in photosynthetic activity upon changing the CO2 concentration from 350ppm to 2200ppm. Plants were clamped with a LI-6400 apparatus as described for (A). When they reached maximal photosynthetic activity at 350ppm CO2 the concentration of CO2 was changed to 2200ppm and the new maximal photosynthetic activity was measured. The graph shows the fold-increase in activity calculated from the two photosynthetic values, i.e., at 350 and at 2200ppm. Data shown is mean and standard deviation of 3-5 independent measurements. Abbreviations: µE, µmol photons m-2 sec-1.

Figure 5. DNA Filter Arrays and Protein Blot Analysis of Gene Expression in the Different Antisense Plants. **(A)** Filter array hybridization comparing the expression pattern of 200 stress response cDNAs between wild type (WT), APX antisense (AS-APX), CAT antisense (AS-CAT), and APX and CAT antisense (dAS) plants. Overall about 500 genes were tested using this approach. A short summary of the results shown in (A) is presented in Table 1. **(B)** Protein blot analysis comparing the level of different proteins involved in photosynthesis between WT and dAS plants. Samples were loaded in 3 different dilutions (1:1, 1:5, 1:20) based on equal protein or chlorophyll content with similar results. No differences were detected between dAS and WT plants. Abbreviations used: Activase, Ribulose-1,5-bisphosphate carboxylase/oxygenase activase; D1, Photosystem II D1 subunit; LHCP, light harvesting chlorophyll binding protein; PsaH, subunit H of photosystem I; RbcS/L, ribulose-1,5-bisphosphate carboxylase/oxygenase small (S) or large (L) subunit.

Figure 6. Enhanced Expression of Chloroplastic Alternative Oxidase (chlAOX) in Double Antisense Plants and in Arabidopsis Plants Subjected to High Light Stress. **(A)** RNA gel blot analysis performed on leaves obtained from wild type (WT), APX antisense (AS-APX), CAT antisense (AS-CAT), and APX and CAT antisense (dAS) plants grown under low (75 µmol photons m-2 sec-1), moderate (150-200 µmol photons m-2 sec-1), or high (600-800 µmol photons m-2 sec-1) light intensity, showing that chlAOX is specifically induced in dAS plants at low light. Chloroplastic AOX is also shown to be induced in AS-CAT plants at moderate light and in all plants, at high light, suggesting that it may be involved in the suppression of ROI production in plants. **(B)** RNA (top) and Protein (bottom) blots showing that chlOX is induced in Arabidopsis plants subjected to high light stress. ChlAOX is shown to be induced after 5 hours of high light stress. This induction is both at the steady state transcript and protein levels. For the analysis of chlAOX protein, chloroplast extracts were loaded in 3 different concentrations: 1, 2.5, and 5-µg chlorophyll/µl.

Figure 7. Suppression of Paraquat-Induced Cell Death in Transgenic Plants with Decreased Photosynthetic Activity. **(A)** Measurements of photosynthetic activity in wild type (WT) and two independent antisense plants with reduced expression of *rbcS* (AS-RbcS1 and AS-RbcS2), showing that AS-RbcS plants have reduced photosynthetic activity. **(B)** Expression of PR-1a in AS-RbcS plants compared to WT plants or to WT plants treated with paraquat. **(C)** Decreased cell death of AS-RbcS plants compared to WT plants in response to a 5-hour treatment with paraquat. Cell death was assayed by measuring ion leakage from leaf discs. Data in (A) and (C) is shown as mean and standard deviation of 3 independent measurements performed on 3 week old plants grown under low light intensity (75 µmol photons m-2 sec-1).

Figure 8. Response of Double Antisense Plant to Infection with an HR-Inducing Bacterium. **(A)** Induction of HR-cell death in WT, AS-APX, AS-CAT, and dAS plants 12 hours following infection with *Pseudomonas syringae* pv *phaseolicola* at different concentrations. Cell death was measured by leakage of ions from cells as described in Methods. Results shown are mean and standard deviation of 3 independent measurements performed on 3 week-old plants grown under low light intensity (75 µmol photons m-2 sec-1). All antisense plants are shown to be hyper-responsive to bacterial infection compared to WT plants. **(B)** RNA gel blots showing the induction of PR-1 transcripts 12 hours following bacterial infection (OD600=0.1). PR-1 is shown to be induced in all plants including WT plants. These results are in agreement with Mittler et al., (1999).

FIGURES

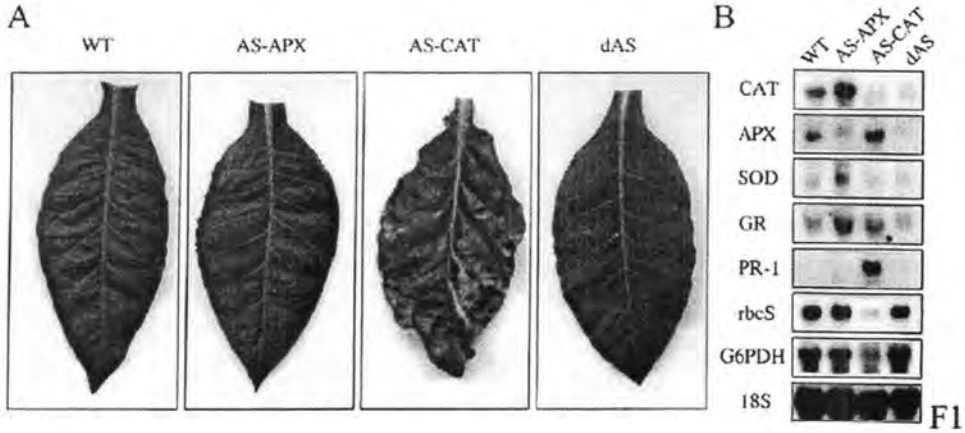

F1

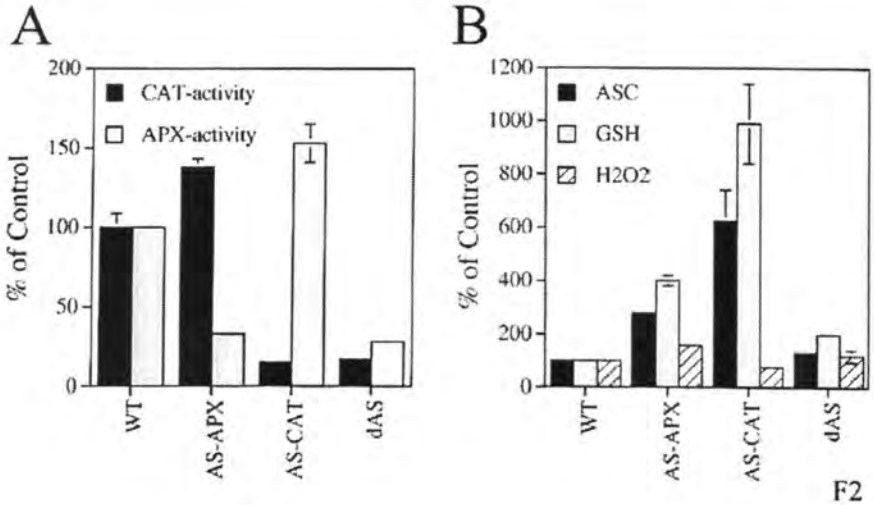

F2

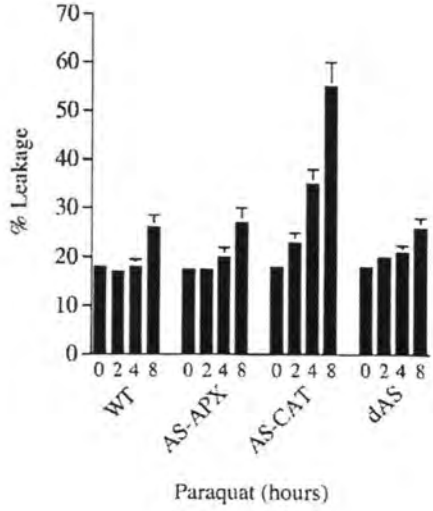

F3

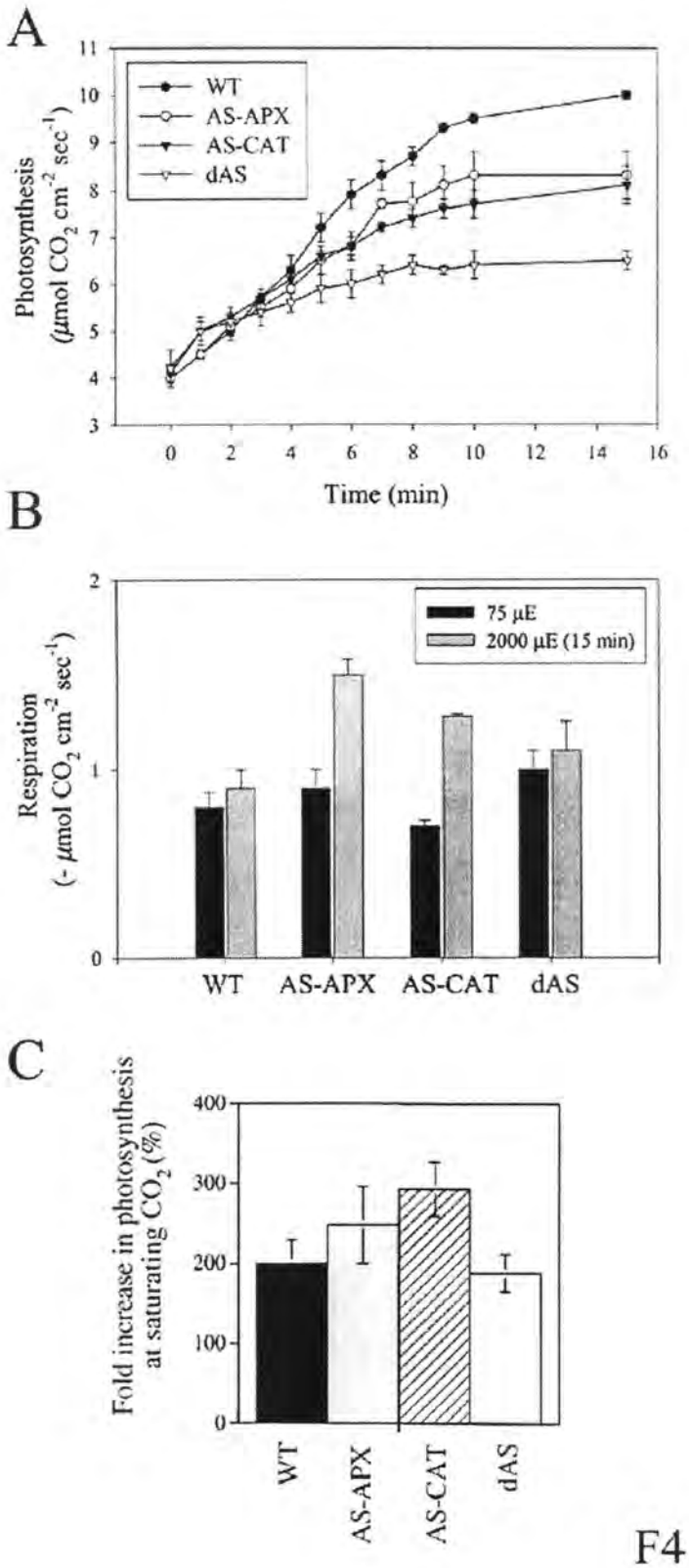
A
Photosynthesis
(μmol CO2 cm-2 sec-1)
WT
AS-APX
AS-CAT
dAS
Time (min)
B
Respiration
(- μmol CO2 cm-2 sec-1)
75 μE
2000 μE (15 min)
WT
AS-APX
AS-CAT
dAS
C
Fold increase in photosynthesis
at saturating CO2 (%)
WT
AS-APX
AS-CAT
dAS

F4

A

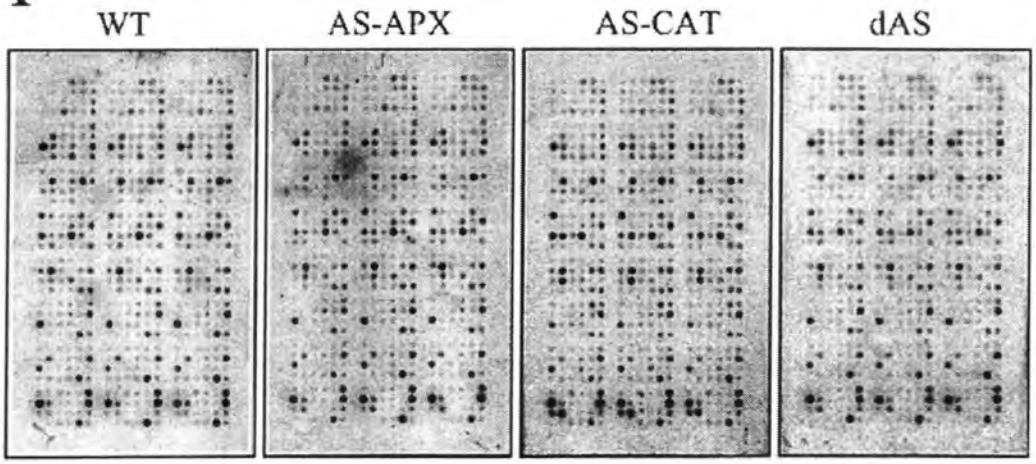

B

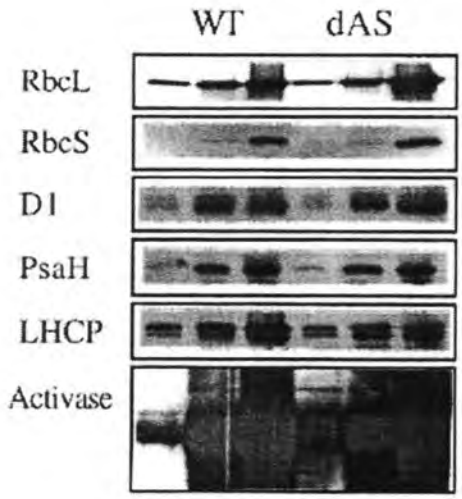

F5

A

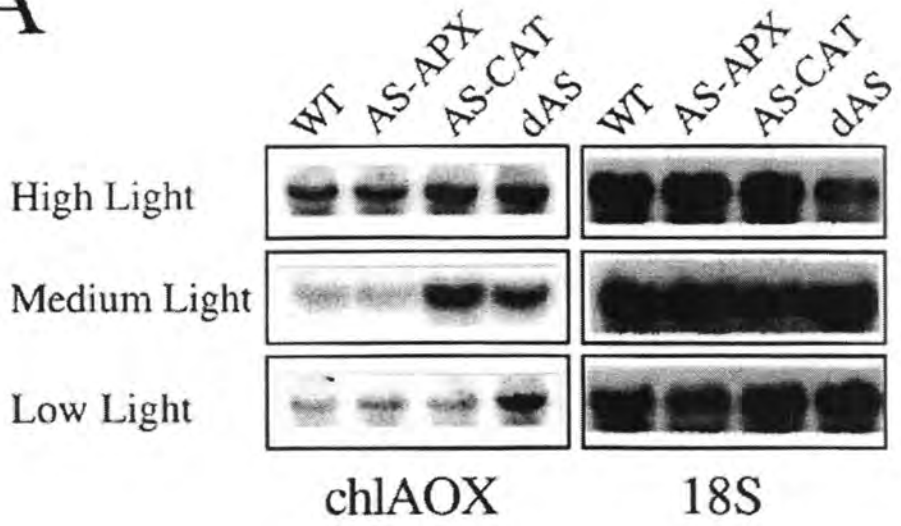
WT
AS-APX
AS-CAT
dAS
WT
AS-APX
AS-CAT
dAS
High Light
Medium Light
Low Light
chlAOX
18S

B

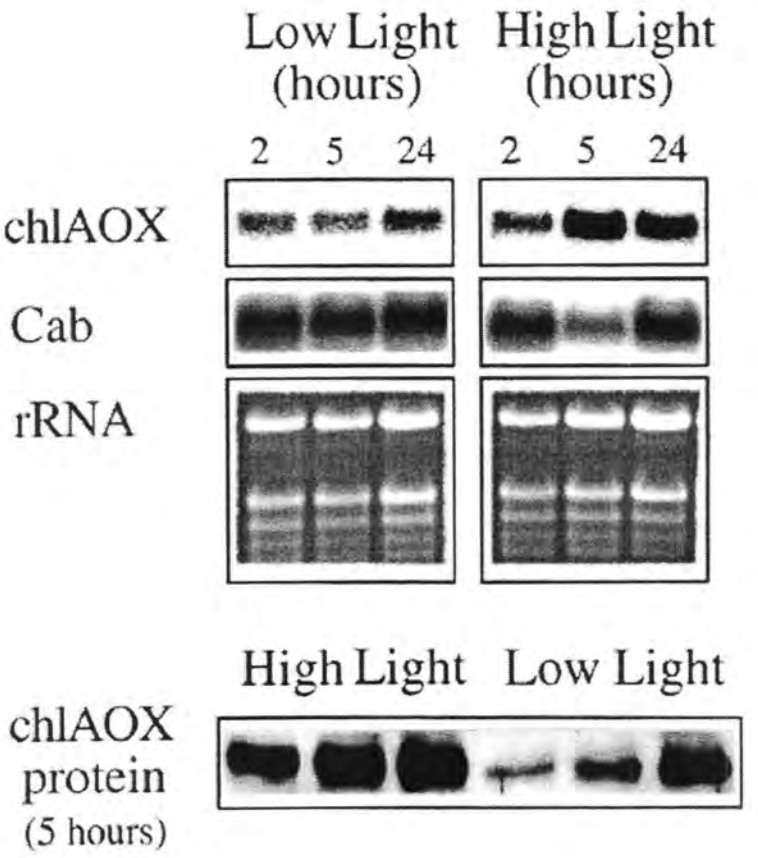
Low Light (hours)
High Light (hours)
2
5
24
2
5
24
chlAOX
Cab
rRNA
High Light
Low Light
chlAOX protein (5 hours)

F6

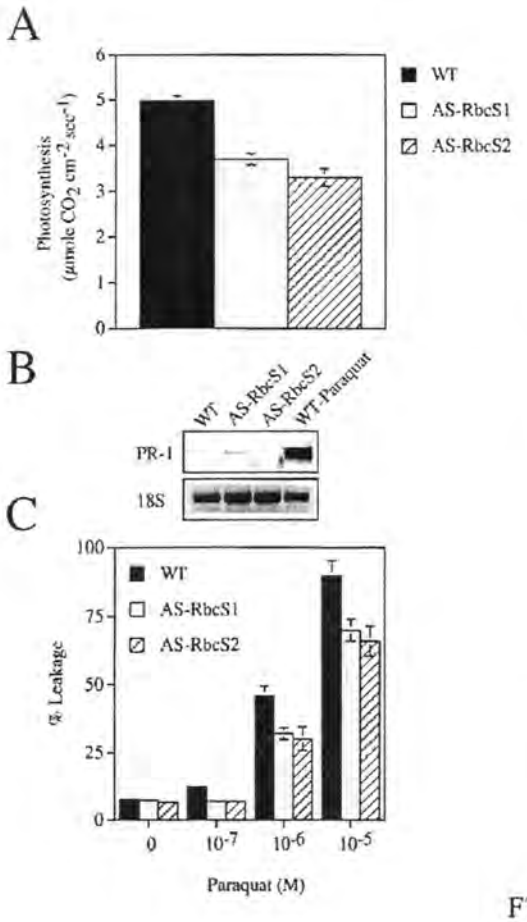
A
Photosynthesis (μmole CO_2 cm^{-2} sec^{-1})
WT
AS-RbcS1
AS-RbcS2
B
WT
AS-RbcS1
AS-RbcS2
WT-Paraquat
PR-1
18S
C
% Leakage
WT
AS-RbcS1
AS-RbcS2
0
10^{-7}
10^{-6}
10^{-5}
Paraquat (M)

F7

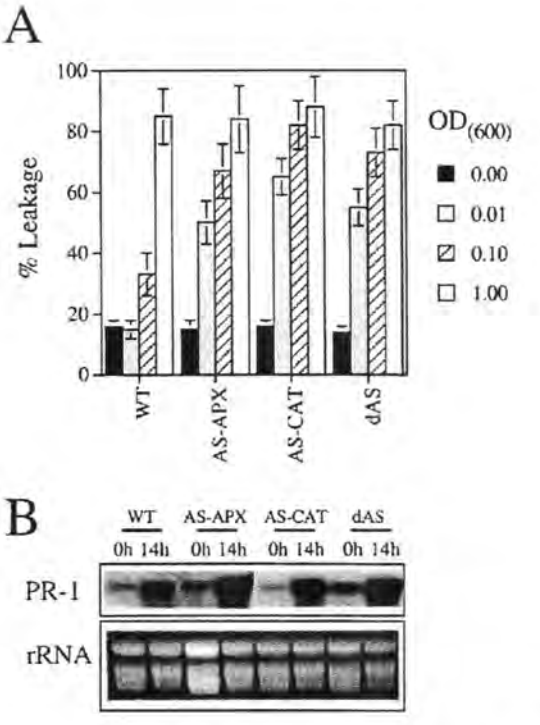
A
% Leakage
$OD_{(600)}$
0.00
0.01
0.10
1.00
WT
AS-APX
AS-CAT
dAS
B
WT
AS-APX
AS-CAT
dAS
0h 14h
PR-1
rRNA

F8

Table 1. Changes in Gene Expression Measured by Filter Arrays.

Gene / Class	Expression Level Compared to WT (as % of Control)		
	AS-APX	AS-CAT	dAS
ROI-related genes:			
Thylakoid APX	51	2	69
Stromal APX	71	49	115
Glutathoine Peroxidase	91	185	117
Thioredoxin Peroxidase	75	64	148
Thioredoxin H1	48	298	149
MDA Reductase	156	256	313
Glutathione-S-transferase	87	320	185
Mitochondrial AOX	32	260	148
Induced genes:			
Cytosolic sHSP	40	327	81
Chloroplastic sHSP	141	1423	142
Cytosolic HSP100	335	182	31
PR-1a (See also Fig. 1B)	28	4660	203
PR-3	18	864	219
PR-5	150	7362	45
ACC Oxidase	58	376	179
Ribulose-5-Phosphate Isomerase	93	20	281
Transaldolase	33	164	455
Transketolase	12	46	514
Invertase	99	297	389
Histone H3	86	497	132
Housekeeping Genes:			
ATP Synthase	90	65	94
Actin	65	67	115
Tubulin	66	60	67
RbcS (See also Fig. 1B)	64	8	87

REFERENCES

Allen, R. (1995) Dissection of oxidative stress tolerance using transgenic plants. Plant Physiol. 107, 1049-1054 .

Asada, K., and Takahashi, M. (1987) Production and scavenging of active oxygen in photosynthesis. In: *Photoinhibition* (DJ Kyle, CB Osmond, CJ Arntzen; Elsevier, Amsterdam), pp. 227-287.

Carol, P., Stevenson, D., Bisanz, C., Breitenbach, J., Sandmann, G., Mache, R., Coupland, G., and Kuntz, M. (1999) Mutations in the Arabidopsis gene IMMUTANS cause a variegated phenotype by inactivating a chloroplast terminal oxidase associated with phytoene desaturation. Plant Cell 11, 57-68.

Clark, D., Durner, J., Navarre, D.A., and Klessig, D.F. (2000) Nitric oxide inhibition of tobacco catalase and ascorbate peroxidase. Mol. Plant Micro. Inter. 13, 1380-1384.

Conklin, P.L., Williams, E.H., and Last, R.L. (1996) Environmental stress sensitivity of an ascorbic acid-deficient Arabidopsis mutant. Proc. Natl. Acad. Sci. USA 93, 9970-9974.

Corpas, F.J., Barroso, J.B., and del Rio, L.A. (2001) Peroxisomes as a source of reactive oxygen species and nitric oxide signal molecules in plant cells. Trends Plant Sci. 6, 145-150.

Cournac, L., Redding, K., Ravenel, J., Rumeau, D. Josse, E.M., Kuntz, M., and Peltier, G. (2000) Electron flow between photosystem II and oxygen in

chloroplasts of photosystem I-deficient algae is mediated by a quinol oxidase involved in chlororespiration. J. Biol. Chem. 275, 17256-17262.

Dangl, J.L., Dietrich, R.A., and Richberg, M.H. (1996) Death don't have no mercy: cell death programs in plant-microbe interactions. Plant Cell 8, 1793-1807.

Dat, J., Vandenabeele, S., Vranova, E., Van Montagu, M., Inze, D., and Van Breusegem, F. (2000) Dual action of the active oxygen species during plant stress responses. Cell Mol. Life Sci. 57, 779-795.

Delledonne, M., Zeier, J., Marocco, A., and Lamb, C. (2001) Signal interactions between nitric oxide and reactive oxygen intermediates in the plant hypersensitive disease resistance response. Proc. Natl. Acad. Sci. USA 98, 13454-13459.

Durner, J., and Klessig, D.F. (1995) Inhibition of ascorbate peroxidase by salicylic acid and 2,6-dichloroisonicotinic acid, two inducers of plant defense responses. Proc. Natl. Acad. Sci. USA 92, 11312-11316.

Fahrendorf, T., Ni, W., Shorrosh, B.S., Dixon, R.A. (1995) Stress responses in alfalfa (Medicago sativa L.) XIX. Transcriptional activation of oxidative pentose phosphate pathway genes at the onset of the isoflavonoid phytoalexin response. Plant Mol. Biol. 28, 885-900.

Foyer, C.H., and Halliwell, B. (1976) The presence of glutathione and glutathione reductase in chloroplasts: a proposed role in ascorbic acid metabolism. Planta 133, 21-25.

Grant, J.J., Yun, B.W., and Loake, G.J. (2000) Oxidative burst and cognate redox signaling reported by luciferase imaging: identification of a signal network that functions independently of ethylene, SA and Me-JA but is dependent on MAPKK activity. Plant J. 22, 87-95.

Haake, V., Zrenner, R., Sonnewald, U. and Stitt, M. (1998) A moderate decrease of plastid aldolase activity inhibits photosynthesis, alters the levels of sugars and starch, and inhibits growth of potato plants. Plant J 14, 147-157.

Hammond-Kosack, K.E., and Jones, J.D.G. (1996) Resistance gene-dependent plant defense responses. Plant Cell 8, 1773-1791.

Herouart, D., Van Montagu, M. and Inze, D. (1993) Redox-activated expression of the cytosolic copper/zinc superoxide dismutase gene in Nicotiana. Proc Natl Acad Sci USA 90, 3108-3112.

Hirt, H. (2000) Connecting oxidative stress, auxin, and cell cycle regulation through a plant mitogen-activated protein kinase pathway. Proc. Natl. Acad. Sci. USA 97, 2405-2407.

Jiang, C.Z., and Rodermel, S. (1995) Regulation of photosynthesis during leaf development in *RbcS* antisense DNA mutants of tobacco. Plant Physiol. 107, 215-224.

Karpinski, S., Reynolds, H., Karpinska, B., Wingsle, G., Creissen, G., and Mullineaux, P. (1999) Systemic signaling and acclimation in response to excess excitation energy in Arabidopsis. Science 284, 654-657.

Josse, E.M., Simkin, A.J., Gaffe, J., Labore, A-M, Kuntz, M., and Carol, P. (2000) A plastid terminal oxidase associated with carotenoid desaturation during chromoplast differentiation. Plant Physiol. 123, 1427-1436.

Juhnke, H., Krems, B., Kotter, P., and Entian, K.D. (1996) Mutants that show increased sensitivity to hydrogen peroxide reveal an important role for the pentose phosphate pathway in protection of yeast against oxidative stress. Mol. Gen. Genet. 252, 456-464.

Klessig, D.F., Durner, J., Noad, R., Navarre, D.A., Wendehenne, D., Kumar, D.,
Zhou, J.M., Shah, J., Zhang, S., Kachroo, P., Trifa, Y., Pontier, D., Lam, E., and Silva, H. (2000) Nitric oxide and salicylic acid signaling in plant defense. Proc Natl Acad Sci USA 97, 8849-8855.

Knight, H., and Knight, M.R. (2001) Abiotic stress signalling pathways: specificity and cross-talk. Trends Plant Sci. 6, 262-267.

Kovtun, Y., Chiu, W.L., Tena, G., and Sheen, J. (2000) Functional analysis of oxidative stress-activated mitogen-activated protein kinase cascade in plants. Proc. Natl. Acad. Sci. USA 97, 2940-2945.

Lam, E., Kato, N., and Lawton, M. (2001) Programmed cell death, mitochondria and the plant hypersensitive response. Nature 411, 848-853.

Maxwell, D.P., Wang,Y., and McIntosh, L. (1999) The alternative oxidase lowers mitochondrial reactive oxygen production in plant cells. Proc. Natl. Acad. Sci. USA 96, 8271-8276.

Mittler, R. and Tel-Or, E. (1991) Oxidative stress response and shock proteins in the unicellular cyanobaterium *Synechococcus* R2 (PCC 7942). Arch. Microbiol. 155, 125-131.

Mittler, R., Nir, M. and Tel-Or, E. (1991) Antioxidative enzymes in Retama and their seasonal variation. Free Radical Res. Comm. 14, 17-25.

Mittler, R., Feng, X., and Cohen, M. (1998) Post-transcriptional suppression of cytosolic ascorbate peroxidase expression during pathogen-induced programmed cell death in tobacco. Plant Cell 10, 461-474.

Mittler, R., Hallak-Herr, E., Orvar, B.L., Van Camp, W., Willekens, H., Inze, D., and Ellis, B.E. (1999) Transgenic tobacco plants with reduced capability to detoxify reactive oxygen intermediates are hyper-responsive to pathogen infection. Proc. Natl. Acad. Sci. USA. 96, 14165-14170.

Mittler, R., Merquiol, E., Hallak-Herr, E., Rachmilevitch, S., Kaplan, A., and Cohen, M. (2001) Living under a 'dormant' canopy: a molecular acclimation mechanism of the desert plant *Retama raetam*. Plant J. 25, 407-416.

Mittler, R. (2002) Antioxidants and stress tolerance. Trends Plant Sci. *in preparation* Moehs, C.P., Allen, P.V., Friedman, M., Belknap, W.R. (1996) Cloning and expression of transaldolase from potato. Plant Mol. Biol. 32, 447-452.

Murthy, S.S., and Zilinskas, B.A. (1994) Molecular cloning and characterization of a cDNA encoding pea monodehydroascorbate reductase. J. Biol. Chem. 269, 31129-31133.

Noctor G., and Foyer, C.H. (1998) Ascorbate and glutathione: keeping active oxygen under control. Annu. Rev. Plant Physiol. Plant Mol. Biol. 49, 249-279.

Orvar, B.L., and Ellis, B.E. (1997) Transgenic tobacco plants expressing antisense RNA for cytosolic ascorbate peroxidase show increased susceptibility to ozone injury. Plant J. 11, 1297-1305.

Pandolfi, P.P., Sonati, F., Rivi, R., Mason, P., Grosveld, F., and Luzzatto, L. (1995) Targeted disruption of the housekeeping gene encoding glucose 6-phosphate dehydrogenase (G6PD): G6PD is dispensable for pentose synthesis but essential for defense against oxidative stress. EMBO J. 14, 5209-5215.

Pei, Z.M., Murata, Y., Benning, G., Thomine, S., Klusener, B., Allen, G.J., Grill, E., and Schroeder, J.I. (2000) Calcium channels activated by hydrogen peroxide mediate abscisic acid signaling in guard cells. Nature 406, 731-734.

Polle, A (2001) Dissecting the superoxide dismutase-ascorbate-glutathione-pathway in chloroplasts by metabolic modeling. Computer simulations as a step towards flux analysis. Plant Physiol. 126, 445-462.

Wetzel, C.M., Jiang, C.Z., Meehan, L.J., Voytas, D.F., and Rodermel, S.R. (1994) Nuclear-organelle interactions: the immutans variegation mutant of Arabidopsis is plastid autonomous and impaired in carotenoid biosynthesis. Plant J. 6, 161-175.

Willekens, H., Chamnongpol, S., Davey, M., Schraudner, M., Langebartels, C.,Van Montagu, M., Inze, D., and Van Camp, W. (1997) Catalase is a sink for H2O2 and is indispensable for stress defence in C-3 plants. EMBO J. 16, 4806-4816.

Wu, D., Wright, D.A., Wetzel, C., Voytas, D.F., and Rodermel, S. (1999) The IMMUTANS variegation locus of Arabidopsis defines a mitochondrial alternative oxidase homolog that functions during early chloroplast biogenesis Plant Cell 11,43-55.